

University of Windsor

## Scholarship at UWindor

---

Electronic Theses and Dissertations

Theses, Dissertations, and Major Papers

---

1-1-2007

### An investigation of Cazaly hanger behaviour.

Anthony Mandarino  
*University of Windsor*

Follow this and additional works at: <https://scholar.uwindsor.ca/etd>

---

#### Recommended Citation

Mandarino, Anthony, "An investigation of Cazaly hanger behaviour." (2007). *Electronic Theses and Dissertations*. 6992.

<https://scholar.uwindsor.ca/etd/6992>

This online database contains the full-text of PhD dissertations and Masters' theses of University of Windsor students from 1954 forward. These documents are made available for personal study and research purposes only, in accordance with the Canadian Copyright Act and the Creative Commons license—CC BY-NC-ND (Attribution, Non-Commercial, No Derivative Works). Under this license, works must always be attributed to the copyright holder (original author), cannot be used for any commercial purposes, and may not be altered. Any other use would require the permission of the copyright holder. Students may inquire about withdrawing their dissertation and/or thesis from this database. For additional inquiries, please contact the repository administrator via email ([scholarship@uwindsor.ca](mailto:scholarship@uwindsor.ca)) or by telephone at 519-253-3000ext. 3208.

# An Investigation of Cazaly Hanger Behaviour

By

Anthony Mandarino

A Thesis

Submitted to the Faculty of Graduate Studies

through

Civil Engineering

in Partial Fulfillment of the Requirements for  
the Degree of Master of Applied Science at the  
University of Windsor

Windsor, Ontario, Canada

2007

© 2007 Anthony Mandarino



Library and  
Archives Canada

Bibliothèque et  
Archives Canada

Published Heritage  
Branch

Direction du  
Patrimoine de l'édition

395 Wellington Street  
Ottawa ON K1A 0N4  
Canada

395, rue Wellington  
Ottawa ON K1A 0N4  
Canada

*Your file* *Votre référence*  
*ISBN: 978-0-494-35017-1*  
*Our file* *Notre référence*  
*ISBN: 978-0-494-35017-1*

#### NOTICE:

The author has granted a non-exclusive license allowing Library and Archives Canada to reproduce, publish, archive, preserve, conserve, communicate to the public by telecommunication or on the Internet, loan, distribute and sell theses worldwide, for commercial or non-commercial purposes, in microform, paper, electronic and/or any other formats.

The author retains copyright ownership and moral rights in this thesis. Neither the thesis nor substantial extracts from it may be printed or otherwise reproduced without the author's permission.

#### AVIS:

L'auteur a accordé une licence non exclusive permettant à la Bibliothèque et Archives Canada de reproduire, publier, archiver, sauvegarder, conserver, transmettre au public par télécommunication ou par l'Internet, prêter, distribuer et vendre des thèses partout dans le monde, à des fins commerciales ou autres, sur support microforme, papier, électronique et/ou autres formats.

L'auteur conserve la propriété du droit d'auteur et des droits moraux qui protègent cette thèse. Ni la thèse ni des extraits substantiels de celle-ci ne doivent être imprimés ou autrement reproduits sans son autorisation.

---

In compliance with the Canadian Privacy Act some supporting forms may have been removed from this thesis.

Conformément à la loi canadienne sur la protection de la vie privée, quelques formulaires secondaires ont été enlevés de cette thèse.

While these forms may be included in the document page count, their removal does not represent any loss of content from the thesis.

Bien que ces formulaires aient inclus dans la pagination, il n'y aura aucun contenu manquant.

  
**Canada**

## ABSTRACT

The Cazaly hanger connection has been used in thousands of precast prestressed concrete beams since its introduction in the mid-1950s. Design methods for these connections have remained largely unchanged over this time. Both full scale and lab scale prestressed concrete tee beams containing Cazaly hanger connections were tested under service and ultimate load conditions. Excessive crack formation at service load levels was identified as an area of concern, especially in areas where corrosive ions are likely to ingress. The use of increased hanger strap steel areas is recommended as a potential means to minimize such cracking, and epoxy injection is identified as a means to repair existing cracks. A critical examination of existing design mechanics was undertaken. Load transfer mechanisms additional to those assumed in common Cazaly hanger design practice have been identified. Areas for future research are detailed.

## DEDICATION

To my family and friends for tolerating this long and drawn out affair.

This work is also dedicated to the late Mr. Richard Clark, a Technician at the University of Windsor, who recently succumbed to a long and courageous battle with cancer. I first met Mr. Clark a number of years ago as a high school summer research assistant. Mr. Clark had an exceptional eye for quality, and constantly demanded the precision, consistency, and integrity that Academic Research should be. He will truly be missed.

"A rock pile ceases to be a rock pile the moment a single man contemplates it, bearing within him the image of a cathedral." Antoine de Saint-Exupery

## **ACKNOWLEDGEMENTS**

The Author is indebted to the following companies and individuals for their support throughout this project:

- Prestressed Systems Incorporated for their donation of test specimens, and specifically, Mr. Loris Collavino, P.Eng.
- Intrepid General Limited for their funding and logistical support of this project.
- Dr. Sreekanta Das, Professor, University of Windsor my advisor, for advising me and providing many useful discussions
- Dr. William Tape, P.Eng (formerly of Prestressed Systems Incorporated), for his guidance and discussion of the technical aspects of Cazaly design.
- Lucien Pop, Technician, and Patrick Seguin, Technicians, University of Windsor

## TABLE OF CONTENTS

ABSTRACT.....	iii
DEDICATION.....	iv
ACKNOWLEDGEMENTS.....	v
LIST OF TABLES.....	viii
LIST OF FIGURES.....	ix
CHAPTER	
I. INTRODUCTION	
Introduction.....	1
Prestressed Concrete Industry in Canada.....	5
Codes and Standards.....	6
Prestressed Concrete Industry in the United States.....	7
Dapped Ends.....	8
Connections and Connection Design.....	10
B-Regions and D-Regions.....	11
Strut-and-Tie Modelling.....	13
Research Objectives.....	15
II. REVIEW OF LITERATURE	
Conception of the Cazaly Hanger.....	16
PCI Design Methodology.....	19
Practical Considerations:.....	21
Strut-Tie Modelling.....	22
Literature surrounding alternate connection methods.....	22
Literature regarding Strut-Tie Modelling.....	28
and End-Regions of Beams.....	28
III. TESTING PROGRAMME	
Overview:.....	31
Full Scale Test Programme.....	31
Specimen Geometry & Fabrication.....	32
Simulated Transportation Damage Test.....	35
Full Scale Test Setup.....	37
Instrumentation.....	38

Full Scale Test Procedure.....	40
Lab Scale Test Programme .....	41
Specimen Geometry & Fabrication.....	42
Lab Scale Test Setup .....	44
<b>IV. RESULTS AND DISCUSSION</b>	
Full Scale Test Results .....	45
Simulated Transportation Test: Qualitative Results .....	47
Preloading:.....	47
Ultimate Testing:.....	49
Lab Scale Test Results.....	51
Qualitative Observations:.....	52
Quantitative Observations:.....	53
Test Beam 1-Quantitative Observations .....	53
Test Beam 2-Quantitative Observations .....	57
Sources of Error.....	60
<b>V. REPAIR METHOD</b>	
Method.....	64
<b>VI. CONCLUSIONS</b>	
Future Research:.....	69
<b>VII. REFERENCES.....</b>	<b>70</b>
<b>VIII. APPENDIX A.....</b>	<b>73</b>
<b>IX. VITA AUCTORIS.....</b>	<b>113</b>



## LIST OF TABLES

Table 1: Concrete Testing Results-Full Scale Test.....	34
Table 2: Concrete Strengths for Lab Scale Testing .....	43
Table 3: Preloading Increments .....	48
Table 4: Ultimate Test Loading Increments .....	49

## LIST OF FIGURES

Figure 1: Examples of Ancient and Modern Monuments. ....	3
Figure 2: Typical Procedures for Prestressing. ....	4
Figure 3: Codes and Standards Applicable to Modern Prestressed Concrete Production (Adapted from CPCI 2005) .....	7
Figure 4: Comparison of Standard Vs. Dapped-End Beams.....	9
Figure 5: Anatomy of a Dapped End.....	9
Figure 6: B- and D- Regions in Typical Beams .....	12
Figure 7: Potential Strut Tie Models of a Dapped-End Beam .....	14
Figure 8: Typical Cazaly Hanger Designs.....	17
Figure 9: Typical Loov Hanger Connection.....	23
Figure 10: Dapped-End Reinforcement Scheme .....	24
Figure 11: Reinforcement scheme proposed by Nanni and Huang (2002) .....	25
Figure 12: Hangers designs examined in the 1986 PCI Research Programme ..	26
Figure 13: Hanger “Type 4” tested by PCI .....	27
Figure 14: Cross section of the Full Scale Specimen.....	32
Figure 15: Elevation Drawing of Cazaly Hanger .....	33
Figure 16: Wire Mesh Reinforcement on Flanges.....	34
Figure 17: Preparation for Road Test.....	37
Figure 18: Beam being set upon concrete support ledge.....	38
Figure 19: Load Cell under Nib of Beam.....	39
Figure 20: Loading of the Test Specimen .....	41
Figure 21: Cazaly Hangers employed in lab scale tests .....	42
Figure 22: Cross Section of the Lab Scale Specimens .....	43

Figure 23: Cracking near the dap on the full scale specimen .....	45
Figure 24: Propagation of cracks prior to stripping.....	46
Figure 25: Preloading of the specimen .....	48
Figure 26: Ultimate loading of the full scale specimen.....	50
Figure 27: Strains along the top bar of the Cazaly hanger.....	53
Figure 28: Strains along top and bottom, respectively .....	54
Figure 29: Strains along the Top Bar of the Cazaly Hanger.....	55
Figure 30: Strains in the bottom bar of the hanger.....	56
Figure 31: Strains in the concrete adjacent the bottom rebar .....	56
Figure 32: Cracking at the re-entrant corner prior to testing .....	58
Figure 33: Propagation of cracks to 150kN.....	58
Figure 34: Specimen at failure [310kN].....	59
Figure 35: Post-failure condition of Cazaly Hanger (concrete removed).....	59
Figure 36: Typical Three-wire strain gage circuit .....	62
Figure 37: Injection of epoxy into existing cracks.....	65
Figure 38: Evidence of epoxy permeating small cracks.....	66
Figure 39: Core of repaired area.....	66

## CHAPTER I

### INTRODUCTION

#### INTRODUCTION

For millennia, the great civilizations of the world looked to stone as a material from which to build their enduring monuments. Many of these structures are still present today. The pyramids, statues and temples of the Egyptians dating from 2700BC are well known, and the ruins of the Olmecs dating from some 1200BC are still found near the Gulf of Mexico; the Great Wall and the temples of the Chinese, the ruins of the Greeks, Romans and Mayans, as well as the ruins of Stonehenge have all survived. These monuments, in addition to their ability to endure time, share another common trait: Their mass. As is exemplified by the pyramids, these structures achieved equilibrium by successive layers of stone bearing on each other. This is to be expected as stone has a limited tensile capacity, but a relatively large compressive strength. Long slender members do not exist in any of these structures, and there are few examples of members in true flexure. Rather, structural form is achieved primarily by large, massive members able to bear incredible loads.

Concrete, a construction material familiar to modern Engineers and Builders, like stone, has a limited tensile capacity. The material in its modern incarnation is a composite of aggregates bonded together by hydraulic cement that is activated by hydration. This modern concrete results from the cements developed by British engineer John Smeaton in 1756, and Joseph Aspdin in 1824. Aspdin's "Portland Cement", developed by burning limestone and clay, is the basis on which modern cements are based. However, the Egyptians were known to have used a lime and gypsum based cement.

Concrete by itself has a tensile capacity on the order of one tenth of its compressive strength, and early concrete structures were largely limited by this lack of tensile capacity. Its ease of casting afforded it the ability to achieve virtually any form, but the span of members constructed in this manner was again, limited. However, in 1849, a Frenchman by the name of Joseph Monier began to produce concrete with embedded steel wire reinforcement. Steel, a material with excellent tensile capacity, could be relied upon to take up the tensile stresses in the concrete. This new "reinforced concrete" allowed for longer, more slender spans. Perhaps the greatest examples of the elegant forms that could be achieved are the bridges of Maillart and Calatrava and the structures of Nervi, shown in Figure 1. Nervi even adopted the use of reinforced concrete for the production of yachts.

However, despite the advances made using reinforced concrete, others realized that given the great compressive strength of concrete was not fully utilized: Yet greater capacity could be achieved by "pre-loading", or "pre-compressing" structural members so as to counteract tensile forces from developing. This concept of "pre-stressing" concrete was first invented the Frenchman Eugene Freyssinet in 1928, and slowly gained acceptance in North America.

For reasons of brevity, the process of prestressing is not described in great detail in this work, except to say that modern prestressing involves the use of high strength tendons or rods made from steel, or less commonly, composite materials. These tendons or rods are placed within the concrete formwork and stressed to a specified load, after which they are "locked off" using appropriate hardware. During pouring and prior to curing, the stressing forces are carried by either the formwork itself, or another suitable anchorage. At such time as the concrete reaches sufficient strength, the tendon anchorages are released and the forces are allowed to transfer into the concrete. The prestressed member is then stripped from its formwork and shipped to the jobsite. This entire process is

described schematically in Figure 2. This process is also known as “pre-tensioning”, however, it is the steel tendons themselves that undergo tensioning with the objective of introducing compressive force into the concrete.

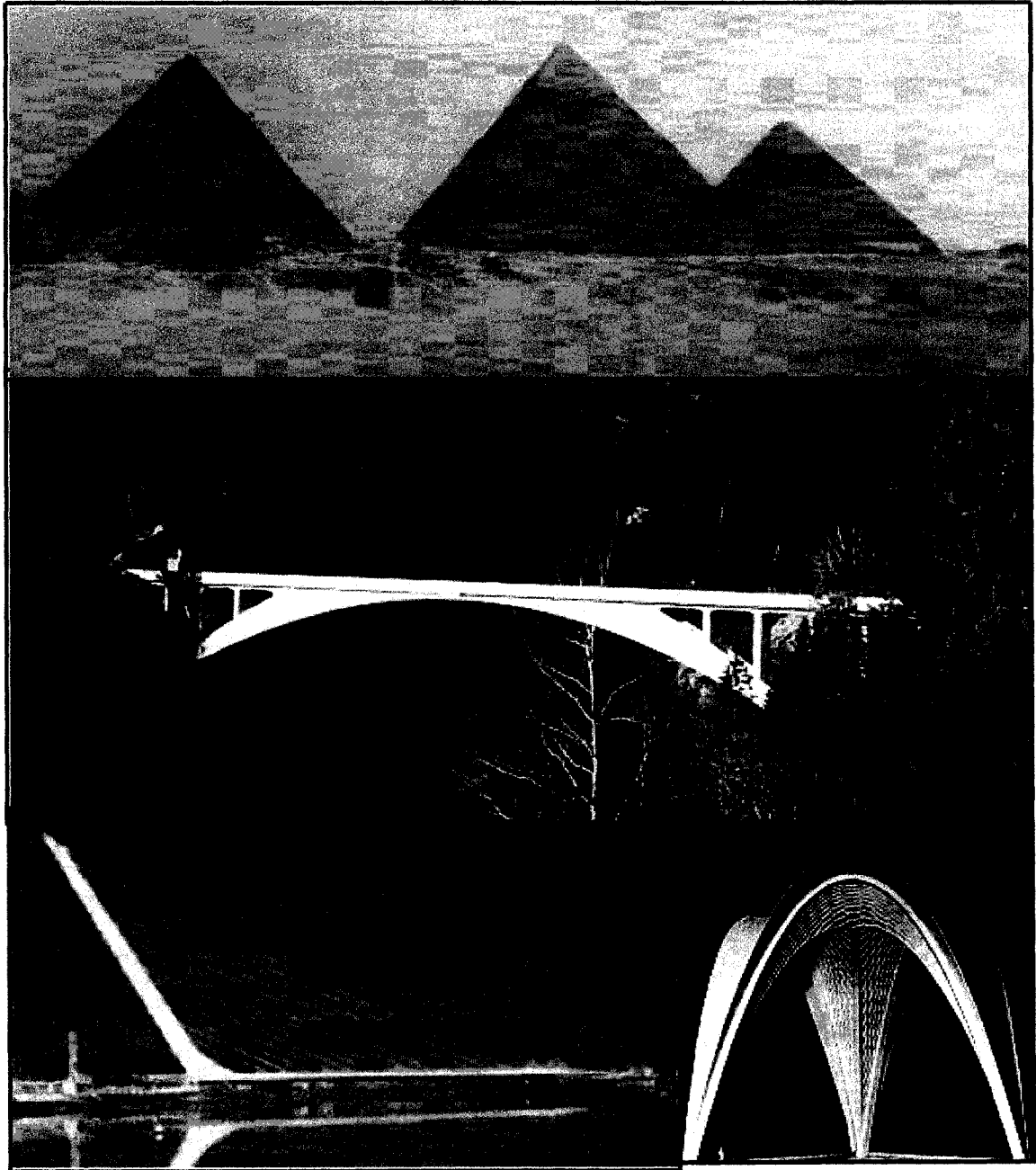


**Figure 1: Examples of Ancient and Modern Monuments.**

(From Top) The Pyramids of Giza, The Salginatobel Bridge by Robert Maillart, the Alamirra Bridge, by Santiago Calatrava, and a concrete archway concept by Pier Luigi Nervi (Billington 1997)

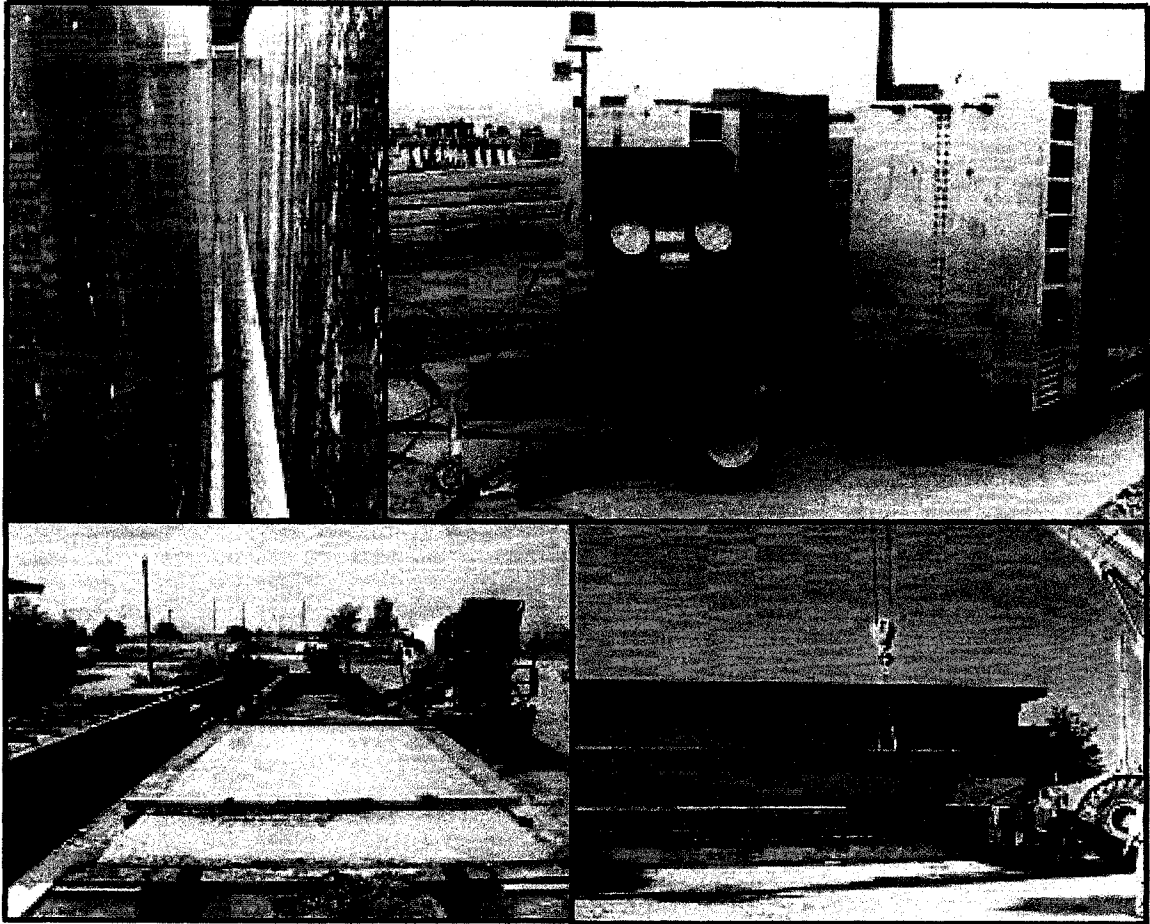


**Figure 2: Typical Procedures for Prestressing.**

Top Left: Prestressing tendons (see arrows) are installed within the formwork. Top Right: Tendons are stressing using a hydraulic jack. Bottom Left: Concrete is poured into formwork, and allowed to cure. Bottom Right: Beam is stripped from formwork.

Prestressing of concrete members affords a number of luxuries: In addition to allowing for longer, more slender spans than plain and reinforced concrete, the presence of compressive force can be used to minimize the size of cracks that form. Architects are particularly fond of the aesthetic advantages of slender members. Improved deflection control can also be achieved.

David Billington, engineering historian and Princeton professor of engineering wrote that:

“The idea of prestressing, a product of the twentieth century, announced the single most significant new direction in structural engineering of any period in history.

It put into the hands of the designer an ability to control structural behavior at the same time as it enabled him or her – or forced him or her – to think more deeply about construction.

Moreover, the idea of prestressing opened up new possibilities for form and aesthetics. Ultimately, it is the new forms that influence the general culture, and because these forms are visual, we can expect visual artists to be the first to sense a new direction.” (Billington 2004)

It should be noted that a similar process, known as “post-tensioning” is commonly used to achieve similar properties, but is not discussed in this work. In this case, stressing of the tendons or rods occurs after the concrete has cured.

### PRESTRESSED CONCRETE INDUSTRY IN CANADA

In Canada, structural precast prestressed products such as double tee beams, of the type discussed in this work, are produced by many of the larger fabricators throughout the country. The Canadian industry is represented by the Canadian Prestressed Concrete Institute (CPCI), founded in 1961, that takes a role in organizing the industry, and promoting and providing information about prestressed concrete. Canadian prestressed concrete designers were among the first to conduct extensive research on prestressed member designs, ultimately leading to the publication of the first North American prestressed concrete handbook in 1964 by Cazaly and Huggins. (Canadian Prestressed Concrete Institute 2006) The first prestressed structure in Canada, however, was erected in 1952 in Vancouver at a time when there was still a tremendous amount of skepticism amongst Canadian engineers about the safety of prestressed structures. The first prestressed structure in the United States had only just been constructed in 1949. (CPCI 2006)

CPCI has also since published updated design manuals on a regular basis (in 1982, 1987, 1996, and the 2006 edition that was not yet published at the time of this writing), and oversees an industry supported quality assurance programme, as well as the development of texts and software design aids. (CPCI 2006) The



early design manuals were largely based on the CSA-A135-1962 Standard governing the use of prestressed concrete at that time.

### CODES AND STANDARDS

It is important that some time be devoted to clarifying the roles of Standards and Codes in the Canadian engineering community.

Codes are generally broad in scope, but are intended to have the force of law by being adopted by a provincial, territorial, or municipal authority. A standard, on the other hand, is quite specific in scope, and does not have the force of law itself unless adopted by a particular code. (National Research Council 2005) As an example, the National Building Code of Canada (NBCC) is adopted almost universally in most jurisdictions as the Code by which buildings are to be designed and constructed. The NBCC, in turn, will reference Canadian Standards dealing with requirements for material properties and construction methods. CAN/CSA A23.4, for example, deals with the materials and construction practices for precast concrete. In addition, most specifications for Canadian construction projects will explicitly reference Canadian Standards in their language when used to procure materials.

In the case of the Canadian prestressed concrete industry, a broad range of standards applies to the materials and practices employed, summarized in Figure 3. However, in general, a prestressed member will be designed according to the loads set out in either the NBCC (or the Canadian Highway Bridge Design Code (CHBDC), in the case of bridges). The materials and practices employed therein, from the concrete ingredients to the reinforcement to the quality control, are set out in various standards.

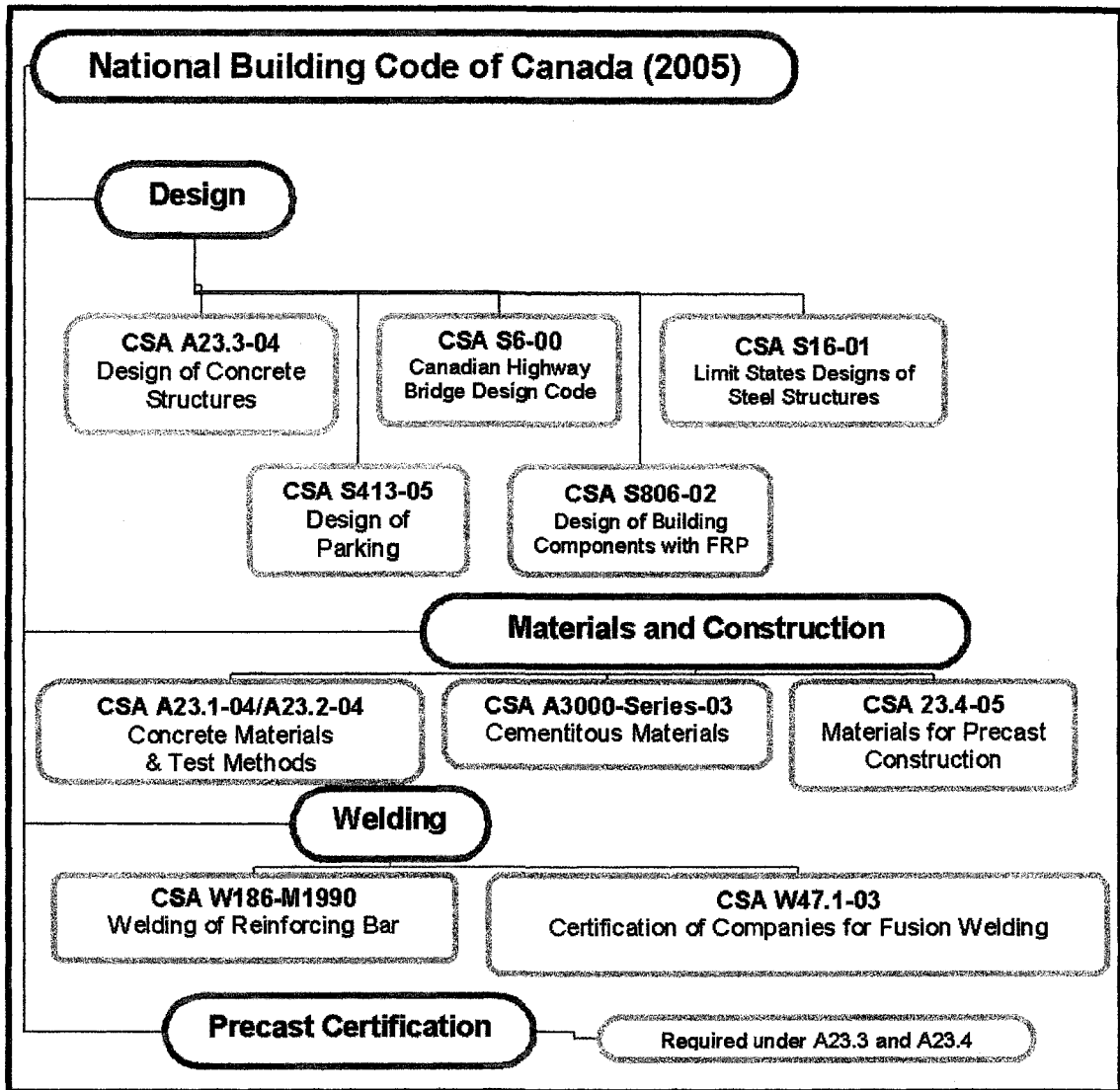


**Figure 3:** Codes and Standards Applicable to Modern Prestressed Concrete Production (Adapted from CPCI 2005)

### PRESTRESSED CONCRETE INDUSTRY IN THE UNITED STATES

The Prestressed Concrete Institute (PCI) is United States' equivalent of CPCI. The two organizations cooperate extensively with each other given the similarities in practices and applications between the United States and Canada. The most notable exception is the continued use of imperial units in the United States, and the slow adoption of Limit States Design methods. The first PCI

design handbook was published in 1971. Much of the research contributing to the development of the practices in this manual was completed in Canada during the mid- to late-1960s. (PCI 1971)

While the individual methods of design differ slightly, the end products produced are generally quite similar in design.

### DAPPED ENDS

As the focus of this Work is upon the particulars of a connection design for dapped-ended members, some understanding of the anatomy and nomenclature of dapped ends is necessary.

Building construction using precast beams can be thought of as a system in which floors are made up of single- or double-tee beams. These beams then carry their loads to columns either directly or through other members that connect to the columns. The building services (HVAC, plumbing, wiring, etc) are typically run within the spaces between the tees. This system is often used for parking structures, office buildings, or warehouses.

In the design of the floor beams, the required depth of a beam is generally a function of the flexural loads imposed upon it. Greater loads, *in general*, necessitate deeper beams. Practically speaking, however, the use of deeper beams bearing on end becomes structurally wasteful: The inter-floor space is controlled by the depth of the beams. The resulting increased structure height results in increased structure weight, increased loadings, and ultimately cost.

The height of a structure (and hence, cost) can be reduced by bearing the floor beams at some location less than their full depth, as in shown in Figure 4. A “dapped-end” is simply an end region of a beam wherein the structural depth has been reduced by notching into the beam, as shown in Figure 5. That portion of the beam remaining is known as the “nib”, and the cut away area is known as the

“dap”. Dapped ends are commonly used not only in prestressed beams, but also in regular reinforced concrete beams, as well as in steel beams as well.

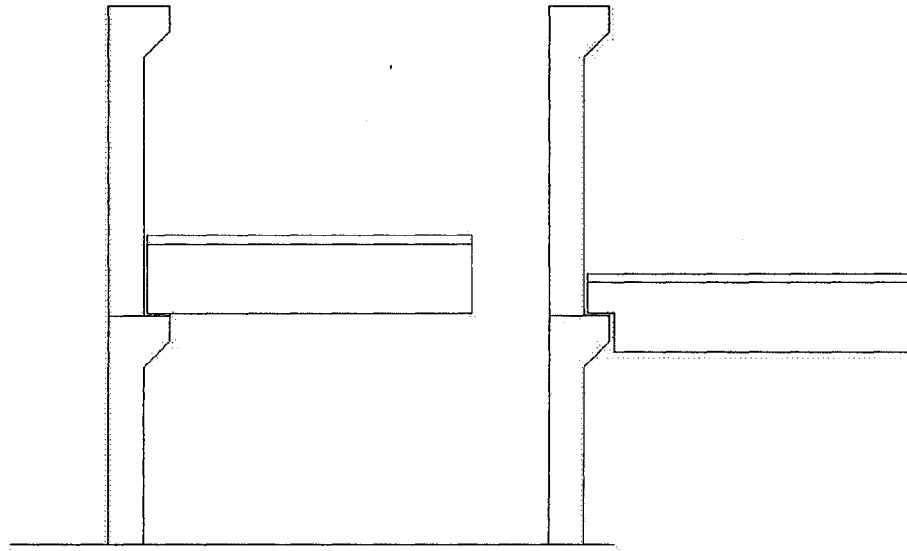


**Figure 4:** Comparison of Standard Vs. Dapped-End Beams: For a given depth of beam, usually governed by flexural design requirements, one can achieve decreased structural depths using dapped ends.

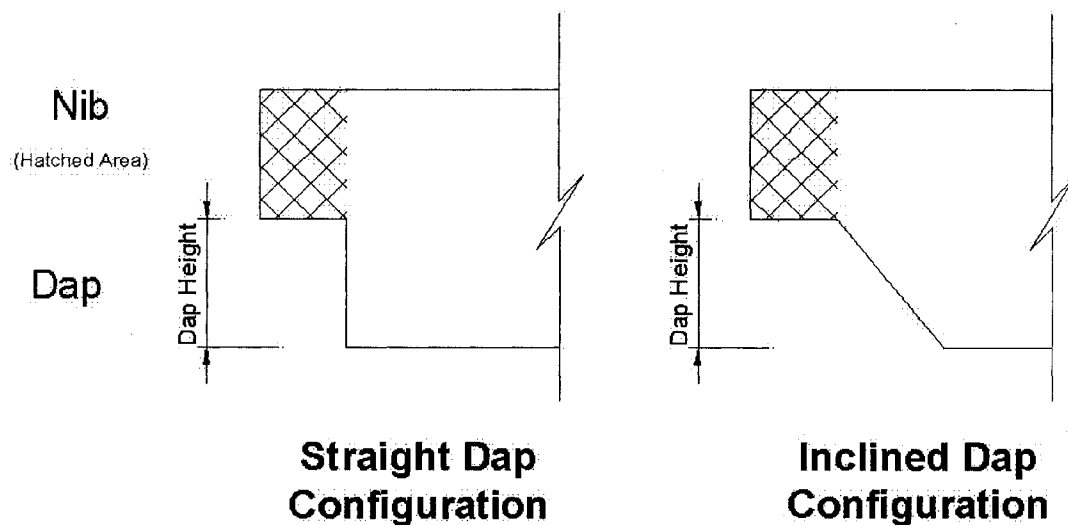


**Figure 5:** Anatomy of a Dapped End.

An additional benefit to the use of dapped end, especially when single tee beams are used, is the increased stability and safety during erection. By resting the member upon a dapped end, one effectively lowers its centre of gravity, thereby reducing the likelihood of tipping over during erection.

Generally, design practice is such that dap height does not exceed half of the member height (Mattock 1979, 1986 and MacGregor 2000). However, by nature of its design, the Cazaly hanger, subject of this work, can be used to achieve much shallower structural depths.

### CONNECTIONS AND CONNECTION DESIGN

Just as a chain is only as strong as its weakest link, so too is a structural member only as strong as its connection: The entire load that a member bears must ultimately be transferred through connections and into other members on its path to the ground.

A structural connection therefore, can be thought of as a device or assembly that transfers forces between two or more members comprising a structural system. The primary objective of connection design, then, is the safe transmission of these forces: The Designer must skillfully proportion the member and connection details so that the strengths of respective materials are not exceeded despite the many potential loads the member may experience. The practical reality of the design process, however, is that there exists the *additional* requirement that implementation of the connection design be as economical as possible. These two, often conflicting objectives, have led to the search for an *optimal* connection. In the specific instance of prestressed concrete beams, the presence of prestressing tendons and prestressing forces introduces additional geometrical constraints that must also be considered.

Numerous connection designs have been proposed for prestressed concrete beams, including the Cazaly hanger. Though the focus of this work is upon the Cazaly hanger, other connection methods will be discussed for comparison later in this work.

### B-REGIONS AND D-REGIONS

Design of concrete member details and connections is extremely dependent upon the region of the member they occupy. The stress trajectories found in a typical concrete beam differ drastically within the end and middle regions of the beam, respectively. Selection of an appropriate design methodology requires an understanding of these differences.

For purposes of choosing an appropriate design methodology, portions of beams have traditionally been classed as either B- (“beam” or “Bernoulli”) regions, or D- (“disturbed” or “discontinuity”) regions. In the case of B-regions, traditional beam theory is assumed to hold true, giving straight line strain profiles. D-regions, however, are assumed to occur where there is an abrupt change in forces or geometry, and traditional beam theory no longer applies. By St. Venant’s principle, and as a common “rule of thumb”, these regions are assumed to extend a distance equal to one member depth from the discontinuity. B- and D-regions for a typical beam are illustrated in Figure 6, below.

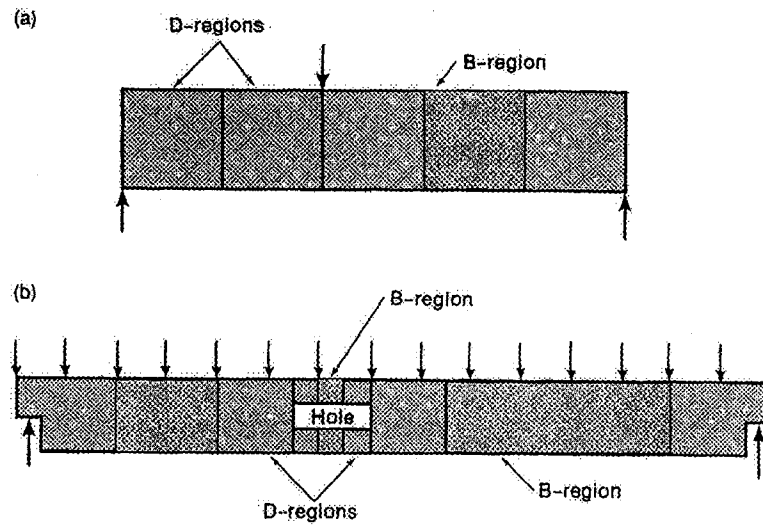


**Figure 6: B- and D- Regions in Typical Beams**

- a) Typical Beam: D-Regions extend outward a distance equal to the depth of the member from the points of application of load.
- b) Dapped-ended beam: D-Regions extend outwards a distance equal to the depth of the member from the re-entrant corners of the dap, as well as the hole through the member. (MacGregor and Bartlett 2000)

Not surprisingly, then, design of B-regions has traditionally been by conventional beam theory for flexure and various models for shear, and D-region design had been by “rule of thumb” or empirical approaches (Bartlett 2000). Early methods of Cazaly design, described subsequently, are a classic example of such an approach.

Relatively recently, a methodology for D-region design emerged from work by Schlaich et al., known as the “Strut-and-Tie Model”. This method has rapidly been assimilated by most major national structural codes and standards, including CSA-A23.3-94, which requires its use for D-region design.

## STRUT-AND-TIE MODELLING

The use of the "Strut-Tie Model" is encouraged in Canada, where it seemingly gained greater use than in the US. The technique is referenced in Clause 11.5 of CSA-A23.3-94 and is based on the work of Schlaich *et. al.*, and expanded by numerous others that followed.

MacGregor and Bartlett (2000) provide an excellent treatment of this technique. It is discussed briefly here to give context to the work that will be discussed in the subsequent literature review.

The Strut-Tie Method, or STM as it has become known, is based upon the idea that concrete, while excellent in compression, can offer little tensile capacity after it has cracked. After this point, the reinforcement is relied upon to carry these forces. Intuitively, it is obvious that this reinforcement must span zones otherwise subject to cracking. For purposes of analysis, analogous trusses for the D-region are formulated that are comprised of concrete compression struts and tensile reinforcement ties. Numerous such analogous trusses may be formulated, and in fact, each load case may require formulation and solution of a unique truss model. This concept is illustrated in Figure 7. The compression struts are shown by dashed lines, whereas the tension ties are shown as solid lines.



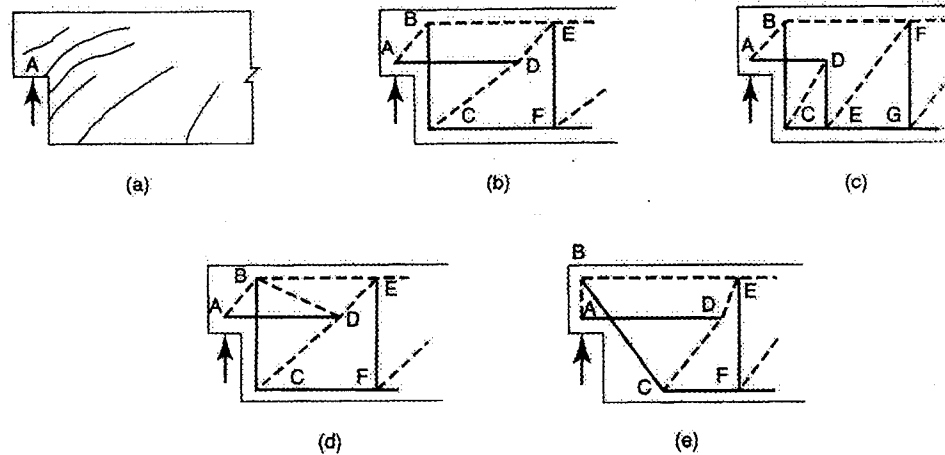


**Figure 7: Potential Strut Tie Models of a Dapped-End Beam**  
 (a) Crack patterns observed during a test of a dapped-end beam  
 (b) – (e) Potential strut-tie models for the dapped-end (Macgregor 2000)

It should be noted that connections of the type and style discussed in this work are always located in the end regions of beams, in the D-regions.

The forces in the STM components can then be evaluated through statics by realizing that these truss forces must be in equilibrium with those outside of the D-region. Once the truss models for each of the load cases are evaluated, the reinforcement scheme selected for a given area of the member is that dictated by the most severe truss model. Minimum steel areas given by CSA A23.3 still apply, however.

This is of course, a simplistic view of the STM technique: In reality, the flow of stress through a member is not accurately depicted as a straight line. The compressive forces, for example, tend to expand or “balloon” on their path to their respective nodes. This, in turn, gives rise to tensile forces which may, if not accounted for, cause a brittle failure. For a reinforced concrete member, A23.3(11.5.2.3) limits the allowable crushing strength,  $f_{cu}$ , to

$$f_{cu} = \frac{f'_c}{0.8 + 170\varepsilon_1} \leq 0.85f'_c$$

where

$$\varepsilon_1 = \varepsilon_s + (\varepsilon_s + 0.002) \cot^2 \alpha_s$$

and  $\alpha_s$  is the smallest angle between the strut and tie.

As well, additional constraints are imposed upon the geometry and reinforcement selection methods to ensure serviceability and ductility.

Presuming that both STM and PCI's approaches are correct, one should obtain similar results using either of the two methods.

### RESEARCH OBJECTIVES

This research aims to investigate concerns over the adequacy of the Cazaly hanger's performance under vertical loads. Cracking at the re-entrant corners of dapped ends is often seen due to the severe stress concentrations at this point. However, in the case of the Cazaly hanger, some concerns have arisen with respect to the opening of these cracks under service load conditions may be excessive. Moreover, the adequacy of current Cazaly hanger design practice is investigated for its contribution to this potential issue.

## **CHAPTER II**

### **REVIEW OF LITERATURE**

A proper treatment of the literature important to Cazaly hanger design requires two things: Firstly, a review of the early works that led to, and supported the development of the Cazaly hanger design, and secondly, the research surrounding the current understanding of dapped-end beams analysis. Within this latter class of literature, one must further understand the differences between reinforced concrete beams and prestressed concrete beams.

#### **CONCEPTION OF THE CAZALY HANGER**

The Cazaly Hanger was first proposed by Canadian consulting engineer Lawrence Cazaly in the 1950s, and saw its first use in January 1957 as a hanger for prestressed concrete purlins on a warehouse project. (Slater 1966) It allowed for extremely shallow structural depths to be achieved, and allowed the purlins to be hung as quickly and as cheaply as steel tie joists. By the mid 1960s, thousands of these connections had been employed successfully throughout North America. (Slater 1966)

The Cazaly hanger consists of three main elements: A steel top bar acting as a cantilever, a strap that transfers the vertical load to the bottom of the unit, and top and bottom dowels, illustrated in the figure below. The shear resistance provided by this connection is due to the shear capacity of the concrete confined by the strap, and by the dowelling action of the bottom bar.

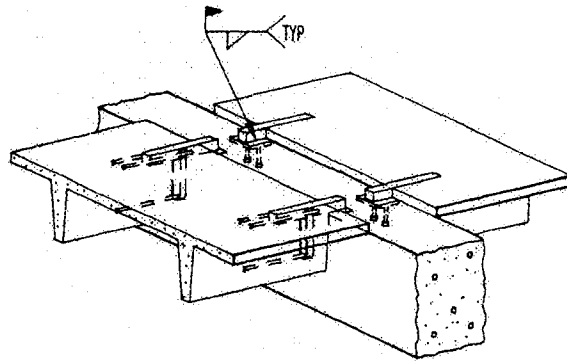
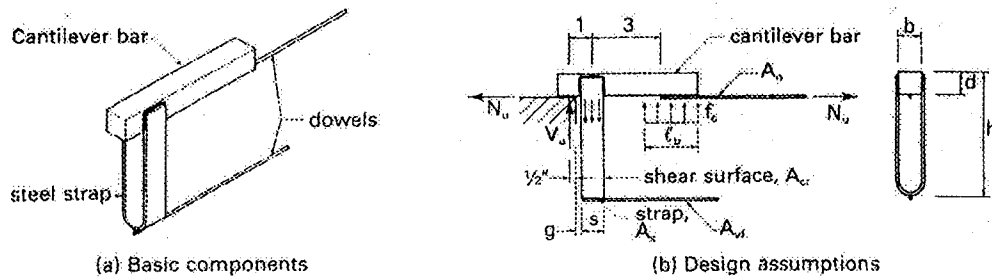


**Figure 8:** Typical Cazaly Hanger Designs

- a) Typical Method of Construction
- b) Typical Design Assumptions
- c) Typical Application

Cazaly's design was based upon empirical design methods at a time when a prestressed concrete design code had yet to be published; the industry had yet to benefit from the concepts of shear-friction and the strut-tie analogy.

The first formal recommendations on Cazaly hanger design emerged in 1964, with the publication of the first edition of the Canadian Prestressed Concrete Institute (CPCI) Prestressed Handbook, authored by Lawrence Cazaly and Michael Huggins. Yet, as late as 1965, the C.P.C.I. undertook a hanger connection research programme as their *lack of knowledge in the field of connection behaviour was [sic] handicapped by a lack of research testing...* (Slater 1966) The Cazaly hanger was the first hanger connection to be tested as part of the C.P.C.I.'s test programme. Again, the design methodology suggested by this research effort relied upon empirical design factors derived from fitting experimental data.

The test regime involved the testing of some six specimens at the University of Alberta, twenty six at the University of Toronto, and twenty at the University of Manitoba. These test specimens had dapped depths of between 250 and 860mm of which only seven beams were prestressed (the others being normally reinforced). The result was the development of an empirical factor,  $K$ , or “key factor” that equated the tensile force in the strap at failure,  $T_c$  to the area of the concrete key,  $A_c$ , concrete strength,  $f'_c$ , area of bottom bar,  $A_b$ , and shear strength of the bottom bar,  $f_v$ .

It was also discovered that should the Cazaly hanger experience any horizontal or axial forces, it would tend to pull out of the member. This mode of failure had been observed in early Cazaly hangers put into service without the top reinforcing bar. (Slater 1966) As a result, a top reinforcing bar was subsequently deemed necessary to prevent this pullout.

Extensive testing subsequently took place in 1968 at the University of Toronto in a series of tests funded by CPCI. In all, fifty two Cazaly hanger connections of varying sizes were subjected to testing in an effort to determine the behaviour of this type of connection when subjected to vertical loading. (Ife *et al.* 1968)

The Toronto series of tests gave tremendous insight into the behaviour of the Cazaly hanger under loading. Firstly, it was determined that at lower loads of perhaps 30% of the service load, the majority of the resistance of the connection resulted simply from its bond to the concrete. Additionally, the bearing area of the top cantilever was confirmed to concentrate in a small region towards the end of the cantilever bar. It should be noted that the tests in question were carried out on relatively shallow hangers which varied from 250 to 400mm in depth. (PCI 1968)

The design methodology that was adopted in early the Canadian and the current American prestressed design manuals is a reflection of this early work, but contains provisions to include the concept of shear friction.

Various authors have noted that little research was done on dapped ended beams prior to the 1970s. (Nanni 2002). Yet, throughout the 1960s, research programmes were being conducted in Canada at various institutions in an attempt to better understand the Cazaly hanger. (Slater 1966 and Ife et al. 1968)

### **PCI DESIGN METHODOLOGY**

The design methodology proposed by the Precast Concrete Institute, the body responsible for overseeing prestressed concrete in the United States, is worthy of examination for a number of reasons. Most importantly, it is closely based upon, and was adapted from the early CPCI design methods. (PCI 1985)

The Cazaly hanger is designed by first assuming that the top steel bar acts as a cantilever: the design reaction,  $V_u$ , is assumed to act at a distance,  $a$ , from the strap, and the bar in turn bears against the concrete a distance  $3a$  from the strap. (The geometrical assumptions are also shown in Figure 8.) The area of steel in the strap can then be given as:

$$A_s = \frac{1.33V_u}{\phi F_y}$$

Where  $F_y$  is the yield strength of the steel and  $\phi$  is the strength reduction factor for steel, 0.9.

The bar dimensions can next be calculated. The moment arm of the cantilever is taken to originate at the centre of the base plate. From the diagram above, the joint width,  $g$ , and the concrete cover,  $c$ , can be assumed to contribute to the length of the moment arm. Thus, the moment is given as:

$$M_u = V_u a = V_u (0.5l_p + g + c + 0.5s)$$

where  $s$  is the width of the strap.

Assuming elastic moment, the bar can conservatively be sized for a width,  $b$ , and depth,  $d$ , of

$$bd^2 = \frac{6M_u}{\phi F_y}$$

The total length of the bar must, of course, be a minimum of

$$0.5l_p + a + 3a + 0.5l_b$$

The concrete at the end of the cantilever must then be checked for sufficient bearing resistance. The ultimate allowable bearing resistance is given by PCI to be:

$$f_{bu} = 0.85\phi f'_c \sqrt{\frac{b_1}{b}} \leq 1.2f'_c$$

And the bearing length to be

$$l_b = \frac{V_u / 3}{bf_{bu}}$$

The top longitudinal dowel or dowels can next be designed by assuming them to resist the entire horizontal or axial component of force that might be present on the hanger assembly. This axial component,  $N_u$ , is generally assumed conservatively to be 20% of the vertical factored reaction. The area of the top longitudinal dowels can then be given as:

$$A_{net} = \frac{N_u}{\phi f_y}$$

where  $\phi$  is the strength reduction factor for reinforcing steel.

The lower dowels are proportioned by applying the shear friction theory:

$$A_{vf} = \frac{1.33V_u}{\phi f_y \mu_e}$$

where  $\mu_e$  is a friction coefficient that is a function of the geometrical and material properties of the member.

Welds connecting the strap to the top cantilever bar and the dowels to the strap and bar, respectively, are designed in accordance with appropriate welding codes or standards. In Canada, applicable standards include CAN/CSA S16 for the proportioning of the steel itself, and CAN/CSA W47.1, for the weld design, as well as CAN/CSA W186 for the weld to the reinforcing bar. The standards of the American Welding Society are applicable in the United States.

#### PRACTICAL CONSIDERATIONS:

A number of issues of practical importance were revealed through the various test programmes conducted on the Cazaly hanger. Firstly, accurate dimensional controls are especially important for this type of connection. Even slight increases in the joint spacing,  $g$ , or the cover,  $c$ , can rapidly result in increases to the connection stresses. Further, the bearing plate on which the top bar rests must be level in both directions: A seat tilted in the axial plane of the member will have the effect of increasing the eccentricity of the connection, thereby increasing the stresses. A seat tilted in the transverse member direction will have the effect of producing un-equal strap forces in the connection. (Slater 1966).

Additionally, given the thickness of steel generally required in the top cantilever bar, care should be given to sufficiently pre-heat the bar prior to welding the strap or the dowels. Failure to properly do so could likely result in premature failure of the welded connection. (Early literature concerning Cazaly hanger research speaks of weld failures-though they were not attributed directly to a lack of preheating.)



Additional consideration should be given to the presence of the prestressing forces. At the end regions of the beams, the forces from the prestressing tendons distribute themselves within the concrete over a distance of about 50 tendon diameters. This added compressive force can be beneficial to the development of rebar pullout capacity and shear resistance, but is not generally relied upon for design.

### **STRUT-TIE MODELLING**

Some discussion should be devoted to the use of strut-tie modeling (STM) for Cazaly hangers. The STM has gained tremendous support for the analysis of D- or disturbed regions. It has been demonstrated to be useful for other types of dapped end designs, but this author wishes to highlight its difficulty for use in Cazaly hanger design. Referring back to Figure 7, it is evident that to successfully formulate a model for the Cazaly hanger would involve passing theoretical truss members through the top cantilever bar to satisfy the equilibrium of the truss. Solving for this design using the strut-tie method would be more intensive and offer few benefits over the existing PCI methodology.

### **LITERATURE SURROUNDING ALTERNATE CONNECTION METHODS**

The Cazaly hanger is but one of many connection designs commonly employed. Numerous researchers have proposed alternative connections, some of which will be discussed briefly here.

The "Loov Hanger", proposed shortly after the Cazaly Hanger came into use and shown in Figure 9 below, was proposed by Robert Loov of the University of Alberta (Loov 1968). The Loov hanger, like the Cazaly, facilitates attaining extremely shallow structural depths. However, Loov recognized the weakness of previous hanger designs under axial loading, and detailed the connection to

resist axial loading through the addition of the top reinforcing bar. (The addition of the top reinforcing bar to the initial Cazaly design corrected this problem in Cazaly hangers.)

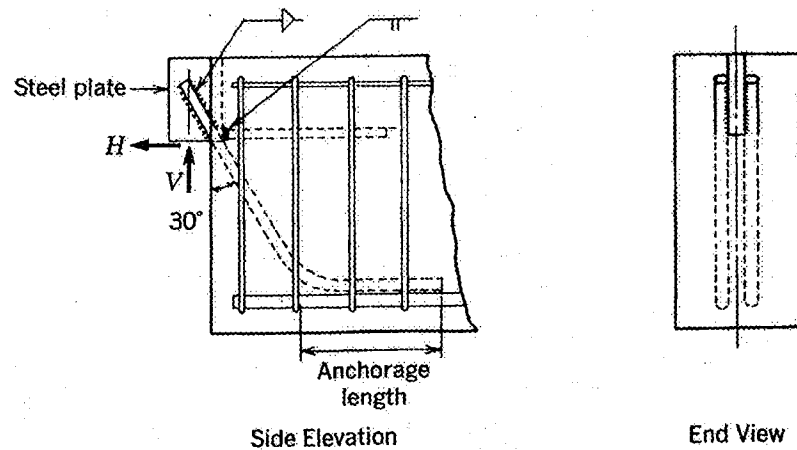


**Figure 9:** Typical Loov Hanger Connection (Libby 1977)

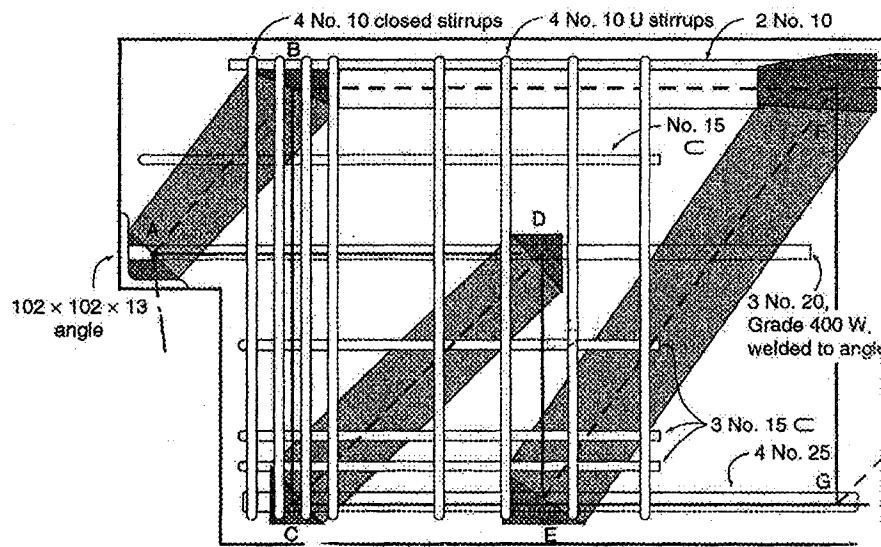
Both the Cazaly and Loov hangers are similar in terms of the assumptions of their basic behavioural mechanics. From Figure 9 it can be seen that the Loov hanger essentially does away with the forward-most portion of the top cantilever bar common to the Cazaly, and replaces it with a top reinforcing bar. Shear resistance is then largely provided by the diagonal reinforcing bar, which acts analogously to the strap in the Cazaly hanger. Component proportioning for the Loov is obtained through basic statics and code-specified bar resistances.

The Loov is notable because it was proposed as an “economical” alternative to the Cazaly. (Libby 1977) This assertion was based upon it weighing approximately half as much as similar Cazaly connections, and requiring less fabrication. (Loov 1968) However, the Loov hanger, in general, is not as easy to position within the precast form as the Cazaly is. Therefore, the decreased material costs associated with the Loov may be offset to a great extent by increased labour requirements. However, this hanger remains a viable and often used alternative to the Cazaly hanger, and has been included in both the CPCI

and PCI design handbooks. Again, many of the design equations outlined in the earliest work for this hanger were empirically derived.

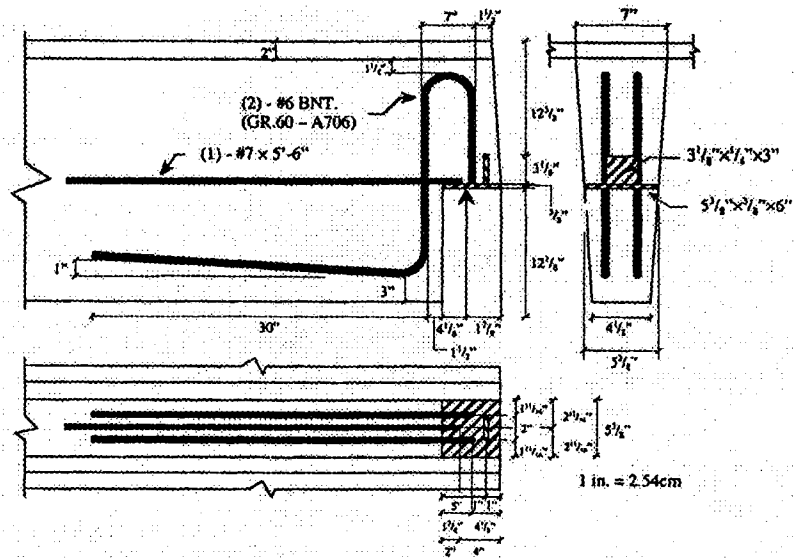
Another advantage of the Loov hanger is the ability to drape a prestressing tendon vertically through the hanger: Subsequent research programmes found that draping approximately 50% of the pre-stressing tendon through the nib would minimize the opening of re-entrant corner cracks.

A number of designs for other hanger connections for dapped-end beams have emerged over the years, often as minor variations on previous designs. One potential connection scheme is shown in Figure 10. The strut-tie model giving rise to this design is also shown.



**Figure 10:** Dapped-End Reinforcement Scheme

More recently, Nanni and Huang (2002) proposed another variant on the dapped end connection, shown in Figure 11.

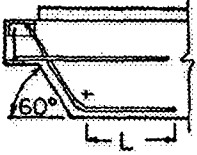
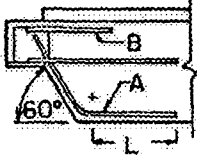
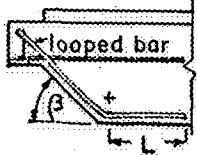
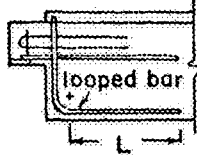
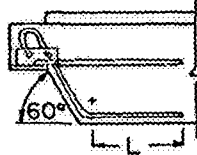


**Figure 11:** Reinforcement scheme proposed by Nanni and Huang (2002)

When examined against the potential crack patterns typically observed in dapped-end beams (Figure 7a), one can see the logic of the design. The top “rounded” portion of the bar intersects the crack planes normally present in the nib region of the dapped-end, where a compression strut exists (See Figure 7b). The horizontal bar at the plane of the bearing seat serves to deal with axial forces in the same manner that early studies recommended for the Cazaly and other hanger connections. Again, examining the figure reveals that the bottom bar intersects the crack plane associated with diagonal tension crack.

A research programme undertaken on behalf of PCI by the University of Washington in 1986 investigated five different types of hanger connections. Although the Cazaly hanger connection was not directly investigated, a modified version bearing many of the same key characteristics as the Cazaly was part of this investigation. Schematics of the hanger connections examined are shown in Figure 12. Hanger method 4, shown below, employs reinforcing steel rods (rebar) in place of the Cazaly’s more typical strap and solid top cantilever bar. The most notable difference is that the rebar acts by the bond developed between it and the concrete, whereas the steel in the Cazaly strap acts by

forming a shear key. Only a small resistance is developed as a result of bonding between the concrete and the strap, and it cannot be relied upon after cracking has occurred. (Mattock 1986a,b). However, overall the design conclusions obtained therein are generally applicable to Cazaly hanger design.

Reinforcement Scheme	Specimen Type				
	A	B	C	D	E
	$L = l_d$ Draped strand	$L = 1.7l_d$ Draped strand	$L = 1.7l_d$ No strand in nib	$L = 1.7l_d$ Draped strand	$L = 1.7l_d$ Draped strand
1A	1B	1C	—	—	
	2A	2B	2C	2D	—
		Bar B omitted	Bar B omitted	Bar B omitted. Cover to A increased.	
	—	3B	3C	3D	3E
		$\beta = 45^\circ$	$\beta = 45^\circ$	$\beta = 60^\circ$	$\beta = 90^\circ$ Slope of bar = $45^\circ$
	—	4B	4C	—	—
	—	5B	—	—	—

**Figure 12:** Hangers designs examined in the 1986 PCI Research Programme (Mattock 1986b)

The specimens examined in the PCI study were beams of only 460mm depth, using concrete of approximately 35MPa specified strength. Both straight and

draped prestressing tendon orientations were examined. A more detailed schematic of the vertical hanger tested can be seen in Figure 13. The authors of the PCI study acknowledge that it is more difficult to accurately locate and maintain reinforcement during casting using this method.

The PCI research programme identified hangers with vertical reinforcement as having poor performance at service loads owing to excessive cracking. A small improvement in performance was obtained by draping approximately 50% of the prestressing tendons through the nib. In fact, this was one of the key recommendations from the testing programme to improve both serviceability cracking and shear capacity. Whereas this may have been possible in the connections tested in the programme, this is very difficult to do when the Cazaly hanger employs a solid top bar.

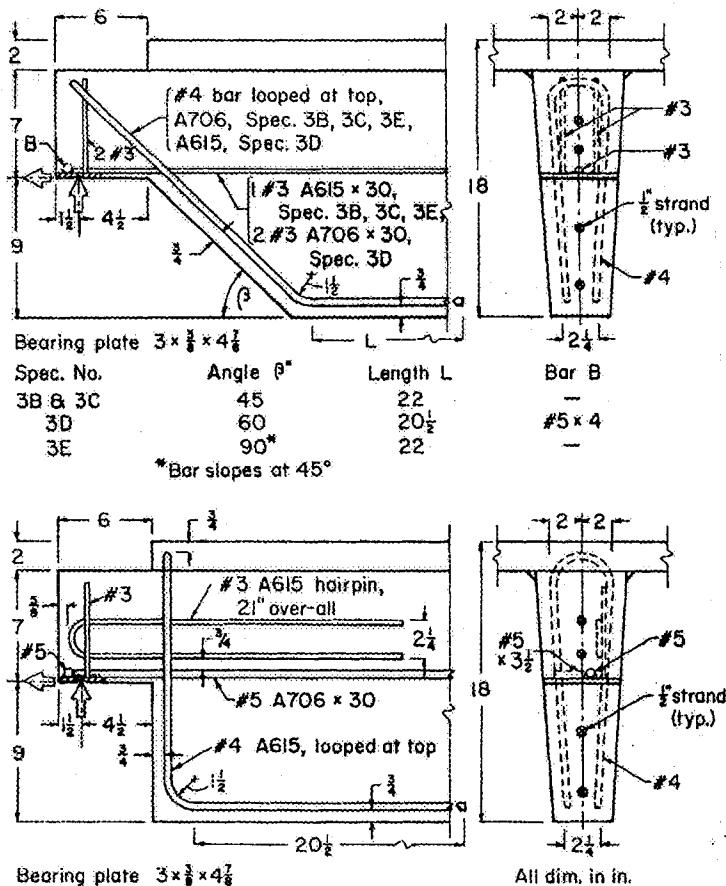


Figure 13: Hanger "Type 4" tested by PCI (Mattock 1986b)

Cracking during the tests of each of these hangers began at the re-entrant corner, and progressed upwards to the web-flange junction. Ultimate failure resulted from the formation of a diagonal tension crack, which was accompanied in some cases by diagonal compression crushing of the concrete in the lower part of the web. Web flexural cracks were evident beginning at about 85% of the ultimate load.

A variant of the vertical hanger using looped rebar using a single bar with a steel plate welded to the bottom is also mentioned by the PCI Report authors as having been used by one manufacturer at the time. However, no testing was completed on this variant.

### **LITERATURE REGARDING STRUT-TIE MODELLING AND END-REGIONS OF BEAMS**

The work of Werner and Dilger (1973) is notable in that it verified computationally and experimentally that the shear force initiating formation of cracks at the re-entrant corner of the dap was equal in magnitude to the shear strength of concrete. Their work involved studies of prestressed concrete beams in shear, employing a variety of reinforcement schemes. Various recommended design details resulted from their work.

Mattock and Theryo (1986) published a summary of the testing programme undertaken by PCI, although the Cazaly hanger itself was not tested. Numerous recommendations for dapped-end reinforcement schemes resulting from the PCI programme, some of which are equally relevant to Cazaly design. The study involved thin-stemmed members (such as double tees) subjected to shear and tension at the bearing plate of the connection. Most notably:

- That the horizontal extension of hanger reinforcement in the bottom of the web should be 1.7 times the specified development length of the reinforcing bar.

- That reinforcement schemes using inclined hanger reinforcement provide better control of cracks than do vertical reinforcement, especially if prestressing strands are terminated at the end face of the beam.
- That hanger reinforcement should be concentric about the centreline of the web, and that special care should be taken to ensure adequate cover to the lower reinforcement and its horizontal extension.
- That in most specimens, it was not possible to develop the full shear strength of the beam greater than the diagonal tension cracking shear using web reinforcement. (Tests by Aswad *et al.* (2004) would later recommend that omitting the web reinforcement in double tees was acceptable.)

For all of the beams tested, crack formation initiated at the re-entrant corner of the dap, and propagated upwards towards the flange. The patterns of subsequent cracks appeared to be dependent, largely, upon the reinforcement schemes selected; in all cases, again, the critical (failure initiating) crack was the diagonal tension crack.

The importance of extending the reinforcement to ensure ductility was also previously discussed by Slater (1966) in his summary of the CPCI's Canadian testing programme. With respect to the Cazaly hanger, this becomes especially important for a number of reasons that will subsequently be discussed.

The conclusion regarding the use of sloped or inclined reinforcement is also significant. The typical Cazaly design employs a steel strap oriented vertically that is essentially responsible for developing a shear key, but offers no inclined reinforcement of the type noted by Mattock and Theryo (1986). The result is a difficulty in controlling cracks, as will also be discussed subsequently.



Tuan *et al.* (2004) also explored end zone reinforcement schemes in prestressed concrete girders in an attempt to develop a reinforcement scheme using less reinforcement while still maintaining adequate crack control. They explored a variety of other methods of end zone analysis including the work of Gergely and Sozen (1967), and the strut-tie method, ultimately concluding that the Gergely-Sozen model was most practical.

Tuan *et al.* note that the strut-tie method does not itself require compatibility of deformations or strains be satisfied, and note that it is analysed at the strength limit state. One must intentionally limit the steel stresses to a level below that which would create undesirable crack widths (140-160MPa). They further conclude that because of the multitude of analogous trusses that may be formulated, and because it presumes concrete tension is non-existent, the solutions derived may be overly conservative.

The Gergely-Sozen model favoured by Tuan *et al.* involves solving for equilibrium on a stress distribution that develops after horizontal cracks have formed.

A number of other potential models for dapped-end analysis have been proposed, including that of Lin *et al.* (2003) and Wang and Guo (2005), but offer little practical benefit to end zone design. Lin *et al.* propose the use of a “softened strut-tie model”, which while shown to be more accurate under the sample set of members tested, is more computationally intensive and complex than the strut-tie method itself. It should be noted that for both of the aforementioned studies, the connections were not of the Cazaly type.

## CHAPTER III

### TESTING PROGRAMME

#### **OVERVIEW:**

As was noted in the review of literature, the early work contributing to the development of the current Cazaly hanger design methodology was, in large part, based upon lab-scale tests of relatively short span beams. In addition, the depths of these beams specimens were shallower than the depths of those beams regularly employed in modern structures. Concrete strengths have also since increased.

An experimental study on a full-scale specimen and two scaled specimens was undertaken to study the performance and mechanics of load sharing at the dap end of the Cazaly hanger. Due to the loads involved and concerns over worker safety, the full scale specimen could not be loaded to failure, whereas specimens tested in the lab were loaded to failure.

#### **FULL SCALE TEST PROGRAMME**

A full-scale double-tee beam was tested under service load. Both ends of the beam were tested so as to maximize the use of the full scale specimen. The tests on this full-scale beam provided the opportunity to subject the specimen to loading similar to that which would occur during transportation of the beam to a job site. The intended factored design reaction of the beam was 486kN per stem, or 972kN per side. As such, each Cazaly hanger was designed for a vertical reaction load of 486kN and a horizontal reaction of 97kN.

Details of the Cazaly hanger fabrication and test setup are described in greater detail, below.

## SPECIMEN GEOMETRY & FABRICATION

The double tee used in the full scale test was 1219mm high x 2777mm wide and approximately 25160mm long, weighing some 39, 500kg. The cross section with tendon spacing and release sequence is shown in Figure 14. Full scale fabrication drawings are provided in Appendix A. A beam of this size is representative of the size and capacity commonly used on the floors and roofs of institutional and commercial buildings.

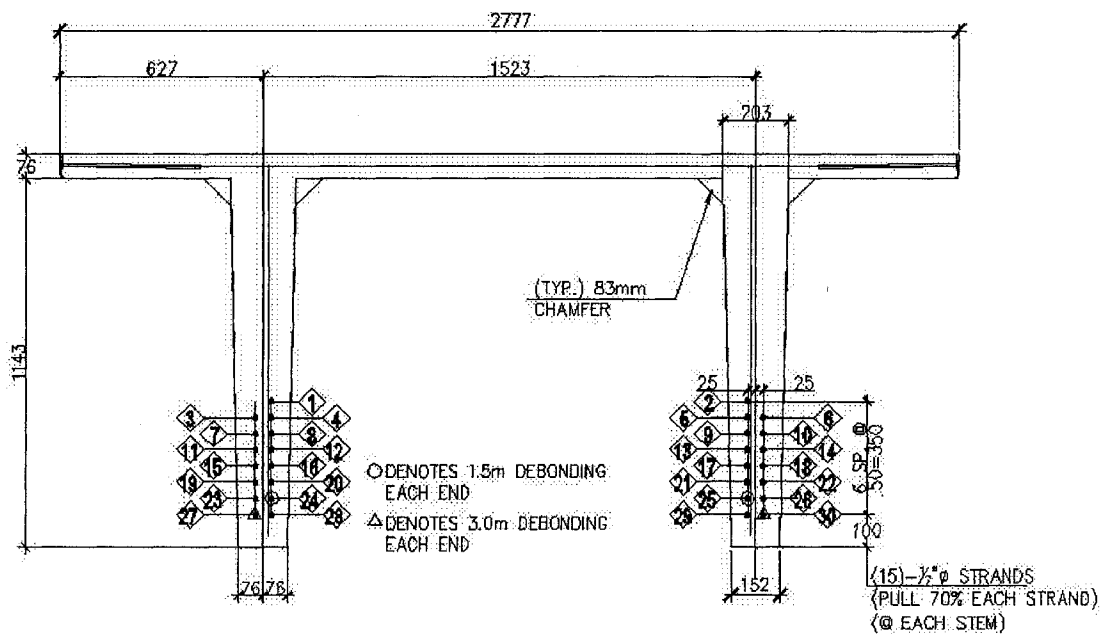


**Figure 14:** Cross section of the Full Scale Specimen showing tendon locations

The Cazaly hanger was embedded in the beam as shown in Figure 15. Referring to the description of Cazaly hanger design in previous chapters, the individual components of the Cazaly hanger were sized according to the calculations in Appendix A.

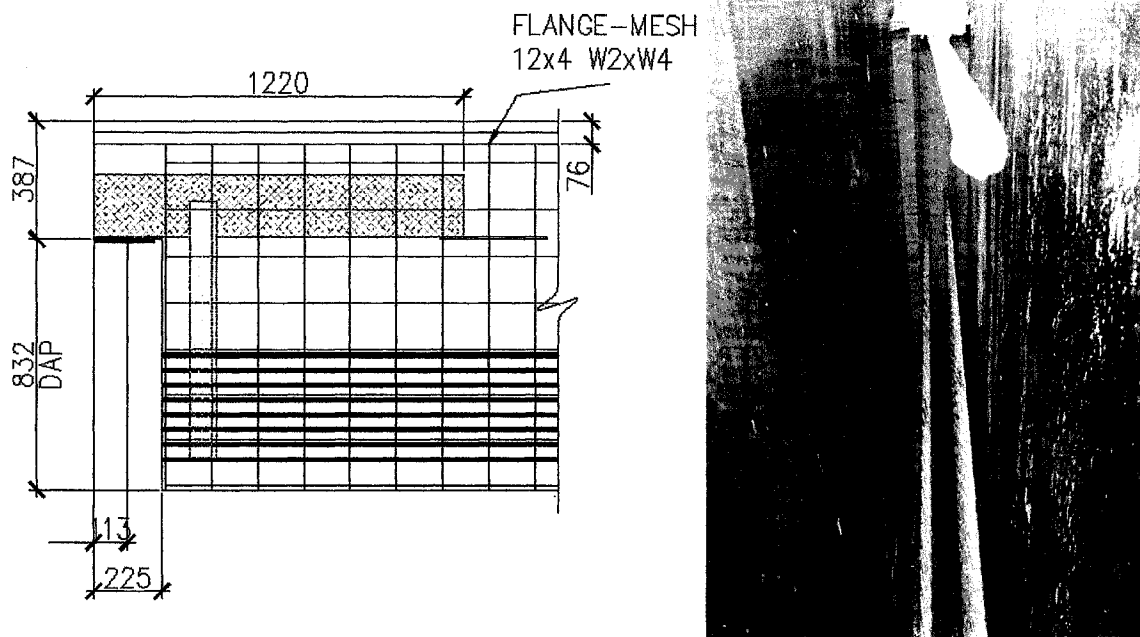


**Figure 15:** Elevation Drawing (Left) and Head On View (Right) Showing Cazaly Hanger

The pre-stressing hardware consisted of fifteen (15) 12.7mm diameter prestressing strands per stem (30 overall) pulled to 70% of ultimate ( $0.70f_{pu}$ ), or 1.75MN per stem. To control stresses at the ends of the beam, the lower tendons were de-bonded for lengths of 1.5 and 3m respectively, as shown in the fabrication drawings in Appendix A. The tendons are visible in Figure 15 as well.

Wire mesh reinforcement was used to further reinforce the stem and flange of the beam (Figure 16).

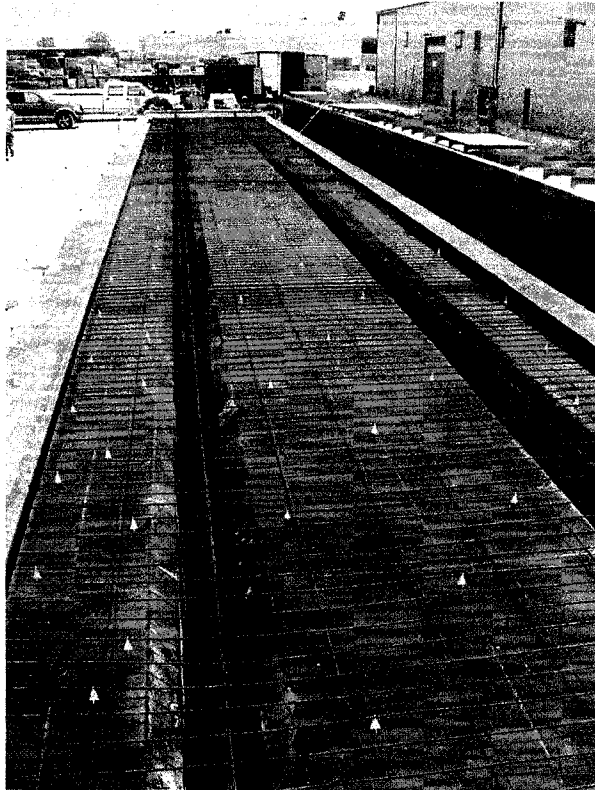


**Figure 16: Wire Mesh Reinforcement on Flanges**

The concrete mix design employed for this beam specified initial concrete strength at transfer,  $f'_{ci}$ , of 28.0MPa, and a 28 day concrete strength,  $f'_c$ , of 48MPa. Air entrainment was specified at  $5\% \pm 1\%$ , and slump was maintained at 230mm through the use of water reducing admixtures. Concrete properties were assured by both in-house by PSI, and by an independent third-party CSA A283 Certified testing laboratory, AMEC Testing Labs, located in Windsor. The results of concrete testing are reported in Table 1 and Appendix A.

**Table 1: Concrete Testing Results-Full Scale Test**

Concrete Test Results - Full Scale Beam		
Specified Strength	F'ci = 28, F'c = 48	MPa
Sample ID	Strength [MPa]	Type
PSI QC	28.0	1 Day @ transfer

AMEC 801	39.6	7 Day
AMEC 802	43.7	14 Day
AMEC 803	48.1	28 Day
AMEC 804	48.1	28 Day
Entrained Air	7%	
Measured Slump	235mm	

The tendons were released 24 hours after casting, and the ends cut flush with the end of the beam. Subsequently, the beam was stripped from the form using two cranes, and temporarily stored on timber bunking. Some cracks were noted immediately after stripping, owing to the stresses of stripping, as well as bursting stresses caused by the tensioning force.

A great deal of effort was made to ensure that the full scale beam, as tested, represented a "real world" design of a double tee beam. The beam itself, as well as all pre-stressing materials, hardware, fabrications, and connections are an exact duplicate of similar beams commonly used buildings.

### **SIMULATED TRANSPORTATION DAMAGE TEST**

Prestressed concrete beams are typically cast at a production facility and then transported to the construction site. Thus, the objective of this test was to simulate the cracks and other damages that may occur due to the transportation of these beams.

As noted previously, this study was undertaken in tandem with a proprietary research programme conducted by PSI. As part of this programme, it was necessary to subject the test specimen to a road trip to simulate transportation loading. This added loading would, in theory, cause some micro cracking which would cause a transported beam to behave slightly differently than a non-

transported beam. This presented a unique opportunity to test a specimen that very closely approximated *in situ* conditions.

A specimen of this size, due to its length and weight, must be transported on specialized trailers. Due to dimensional and axle loading requirements in Ontario, it was necessary to employ a specialized rear-steer carriage for transporting this beam. During transport, the beam itself forms part of the trailer assembly, with the rear dolly simply clamping to the beam. For navigating around intersections, corners, and high-way off ramps, a hydraulically driven rear-steering feature is used on the rear dolly. This is illustrated in Figure 17.

The road trip took place 2 days after stripping the beam from its form, and involved a total round-trip distance of approximately 200km. It was anticipated that this distance accurately reflects the distance and road conditions that most beams are transported to jobsites.



**Figure 17: Preparation for Road Test**  
Top: Loading of test specimen onto the rear-steer dolly transporter.  
Bottom: Steering on the rear dolly being used to negotiate turn.

### **FULL SCALE TEST SETUP**

The loads necessary to produce the desired test reactions for the specimen presented unique challenges: The costs involved in constructing an outdoor reaction frame were prohibitive. Therefore, it was decided to load the specimen incrementally with solid concrete wall panels, which were in abundance at the PSI facility. A specialized reinforced concrete support ledge, shown in Figure 18, was constructed to bear the reaction of the end to be tested. A custom built load cell (described later in this chapter) was used to measure the support reactions. A rubber bearing pad separated the load cell from the steel bearing plate of the



Cazaly assembly and allowed for minor variations in fit. The opposite end of the beam bore on timber bunking.



**Figure 18:** Beam being set upon concrete support ledge

### **INSTRUMENTATION**

Due to the potential for damage in the event of a catastrophic failure, and the costs involved with instrumentation, custom-built reaction load cells were constructed and calibrated at the University of Windsor. (Calibration curves as well as design schematics are included in Appendix A. One of the load cells is shown in Figure 19. The load cells consisted of two 19mm steel plates supported on nine 25mm solid round bars. Electrical resistance strain gages were affixed with cyanoacrylate adhesive to each of the nine bars at their midpoint and wired per the schematic in Appendix A. Strain gages were supplied by Kyowa Industries, had a gage length of 10mm, and were

temperature compensated for mild steel. Strain gages were coated with protective polyurethane to allow them to resist the effects of weather for the duration of the test.



**Figure 19:** Load Cell under Nib of Beam

Strain gages were also affixed to portions of the Cazaly hanger assembly to monitor reinforcing bar strain, strap strains, and cantilever bar strains. These gages were of the same type used for the load cells, and were mounted using the same adhesive. The locations of the installed gages are noted in the Appendix, chosen so as to allow for determining the individual component forces.

Strain gages were also used to measure the strains at various locations on the concrete. Surface-mounted electrical resistance strain gages were fixed at the locations shown in the Appendix. The locations were selected so as to monitor the opening of the re-entrant corner cracks. These gages were supplied by Vishay/Measurements Group, and had a gage length of 30mm.

The longer gage length (30mm vs. 10mm used for steel) is useful when measuring concrete strains: Since concrete is not a homogeneous material, strains over a smaller area may not be representative of the true strain.

An electrical resistance embedment-style strain gage was also used near the strap region of the Cazaly hanger to measure the strains within the concrete itself. The effective gage length of this gage was 50mm.

Installation of all gages was completed in strict accordance with the respective manufacturer's recommended methods of installation.

Strain gages were connected to switch and balance units, which were in turn connected to strain measuring boxes, all manufactured by Vishay/Measurement Group. Strains were recorded in order of the gages, using the switching units to advance to the next gage measurement.

### **FULL SCALE TEST PROCEDURE**

Loading of the test specimen was accomplished by gently placing sections of 200mm thick solid concrete wall panels onto the specimen. Two sizes of wall panels were available, measuring 9.5 and 8.3m, each with a respective mass of 11 360kg and 10 000 kg. However, the actual reaction load was monitored via the load cells. Prior to placing the panels on the specimen, wooden bunking was placed at 2m and 7.6m from the end of the beam so that the points of applied loading would be outside the D-region of the beam end.

The slabs were placed onto the specimen by means of a "straddle lifter" crane, shown in Figure 20. After each load was applied, strains were allowed to stabilize for 30min or until no discernable change in strain occurred prior to taking strain readings. An addition, crack openings were measured using a crack gage and marked on the specimen.

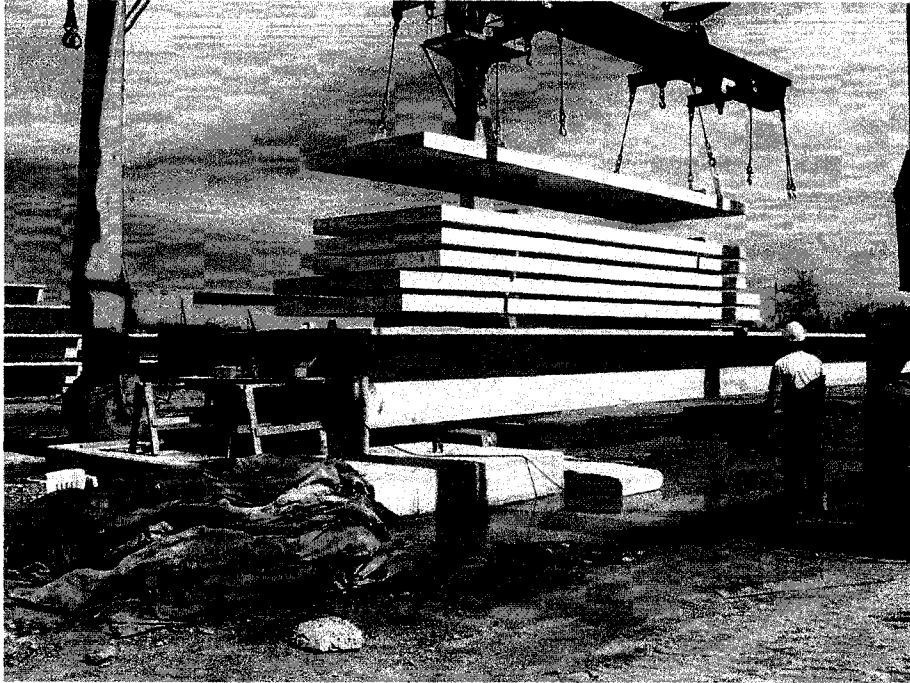


**Figure 20:** Loading of the Test Specimen

### **LAB SCALE TEST PROGRAMME**

The practical reality of selecting a specimen design for lab-scale testing was that the specimen prestressing and casting had to occur offsite (at PSI), and then be transported to the University Structures Laboratory for testing. Both the limitation of lifting capacity and the lack of proper truck access to the Structures Lab severely limited the size of sample that could be tested. Further complicating the issue was the fact that the costs of custom-building a prestressing form for this study were prohibitive. As such, it was decided to use an existing double tee form profile and strand orientation, and cut it in half to yield two single tee beams. The maximum design reaction that could be accommodated for such a specimen was equivalent to  $\frac{1}{4}$  of the design reaction of the full scale beam. This is to say that whereas each stem was sized for 486kN on the full scale beam, the lab scale beam comprised a single stem sized for a reaction of  $\frac{1}{4} \times 486\text{kN}$ , or 122kN.

To further maintain symmetry between the respective tests, the depth to dap ratio (depth: dap) on the lab scale specimen was adjusted to match that of the full scale beam, or 1.45:1.

## **SPECIMEN GEOMETRY & FABRICATION**

Following the design methodology outlined in the previous chapters, the lab scale Cazaly hanger was proportioned for a design reaction of 122kN and an axial force of 24kN, giving the design shown in Figure 21. Calculations are included in Appendix A. During fabrication of the assembly, it was ensured that the cantilever bar was preheated prior to welding the strap and rebar to it.

The cross section and layout of the lab scale specimen is shown in Figure 22 below.

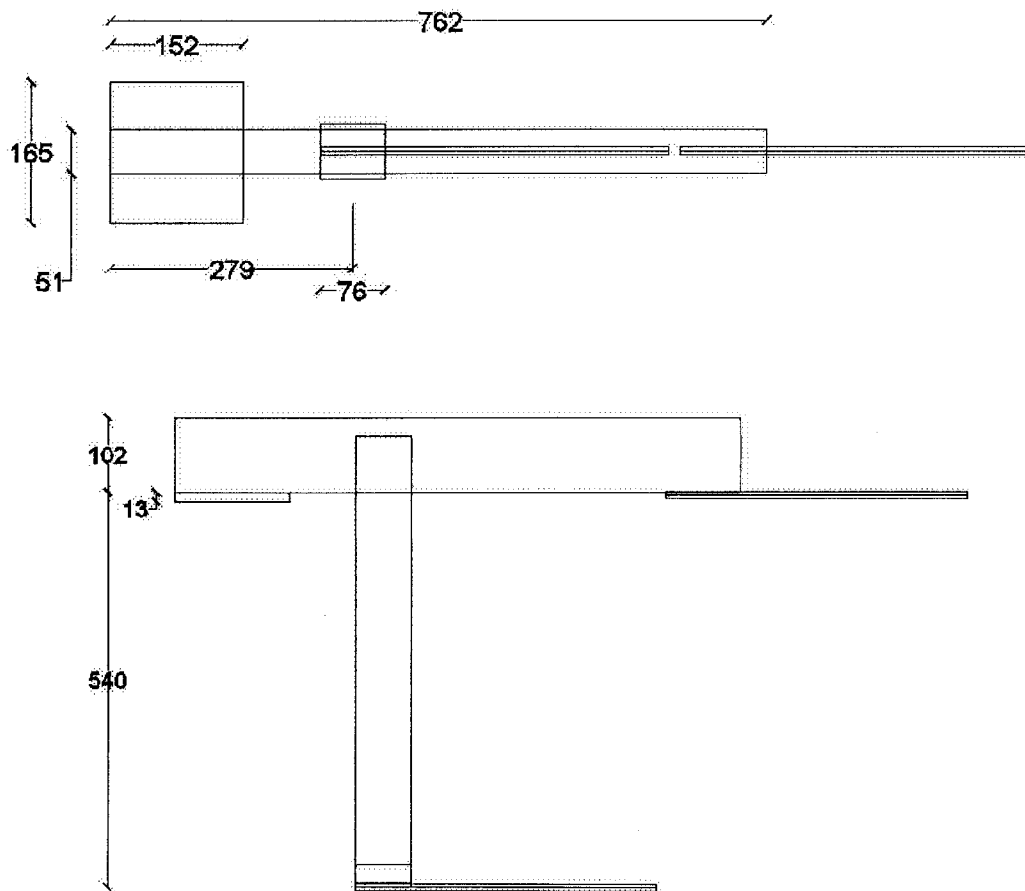


**Figure 21:** Cazaly Hangers employed in lab scale tests

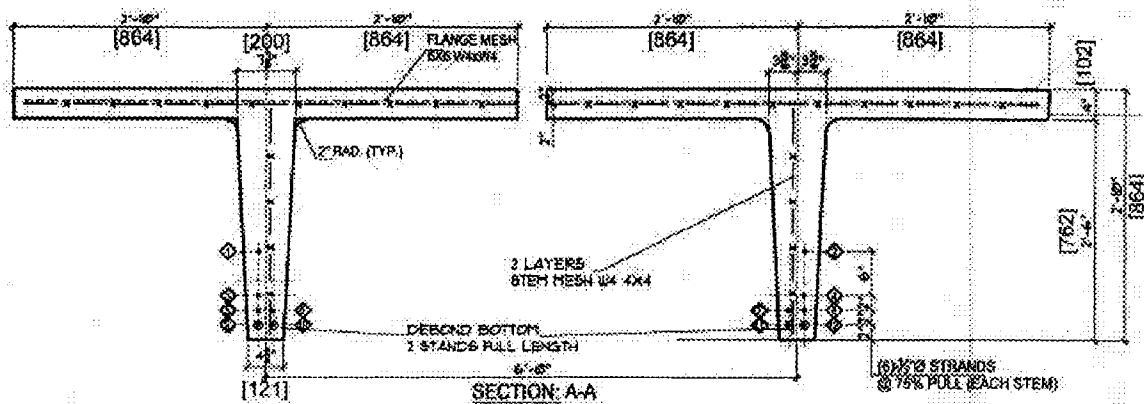


**Figure 22:** Cross Section of the Lab Scale Specimens

The concrete mix design employed for the lab scale beams was identical to that used in the full scale test, having a concrete strength at transfer,  $f'_{ci}$ , of 28.0MPa, and a 28 day concrete strength,  $f'_c$ , of 48MPa. Concrete properties at transfer were assured in-house by PSI, and the “as-tested” concrete strengths obtained from cores taken from the specimen. The concrete strengths are summarized below, in Table 2. (The method of coring and correction factors used is contained in Appendix A and is per ACI recommendations).

**Table 2: Concrete Strengths for Lab Scale Testing**

Concrete Test Results-Full Scale Beam		
Specified Strength	$F'_{ci} = 28, F'_c = 48$	Mpa
Sample ID	Strength [Mpa]	Type
PSI QC	35.9	12 Hour
Beam1-AM1	48.4	At Test*
Beam1-AM2	47.9	At Test*
Beam1-AM3	50.9	At Test*

**Note:** Values obtained from cores drilled from specimen.

## **LAB SCALE TEST SETUP**

The lab scale beams were tested at the University of Windsor's structure's lab. Loads were applied using a hydraulic jack suspended from a reaction frame (detailed drawings are included in the Appendix.) Both the applied load (from the jack), and the resulting reaction load at the Cazaly hanger were monitored using load cells connected to a Data Scan data acquisition system. (Manufactured by MSL Datascan Technology, Berkshire UK) The calibration curves for these load cells are included in the Appendix.

In a manner similar to the full scale tests, strain gages were applied to both the Cazaly hanger, and to the concrete surface. The locations of the gages differed slightly between for the second lab scale beam based upon knowledge learned of the first. Additionally, concrete embedment-style strain gages were included similar to the full scale test. The locations are shown in the Appendix.

## CHAPTER IV

### RESULTS AND DISCUSSION

#### FULL SCALE TEST RESULTS

The test specimen was inspected immediately after stripping from its formwork. A series of cracks were visible at each end owing to both the stripping process, and from the transfer of stressing forces from the tendons to the concrete. These cracks are illustrated in Figure 23.

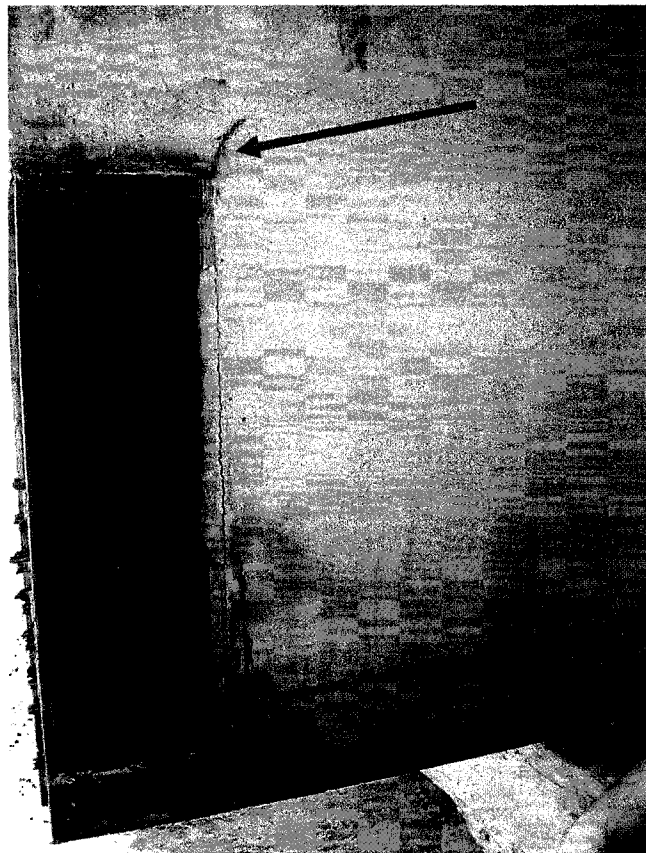


**Figure 23:** Cracking near the dap on the full scale specimen  
Lower Arrow: Cracks resulting from the stripping process  
Top Arrow: Cracks at re-entrant corner due to stressing forces

The stripping crack, illustrated above, results from the stripping process: To facilitate breaking the bond between the beam and the formwork, it must be lifted



from only one end. The force resulting from the beam being tilted out of the form results in these types of cracks.

A small hairline crack can be seen at the re-entrant corner. Over the next several weeks as the beam remained in storage, these cracks continued to propagate slightly (Figure 24). These cracks, resulting from the transfer of stresses from the tendons to the concrete in the end region of the beam, are recognized by PCI and CPCI as regularly occurring in these types of beams. (CPCI 1996 and PCI 1985)

In all, these cracks measured less than 0.4mm in width, as measured visually using a crack comparator card.



**Figure 24:** Propagation of cracks prior to stripping

## SIMULATED TRANSPORTATION TEST: QUALITATIVE RESULTS

The beam was loaded onto the specialized trailer, noted in the previous chapter. In the process of this activity, damage occurred to the concrete on the left side of the north stem of the tee, resulting in damage to one of the two strain gages affixed to the Cazaly hanger strap (lower left side strap gage).

The extents of the cracks were noted prior to loading and transporting the beam, and immediately upon its return. In all, the beam travelled some 200km over roadways representative of transport routes for most beams produced in this area. Neither the extent nor width of the cracks appeared to be appreciably affected by the transportation process itself.

### PRELOADING:

The test specimen was subjected to a “preload” to introduce some cracking into the beam. It was felt that to preload the beam resulted in conditions that more accurately emulated real world “in service” conditions of the beam. This is to say that the preloading results in some micro cracking of the concrete, resulting in a member stiffness that is slightly less than an unloaded (uncracked) beam.

This loading was completed in the manner described in the last chapter, in increments up to a total load of 30% of the design reaction, as outlined in Table 3, and shown in Figure 26. The load applied was consistent with those expected in service.

**Table 3: Preloading Increments**

Increment	Load [kN]
0	0
1	111
2	205
3	97
4*	15

\*It should be noted that although increment 4 represents zero load, this residual load is likely the result of the beam re-seating itself on its support.

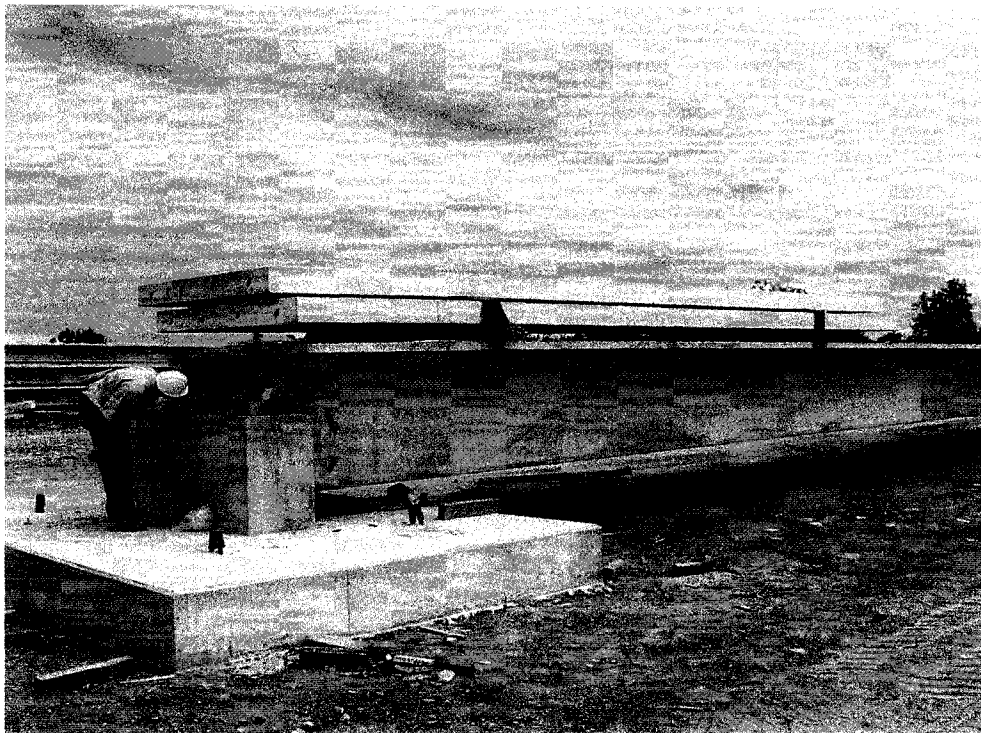


**Figure 25: Preloading of the specimen**

Under this loading regime, many of the cracks were seen to increase in width slightly. Most notably, the diagonal crack, previously 0.4mm in width, increased to 0.8mm in width.

What is interesting to note is that the top rebar, attached to the cantilever bar, actually undergoes tension even at these (relatively) low loadings. The top rebar

is likely helping the cantilever bar to resist being pulled out from the concrete. Also notable are the strains in the Cazaly straps: At loadings of approximately 200kN, these straps are seeing strains of some 150 $\mu\epsilon$ . This corresponds to a stress of approximately 30MPa and a force in each strap of approximately 40kN. The implications of this will be discussed later.

#### ULTIMATE TESTING:

Having completed the preloading, a test of the connection's ultimate capacity was attempted. As noted in the previous chapter, concerns over worker safety prevented the completion of this test. Loading continued in the increments shown in Table 4 below, to a maximum load of approximately 434kN. At this point, it was decided that the addition of further load could potentially result in a catastrophic failure, and injure those conducting the test. As such, further loading was discontinued. This final load corresponds to approximately 65% of the design reaction of the beam (664kN). The loading is also shown in Table 4, below. This decision corresponded with the opening of a diagonal crack, which opened to a width of 2-3mm. The load was allowed to remain on the specimen for many days thereafter. The cracks did not propagate further during this time. However, as worker safety was a concern, no further loading of the specimen was completed.

**Table 4: Ultimate Test Loading Increments**

Increment	Load [kN]
0	0
1	89
2	172
3	236
4	300
5	362
6	434

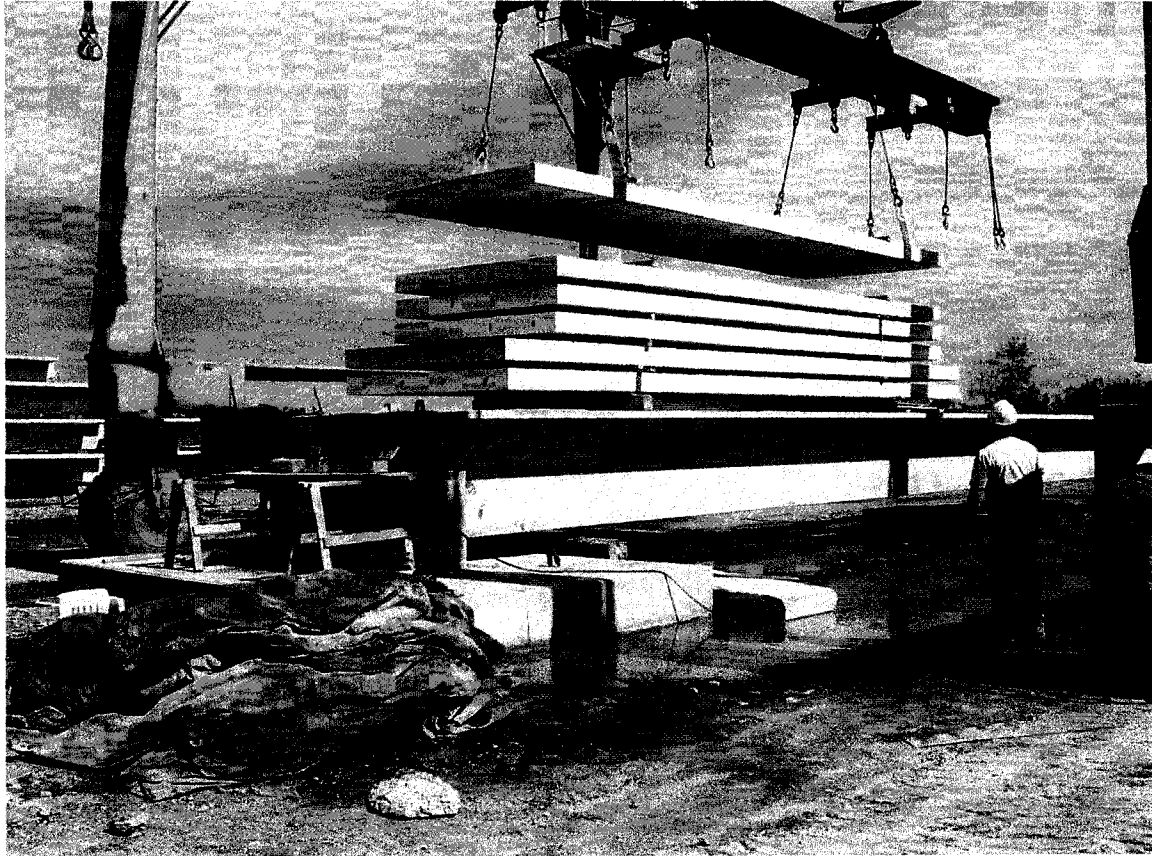


**Figure 26:** Ultimate loading of the full scale specimen

A full account of the data is given in the Appendix, but it is discussed briefly here for clarity.

At the maximum loads obtained the top cantilever bar approaches strains of approximately  $250\mu\epsilon$ . These strain values are consistent on both of the strain gages (top face and bottom face) of the cantilever bar. These correspond to a stress of approximately 50MPa. It should be noted that these stresses are measured at only one location at the middle of the cantilever bar. The lab scale models utilized stain gages at multiple locations along the top bar.

Also at these loads, the strains in the straps were between 325-400 $\mu\epsilon$  at the bottom near the welds, and 475 $\mu\epsilon$  at the midpoint. These correspond to 65-80MPa and 95MPa, respectively, for each leg of the strap.

Considering the bottom region of the strap and the stresses associated with this area, it can be inferred that the strap is carrying some 188kN of the total load at this point, or 74% of the stem load. As one travels up the strap, it can then be calculated that at midpoint, the strap is responsible for carrying some 246kN of load, or 98% of the stem load. Note that there is likely a combined axial and bending effect taking place, so these values do not represent purely tensile values.

### **LAB SCALE TEST RESULTS**

The controlled environment allowed for more accurate control of the test parameters, and allowed for more detailed observation of the test specimens' behaviour under loading. Specimens were loaded in increments of 10kN as outlined in the previous chapter, to an ultimate failure load of approximately 310kN, at which point a catastrophic failure resulted from the initiation of a diagonal shear crack from the bottom corner of the dap extending diagonally upwards to meet the flange.

Prior to loading, both lab scale specimens showed cracking at the re-entrant corner, consistent with that seen on the full scale specimen. The crack widths on the lab scale specimens were less than 0.4mm.

## **QUALITATIVE OBSERVATIONS:**

### **Test Beam 1-Qualitative Observations**

The first beam showed no visible signs of distress until approximately 70kN load, at which point cracks at the re-entrant corner began to open slightly. This crack would serve as the initiation point for some subsequent cracks. At between 100-110kN, a crack of 0.4mm width extended from the re-entrant corner to the near the stem-web interface. (This is taken near the middle of the crack. The width of the crack near its origin is, of course, larger.) This crack slowly propagated upwards upon subsequent loading. At 170kN, a diagonal crack was observed in the nib portion of the beam. At between 200 and 250kN, cracks opened significantly (from 1mm up to 2-2.5mm). At approximately 270kN, the crack at the re-entrant corner grew to be about 5mm in width. At approximately 300kN a diagonal crack appeared suddenly and a loud bang was heard with a subsequent immediate drop in the load supported. Some minor flexural cracking was also evident at the beam mid-span. Some of the concrete in the region above the bottom rebar to strap weld had spalled off, revealing the prestressing tendons and strap.

### **Test Beam 2-Qualitative Observations**

Similar to the first test specimen, there were no visible signs of distress in the specimen until approximately 70-80kN, at which point a crack opened at the re-entrant corner. These cracks were on the order of 0.1 to 0.2mm, and did not grow appreciably until about 150kN, at which point they began to progress to the flange. (This is taken near the middle of the crack. The width of the crack near its origin is, of course, larger.) At approximately 210kN, the cracks grew to about 1-2mm in width. The cracks continued to expand until about 300kN, at which point the cracks at the re-entrant corner were on the order of 5-8mm. At 310kN, two diagonal shear cracks appeared suddenly and simultaneously, intercepting strain gages CG10 and CG5. There were also a pair of vertical cracks in the

region around the bottom bar consistent with those expected of a bar pullout failure.

**QUANTITATIVE OBSERVATIONS:**

**TEST BEAM 1-QUANTITATIVE OBSERVATIONS**

In comparing the strain gage values obtained along the top cantilever bar of the Cazaly hanger, strains at maximum load range from approximately 90 $\mu\epsilon$  at Gage 1 to 1700  $\mu\epsilon$  at Gage 4. Gage 5 failed at 175kN. The strain reading at Gage 4 corresponds to a stress of approximately 340MPa. It seems reasonable, then, to conclude that yielding of the top bar has occurred between gages 4 and 5, as shown in Figure 27.

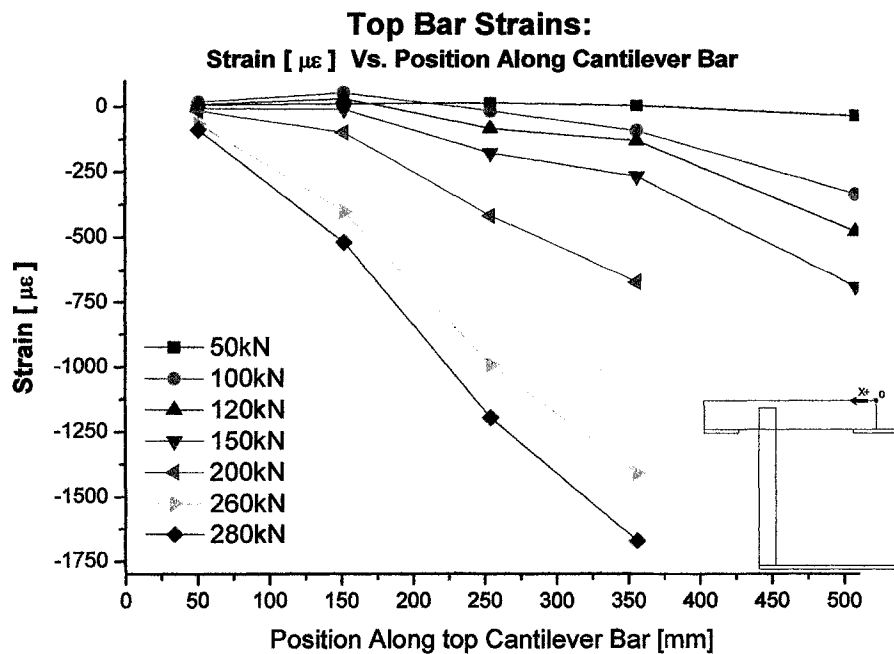


**Figure 27:** Strains along the top bar of the Cazaly hanger

Gages 6, and 7, located near the top and bottom of the strap, respectively, show strain values of approximately 1625 and 1400 $\mu\epsilon$ , corresponding to stresses of



325 and 280MPa, respectively (or 271 and 315kN). It becomes obvious that the strap is entirely responsible for carrying the load immediately prior to failure.

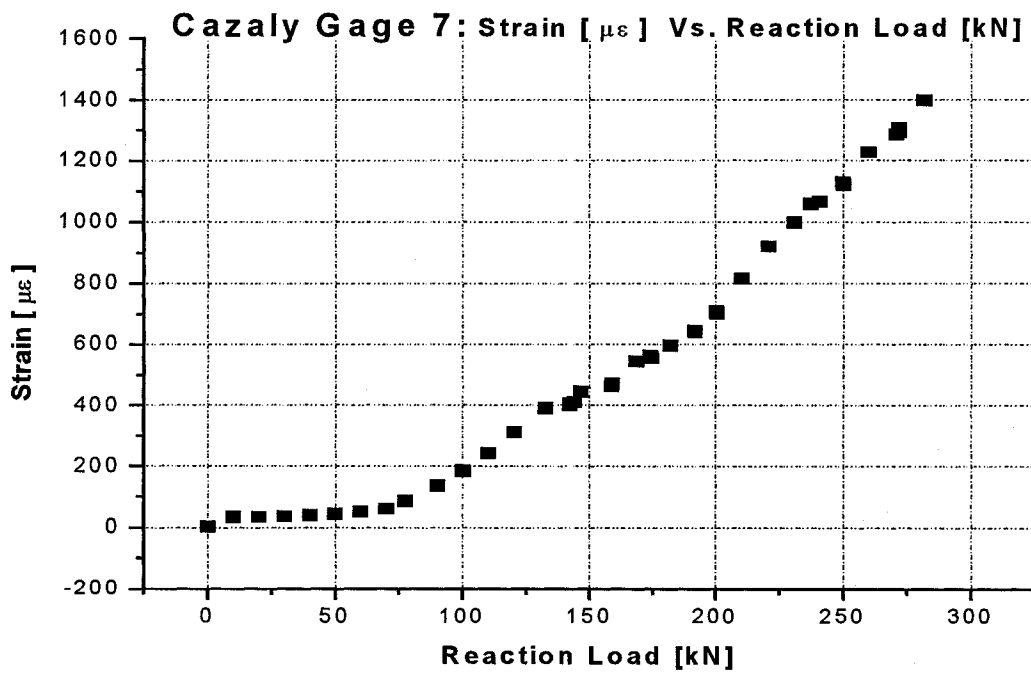
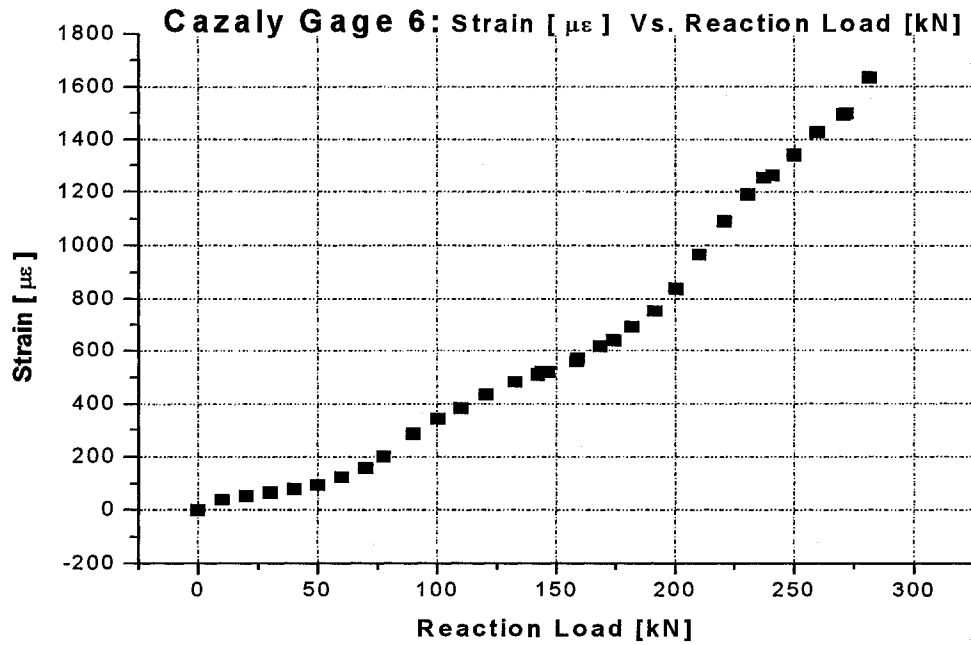
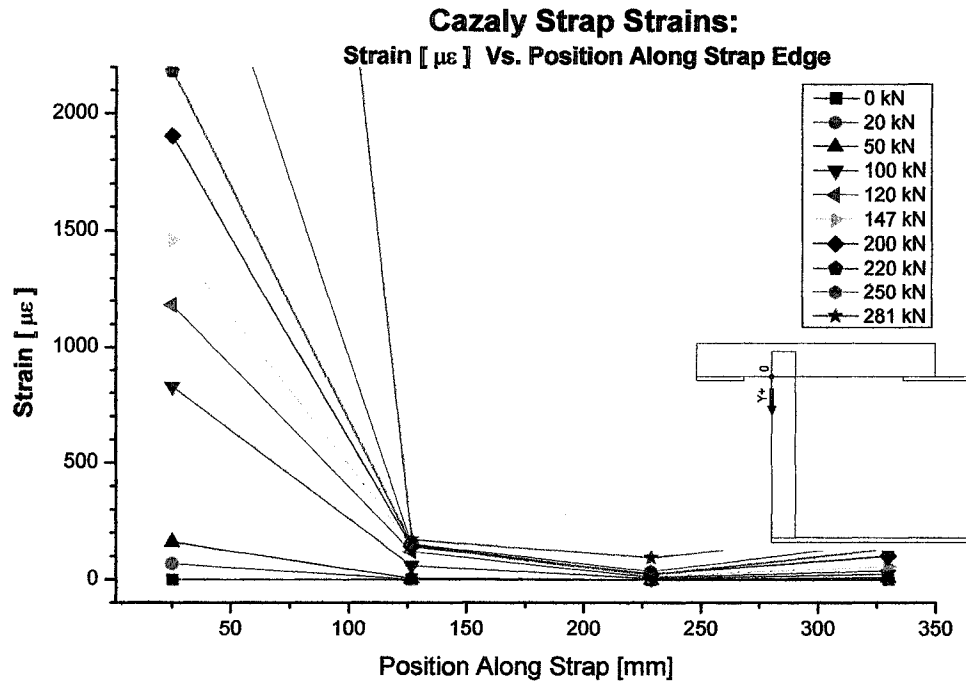


Figure 28: Strains along top and bottom, respectively

There is also some bending strain evident on the Cazaly strap, as evidenced in Figure 29. As can be seen, the strain increases with each load step are greater than would be expected if they were due only to axial load



**Figure 29:** Strains along the Top Bar of the Cazaly Hanger

The strains measured for the top rebar are primarily tensile, but showed a marked increase in tensile strain after approximately 70kN-the point at which cracks at the re-entrant corner began to propagate. Strains on the bottom rebar, as expected, were tensile as well. A strain gage embedded in the concrete adjacent the bar (Embedment Gage 3) showed strain values within the concrete consistent with those on the bar. This is illustrated below in Figure 30 and Figure 31.

The top bar initially showed tensile strains as well, until approximately the same point, at which point it became compressive.

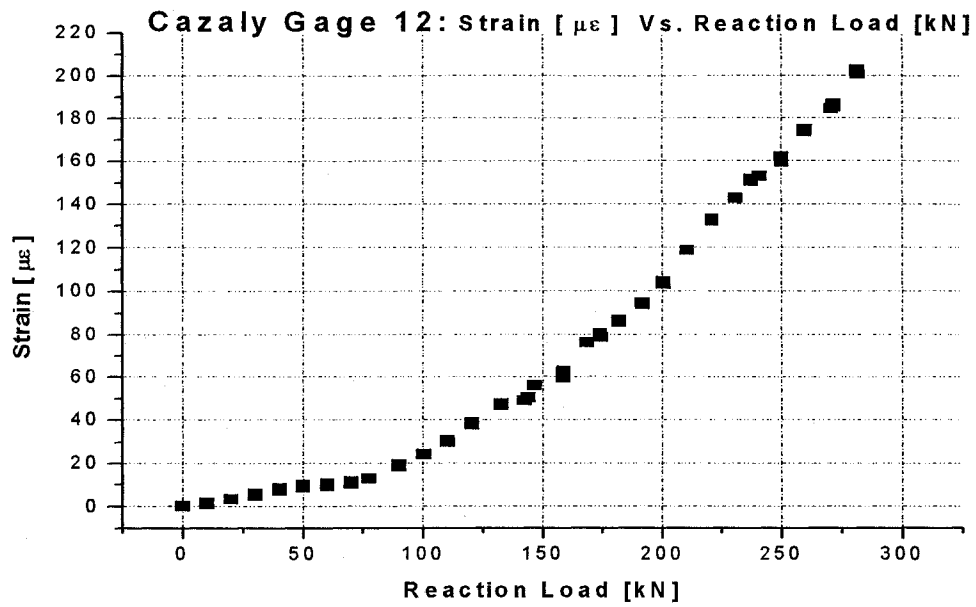


Figure 30: Strains in the bottom bar of the hanger

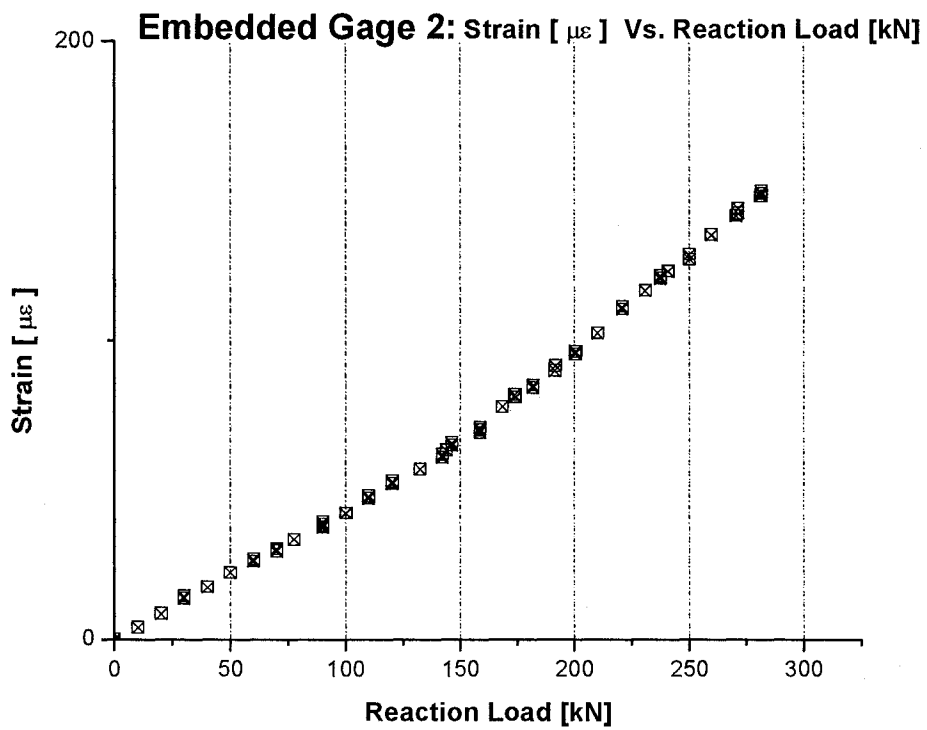


Figure 31: Strains in the concrete adjacent the bottom rebar

## TEST BEAM 2-QUANTITATIVE OBSERVATIONS

The strain data for the second test beam are very similar to the first. As such, for purposes of brevity, it is not discussed here, but rather, is included in the Appendix for reference.

However, the second test beam was outfitted with concrete strain gages in different locations than the first, having benefited from the experience of the first test.

Concrete Gage 3, located on the concrete near the top of the steel strap, was intercepted by a crack at approximately 70kN load, and experienced tensile strains of  $4000\mu\epsilon$  before failing at approximately 180kN load. Gages 4 and 5, located directly adjacent experience compressive strains of  $140\mu\epsilon$  and  $120\mu\epsilon$ , respectively, before failure.

Concrete Gage 6, located on the concrete near the bottom of the steel strap, as well as the adjacent gages 7 and 8, all show compressive strains ( $200\mu\epsilon$ ,  $200\mu\epsilon$ , and  $130\mu\epsilon$ , respectively). Gage 6 was ultimately intercepted by a crack at a failure load of approximately 310kN.

Concrete Gage 9, located at a 45 degree angle near the area where a diagonal tension crack would form, registered a linear increase in tensile strain to a failure value of approximately  $115\mu\epsilon$  at 210kN.

Concrete Gages 10 through 13, located on the concrete surface near the bottom of the stem of the tee in the region of the bottom rebar, were consistent in exhibiting uniformly increasing tensile strains throughout the test.

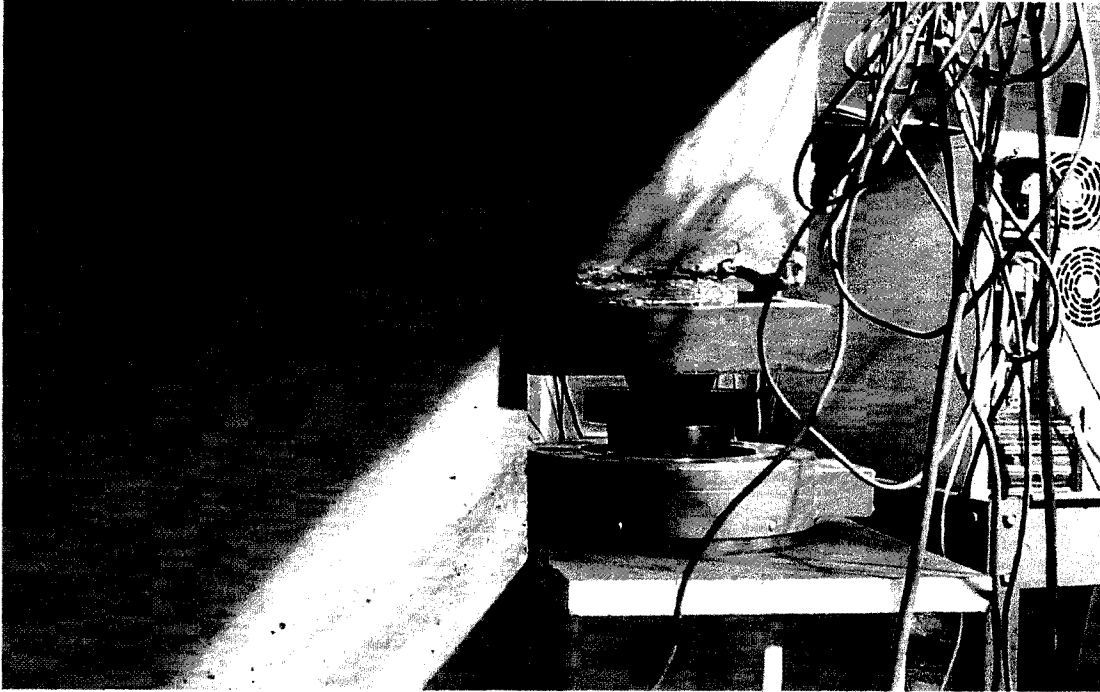


**Figure 32:** Cracking at the re-entrant corner prior to testing

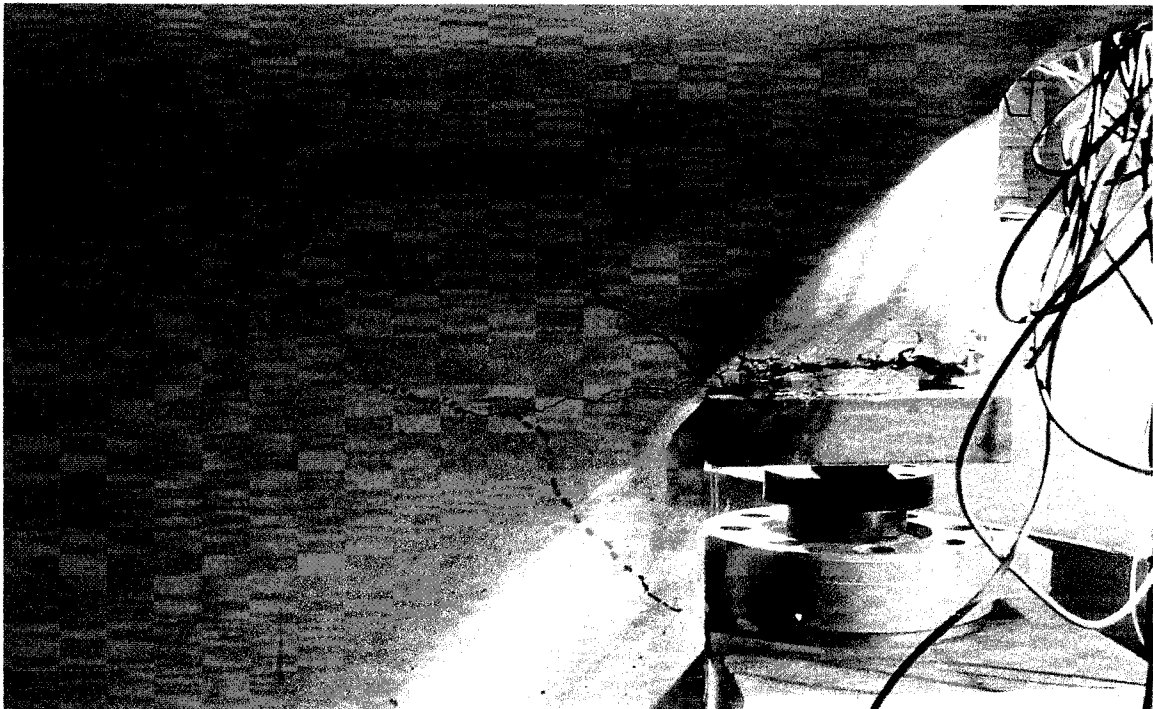


**Figure 33:** Propagation of cracks to 150kN

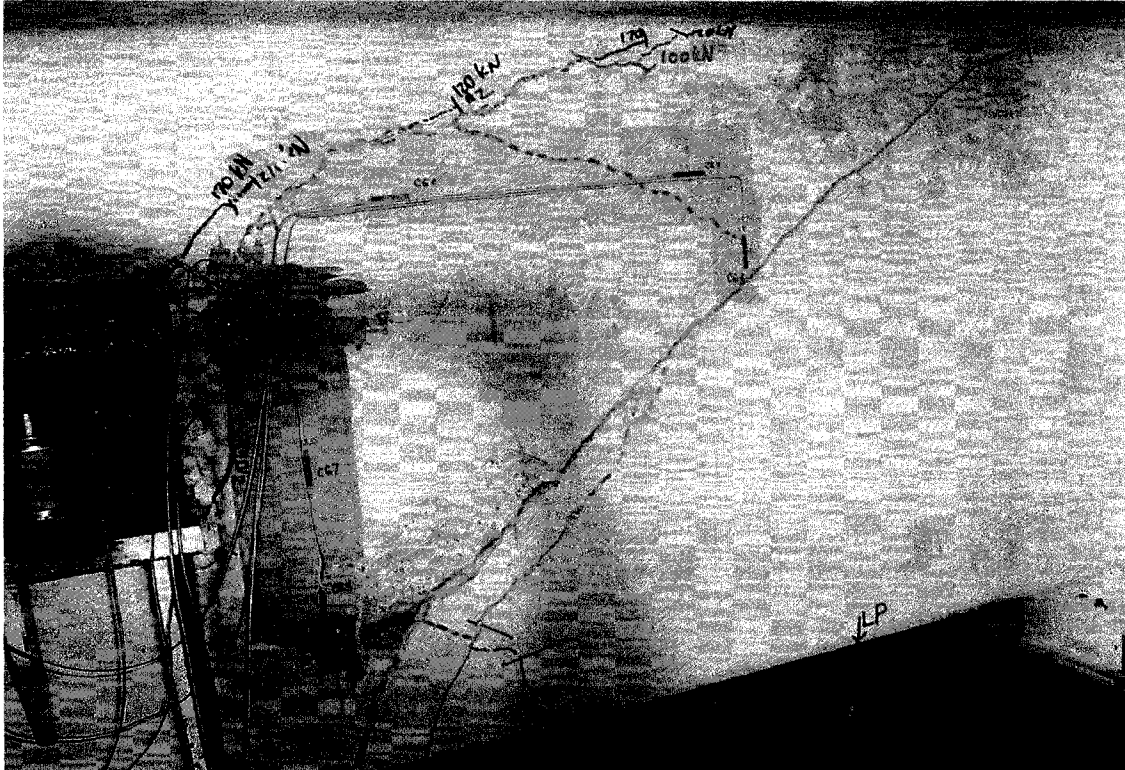


**Figure 34:** Specimen at failure [310kN]. Diagonal crack and spalling is evident.



**Figure 35:** Post-failure condition of Cazaly Hanger (concrete removed)

## SOURCES OF ERROR

No presentation of data is complete without a critical examination of the method by which those data were obtained. As it relates to this work, two fundamental questions arise: Firstly, one can question how accurately the specimens reflect “real world” beams, and secondly, whether the methods of data collection are valid?

Any civil engineering experiment involving concrete, by definition, suffers the effects of the heterogeneity of this material and the variability of workmanship, casting and curing. Wherever possible, every effort was made to minimize the effects of the latter three of these variables. The specimen employed for the full scale tests was identical to beams regularly employed on commercial and institutional structures, and great pains were taken to ensure accurate placement of reinforcement and embedment. Similar quality control was employed for the lab scale beams. In addition, the two lab scale specimens were cast at the same time and cured in the same manner prior to transport to the University of Windsor for testing.

Despite this, the author acknowledges that local strain values-especially those obtained on the surface of the concrete-should be discussed only within the context of all data obtained.

### **Strain Gage Measurements**

Typically, strain gages for use on the surface of concrete are selected with a gage length of at least five times the diameter of the largest aggregate so as to avoid the influence of localized effects. Whereas the large aggregate fraction of the concrete contained aggregates in the 8-10mm range, one would recommend the use of gage lengths of 40-50mm, or five times the diameter of the largest aggregate. (Vishay 2001e) However, the close spacing required for some of the gages coupled with the fact that the mix was a “self consolidating” mix (and thus, had a larger portion of fine aggregate than regular mixes and a lower portion of

coarse aggregate) resulted in the decision to use gages of 30mm gage length. The author does not believe this to have detrimentally affected the data.

The accuracy of strain gage measurements is affected by a number of other factors, most notably:

### **Temperature Effects**

The resistance of a strain gage varies with temperature, thereby producing an apparent strain. Temperature differentials between the gage and test substrate result in a similar effect. This output is known as “thermal output”. An excellent discussion of this is given in Vishay 2001a.

For the purposes of this work, errors resulting from thermal output were minimized by employing self-temperature-compensating (STC) gages that have a coefficient of thermal expansion closely matched to the substrate, and by using a three-wire quarter-bridge sensing circuit, discussed below. From the previous reference, it can be seen that for measurements taken near room temperature, thermal output resulting from these effects is expected to be negligible. (For the sake of completeness, it should be noted that some self-heating of the gage results from the excitation voltage passed through it. However, for short duration tests on large components, as was the case for this work, these effects are minor.)

Gage factor, or the relationship between the applied strain and the change in the strain gage resistance, is also affected by temperature. Again, for tests at or near room temperature, this variation is negligible. (Vishay 2001a)

The use of self-temperature-compensating gages and three wire quarter-bridge sensing circuits is common and well understood. (Vishay 2001d) From Figure 36, it can be seen that the resistance resulting from the strain gage wires is



equilibrated in each side of the circuit, thereby compensating for the thermal effects in the lead wires. Discussion of this is given in Vishay 2001d.

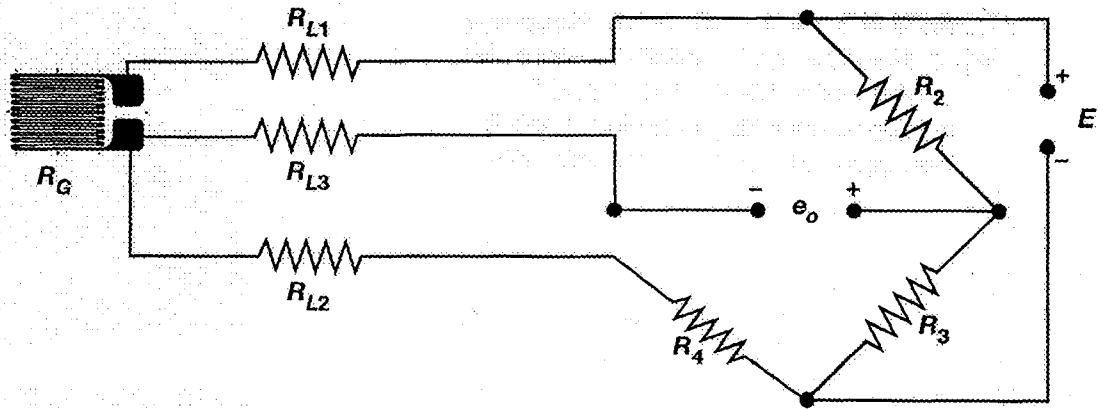


**Figure 36:** Typical Three-wire strain gage circuit

**Misalignment and Transverse Sensitivity of Strain Gages:**

Misalignment of strain gages can have a similar effect as well. (Vishay 2001c and Vishay 2001b, respectively). Examination of the strain gages after the glue had set indicated angular misalignments were on the order of less than 5 degrees. From Vishay 2001d, it can be seen that for such values of angular misalignment, error is less than a few percent.

Transverse sensitivity refers to the degree to which a strain gage is sensitive to strains about an axis perpendicular to its main axis. In all but a purely uni-axial state of strain within a component, one would expect that some transverse strain would be present. Strain gages are not entirely insensitive to this. Examining the concrete surface gages employed on this project, many were placed perpendicular to the opening of cracks in regions where cracks were expected. In these regions, the majority of the strain was expected to be parallel to the major axis of the strain gage.

**Other Factors:**

There is some uncertainty inherent with any measurement device. For the data acquisition system employed for this work, the manufacturer's worst case "Limits of Error" is reported to be  $10 \times 10^{-6}$ . If this is conservatively considered to be a rectangular distribution, the standard deviation can be taken as  $5.33 \times 10^{-6}$ .

## **CHAPTER V**

### **REPAIR METHOD**

There has been a tremendous emphasis in recent years on the repair or rehabilitation of structures. There are both economic and scheduling justifications for choosing to repair versus reconstructing structures.

A number of repair methods have been developed over the years to rehabilitate or strengthen dapped end beams. These have ranged from post-tensioning methods to, most recently, the use of fibre reinforced polymer (FRP) style repairs. Numerous researchers investigated these methods. Taher *et al* (2005) give an excellent summary of the multitude of methods available, and undertake testing of their own. However, these methods focus on restoring, or in some cases, potentially increasing the shear capacity of existing members.

Whereas the prevalence of crack formation was demonstrated in this work, and whereas the ingress of corrosive ions would negatively affect the integrity of the hanger assembly, an effort was made to find a method of sealing these cracks. Injection of an ultra-low viscosity epoxy was tested for efficacy in sealing these cracks. One such method is described below. The reader should not interpret this as a singular endorsement of the particular products used. Rather, there are a number of ultra-low viscosity products available that would likely produce equivalent results. Further, the reader is cautioned that load testing of the repair revealed that no significant gains in member strength were attained. This method is intended for sealing the cracks only.

#### **METHOD**

For the purposes of these tests, the materials employed were Rezi-Weld Gel Paste and Rezi-Weld LV State, manufactured by W.R. Meadows Incorporated. The Gel Paste product is a very viscous epoxy suitable for use on vertical surfaces, and was used to seal overtop the existing cracks, and to glue the

injection ports in place. The LV State product is a two-component ultra-low viscosity epoxy suitable for injection.

Injection ports were glued overtop the cracks at approximately 300mm spacing using the Gel Paste product, ensuring that the Gel Paste did not block the crack in the area of the injection ports. The remaining areas of exposed crack were sealed using the same product and allowed to cure for 24 hours. Prior to injecting the LV State product, and per the manufacturer's recommended practice, the material was tempered to between 18°C and 29°C. Beginning at the lowest injection port, the material was injected until it was seen flowing from the next port. The lower port was then plugged and injection continued from the flowing port. These procedures are shown in Figure 37, below.



**Figure 37:** Injection of epoxy into existing cracks

Closer examination of the cracked areas reveals the extent to which the epoxy was able to travel into small cracks. In this case, this is likely due to capillary action versus the injection process itself. This is shown in Figure 38.



**Figure 38:** Evidence of epoxy permeating small cracks

The successful injection of the epoxy through the thickness of the cracks was confirmed visually on cores obtained from the repaired areas. This is shown in Figure 39, below.

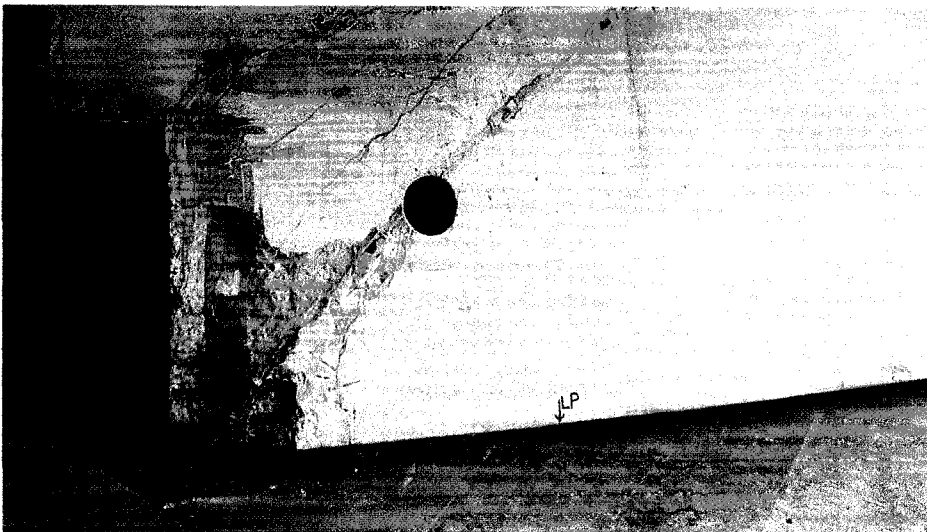


**Figure 39:** Core of repaired area

## CHAPTER VI

### CONCLUSIONS

Overall, the quantitative results obtained from strain gage data are consistent with the qualitative/physical aspects observed during the test. Both the full scale and lab scale test are consistent in the observation that the strap is responsible for virtually all of load carrying capacity of the Cazaly hanger after the concrete has initially cracked. Moreover, examination of the strains along the top bar and the hanger strap indicates the presence of significant flexural forces. In the top bar, these forces remain tolerable throughout the loading range to failure. The magnitude of the forces at the strap, however, is discussed below.

Also notable is the presence of the unexpected compressive strains in the concrete adjacent to the bottom of the strap is consistent with the fact that concrete was observed to be spalling from the specimen prior to failure, shown in Figure 35. This is believed to result from a rotation inwards of the Cazaly hanger under load, resulting in crushing of the concrete between the strap and the bottom bar.

Under service loads (approximately 1/3 of ultimate) rather large cracks are evident in the region around the re-entrant corner. A table listing the recommended maximum values of crack widths is included in the Appendix. It is evident, upon examination, that the cracks experienced by the beams near the re-entrant corner exceed the recommended maximum values for prestressed elements. These cracks, while having no effect on the ultimate strength of the connection *per se*, result in a serviceability concern: depending on the environment, there exists a potential for corrosion to occur as a result of chloride ingress. Under the right circumstances, stress corrosion cracking of the strap in this area may be possible.

Given the particular geometry and construction of the Cazaly hanger, these types of cracks are difficult to control. Whereas other connections can benefit from

draping of the prestressing tendons up into the nib, the Cazaly hanger's construction does not allow this. It can be concluded that the best method to minimize these cracks is to increase the area of steel provided for the straps, and to potentially increase the moment of inertia,  $I$ , of the top bar so as to minimize bending.

The lab scale testing made evident the fact that rather large forces are present at the strap-top bar weld. While this is not a concern for low level cyclic or static loads, this is perhaps an area that deserves greater attention. Other researchers (Theryo *et al.*) have investigated the potential for fatigue failures of flange-to-flange connectors in precast double tee beams, and have concluded also, that more research is needed.

In terms of design methodologies, it appears that the existing design methodologies are sufficient for the design of Cazaly hangers, with the additional caveat that attention be drawn to the areas of steel used for the strap, and the top bar. However, it appears likely that additional load sharing mechanisms are responsible for a portion of the connection strength.

### FUTURE RESEARCH:

Regrettably, the data in this study are limited to a series of two lab scale and one full scale beam test as a result of the costs associated with this type of testing and the lack of funding and assistance available for it. As such, the author urges caution in extending the conclusions resulting from this data to design practices until such time as a larger scale study has been completed.

Should funding and materials become available, the author would urge more detailed examination of the region at which the top bar connects to the strap. Given the observation that the Cazaly hanger strap carries virtually the entire connection load, a catastrophic failure is a certainty should this region fail. Problems in this region are likely to manifest themselves in one of two ways: The potential for corrosive agents to ingress into the connection as already been alluded to. Indeed, a historical study of the in situ condition of existing connections would be of interest, as would an evaluation of the reparability of damaged or failed connections. Secondly, given the stresses observed at this location, some thought might be given to examining the potential for cycle-induced problems at this location. This would, of course, become more pronounced should such a connection have been utilized on a bridge girder.



## REFERENCES

- Aswad, A., Burnley, G. Clelend, N.M., Orndorff, D, Wynings, C. (2004). Load Testing of Prestressed Concrete Double Tees Without Web Reinforcement. *PCI Journal*, 49(2), March-April, 66-77.
- Billington, D.P. (2004). Historical Perspective on Prestressed Concrete. *PCI Journal*. 49(1), 14-30.
- Billington, D.P. (1997). *Robert Maillart: Builder, Designer, and Artist*. New York, New York: Cambridge University Press.
- Canadian Prestressed Concrete Institute (CPCI). (September 1, 2005). CPCI Monthly Vision News. Retrieved August 31, 2005 from [http://www.cpci.ca/downloads/news/CPCI\\_Vision\\_News\\_September\\_2005.pdf](http://www.cpci.ca/downloads/news/CPCI_Vision_News_September_2005.pdf)
- Canadian Prestressed Concrete Institute (CPCI). (1996). Design Manual: Precast and Prestressed Concrete. Ottawa, Ontario: Canadian Prestressed Concrete Institute.
- Gergely, P., and Sozen, M. A. (1967). Design of Anchorage-Zone Reinforcement in Prestressed Concrete Beams. *PCI Journal*, 12(2), April, 63-65.
- Huang, P.C, J.J Myers and A. Nanni. (2000). Dapped-End Strengthening in Precast Prestressed Concrete Double Tee Beams with FRP Composites. *Proc., 3rd Inter. Conf. on Advanced Composite Materials in Bridges and Structures, Ottawa, Canada*, 545-552.
- Huang, P.C., & Nanni, A. (2006). Dapped-End Strengthening of Full-Scale Prestressed Double Tee Beams with FRP Composites. *Advances in Structural Engineering*, 9(2), 293-
- Hurst, M.K. (1998). *Prestressed Concrete Design, Second Edition*. New York, New York: E & FN Spon.
- Ife, J.S., Uzumeri, S.M., Huggins, M. W. (1968). Behaviour of the "Cazaly Hanger" Subjected to Vertical Loading. *PCI Journal*, December.
- Libby, J.R. (1977). *Modern Prestressed Concrete*. Toronto, Ontario: Van Nostrand Reinhold Company International.
- Lin, I-J, Hwang, S-J, Lu, W-Y, and Tsai, J-T. (2003) Shear Strength of Reinforced Concrete Dapped-End Beams. *Structural Engineering and Mechanics*, 16(3), 275-294.

Loov, R. (1968). A Precast Beam Connection Designed for Shear and Axial Load. *PCI Journal*, June.

MacGregor, J.G. and Bartlett, F.M. (2000). *Reinforced Concrete: Mechanics and Design First Canadian Edition*. Scarborough, Ontario: Prentice-Hall Canada Inc.

Mattock, A. H. and Chan, T. C. (1979). Design and Behavior of Dapped End Beams. *PCI Journal*, 24(6) November-December, 28-45.

Mattock, A.H. and Theryo, T.S. (1986). PCISFRAD Project No. 6 Summary Paper: Strength of Precast Prestressed Concrete Members With Dapped Ends. *PCI Journal*, 31(5), September-October, 58-75.

Mattock, A.H. and Theryo, T.S. (1986). *Research and Development Report 06-86: Strength of Members with Dapped Ends*. Chicago, Illinois: Prestressed Concrete Institute.

Nanni, A., Huang, P.C. (2002) Validation of an Alternative Reinforcing Detail for the Dapped Ends of Prestressed Double Tees. *PCI Journal*, January-February 38-50.

Nasser, D. (2000). Open Forum Problems and Solutions: Double Tees With Extreme Daps. *PCI Journal*, November-December, 110-113.

National Research Council of Canada (NRC). (January 31, 2003). Canada's Code Development System. Retrieved January 18, 2007 from [http://www.nationalcodes.ca/ccbfc/ccds\\_e.pdf](http://www.nationalcodes.ca/ccbfc/ccds_e.pdf)

Nawy, E.G. (2003). *Prestressed Concrete: A Fundamental Approach*, Fourth Edition. Toronto, Ontario: Pearson Education Incorporated.

Nilson, A.H. (1978). *Design of Prestressed Concrete*. Toronto, Ontario: John Wiley & Sons, Inc.

PCI Committee on Connection Details. (1988). *Design and Typical Details of Connections for Precast and Prestressed Concrete*. Chicago, Illinois: Prestressed Concrete Institute.

PCI Committee on Industry Handbook: Background and Discussion Task Group. (1998). *Background and Discussion of the PCI Design Handbook Fifth Edition*. Chicago, Illinois: Prestressed Concrete Institute.

PCI Committee on Quality Control Performance Criteria. (1983). Fabrication and Shipment Cracks in Prestressed Hollow-Core Slabs and Double Tees. *PCI Journal*, 28(1), 13-23.

Pillai, S.U., Kirk, D.W., and Erki, M.A. (1999). *Reinforced Concrete Design, Third Edition*. Toronto, Ontario: McGraw-Hill Ryerson Limited.

Prestressed Concrete Institute. (1985). *PCI Design Handbook, Third Edition*. Chicago, Illinois: Prestressed Concrete Institute.

Sheikh, M.A, de Paiva, H.A.R., and Neville, A.M. (1968). Calculation of Flexure-Shear Strength of Prestressed Concrete Beams. *PCI Journal*, February 67-85.

Skoog, D.A., Holler, F.J., and Nieman, T.A. (1998). *Principles of Instrumental Analysis, Fifth Edition*. Orlando, Florida: Harcourt Brace & Company.

Slater, W.M. (1966). Canadian Prestressed Concrete Institute's 1965 Research Program on Hanger Connections. *PCI Journal*, June 1966.

Taher, S.E.-D.M.F. (2005). Strengthening of Critically Designed Girders with Dapped Ends. *Structures and Buildings*, 152(SB2), 141-152.

Tuan, C.Y., Yehia, S.A., Jongpitaksseel, N, and Tadros, M.K. (2004). End Zone Reinforcement for Pretensioned Concrete Girders. *PCI Journal*, 49(3) May-June, 68-82.

Vishay-Measurements Group. (2001). *Application Note TN-504-1: Strain Gage Thermal Output and Gage Factor Variation with Temperature*.

Vishay-Measurements Group. (2001). *Application Note TN-509: Errors Due to Transverse Sensitivity in Strain Gages*.

Vishay-Measurements Group. (2001). *Application Note TN-511: Errors Due to Misalignment of Strain Gages*.

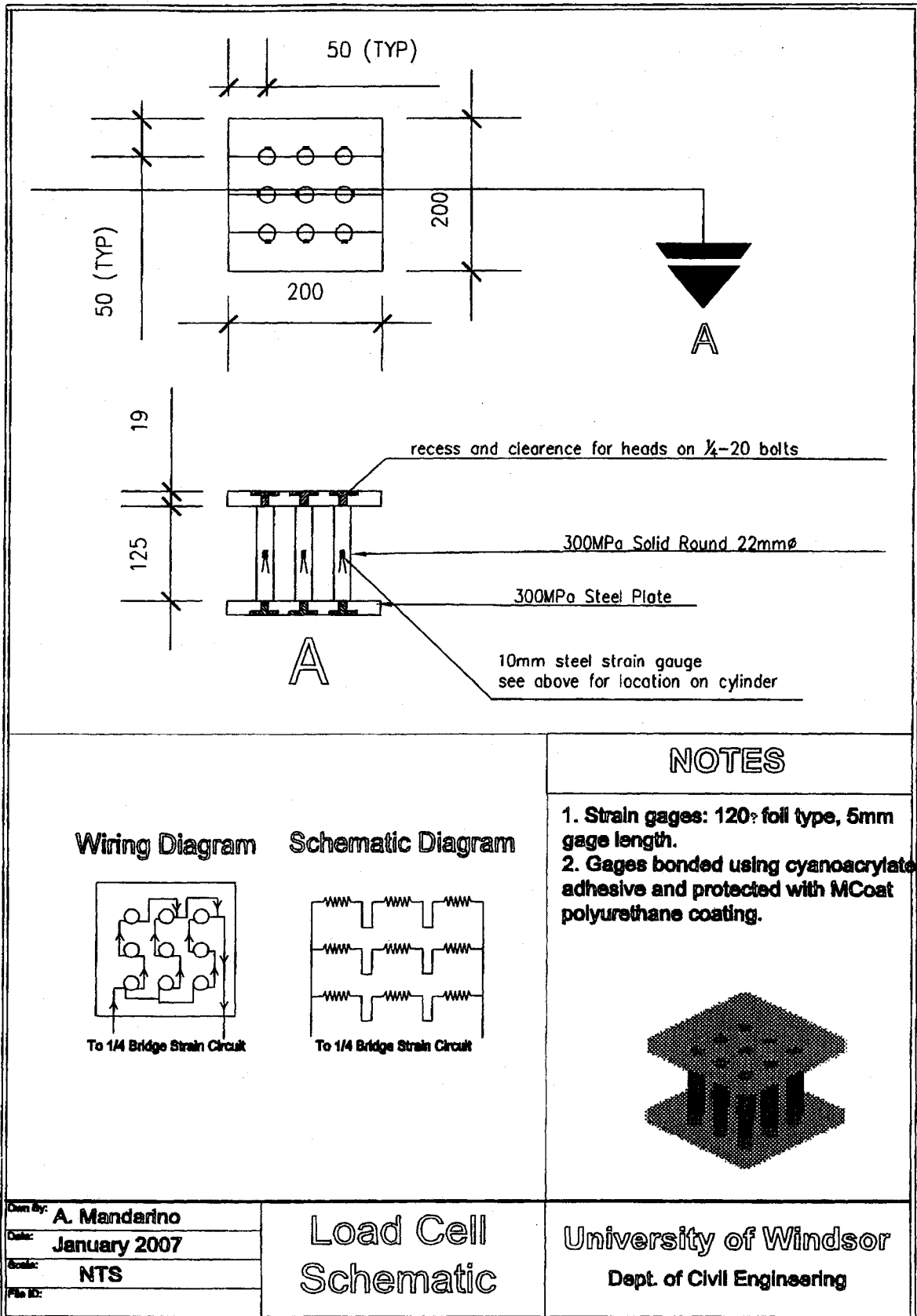
Vishay-Measurements Group. (2001). *Application Note TT-611: Strain Gage Installations for Concrete Structures*.

Vishay-Measurements Group. (2001). *Application Note TT-612: The Three-Wire Quarter-Bridge Circuit*.

Wang, Q, and Guo, Z. and Hoogenboom, P.C.J. (2005). Experimental Investigation on the Shear Capacity of RC Dapped End Beams and Design Recommendations, *Structural Engineering and Mechanics*, 21(2), 221-235.

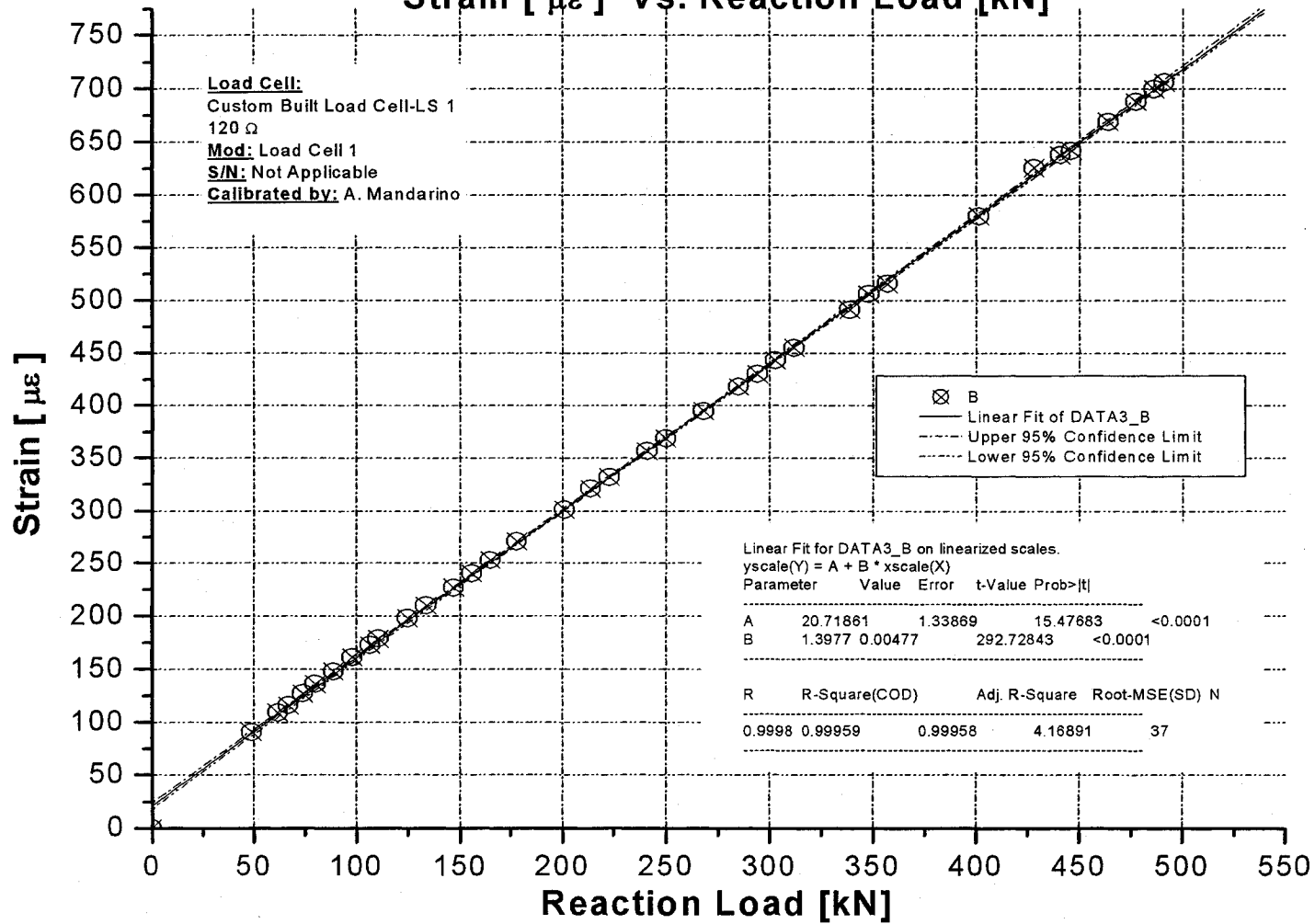
Werner, M.P., and Dilger, W.H. (1973). Shear Design of Prestressed Concrete Stepped Beams. *PCI Journal*, 18(4), July-August, 37-49.

## APPENDIX A



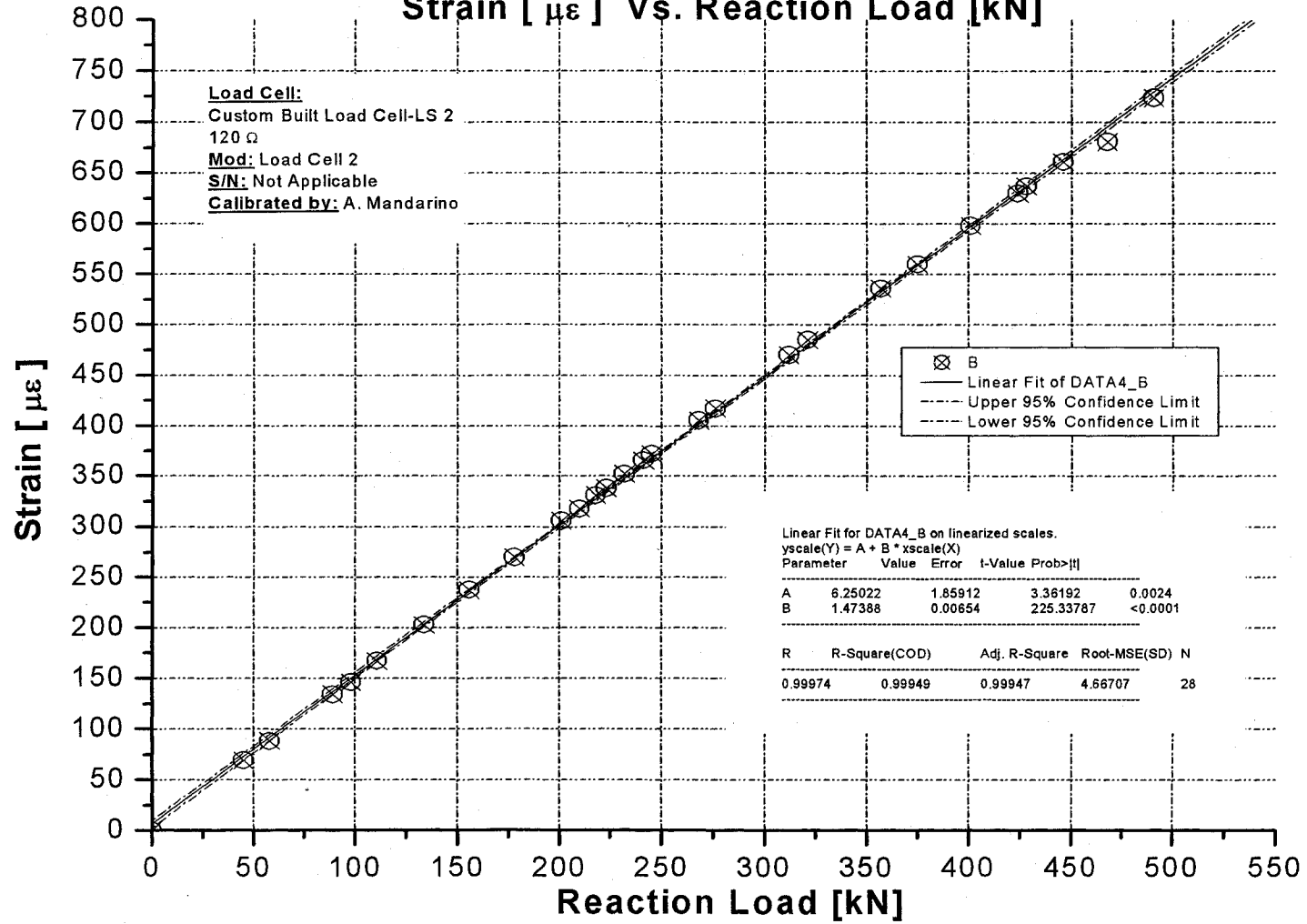
## Load Cell Calibration Curve: LS 1

### Strain [ $\mu\epsilon$ ] Vs. Reaction Load [kN]



## Load Cell Calibration Curve: LS 2

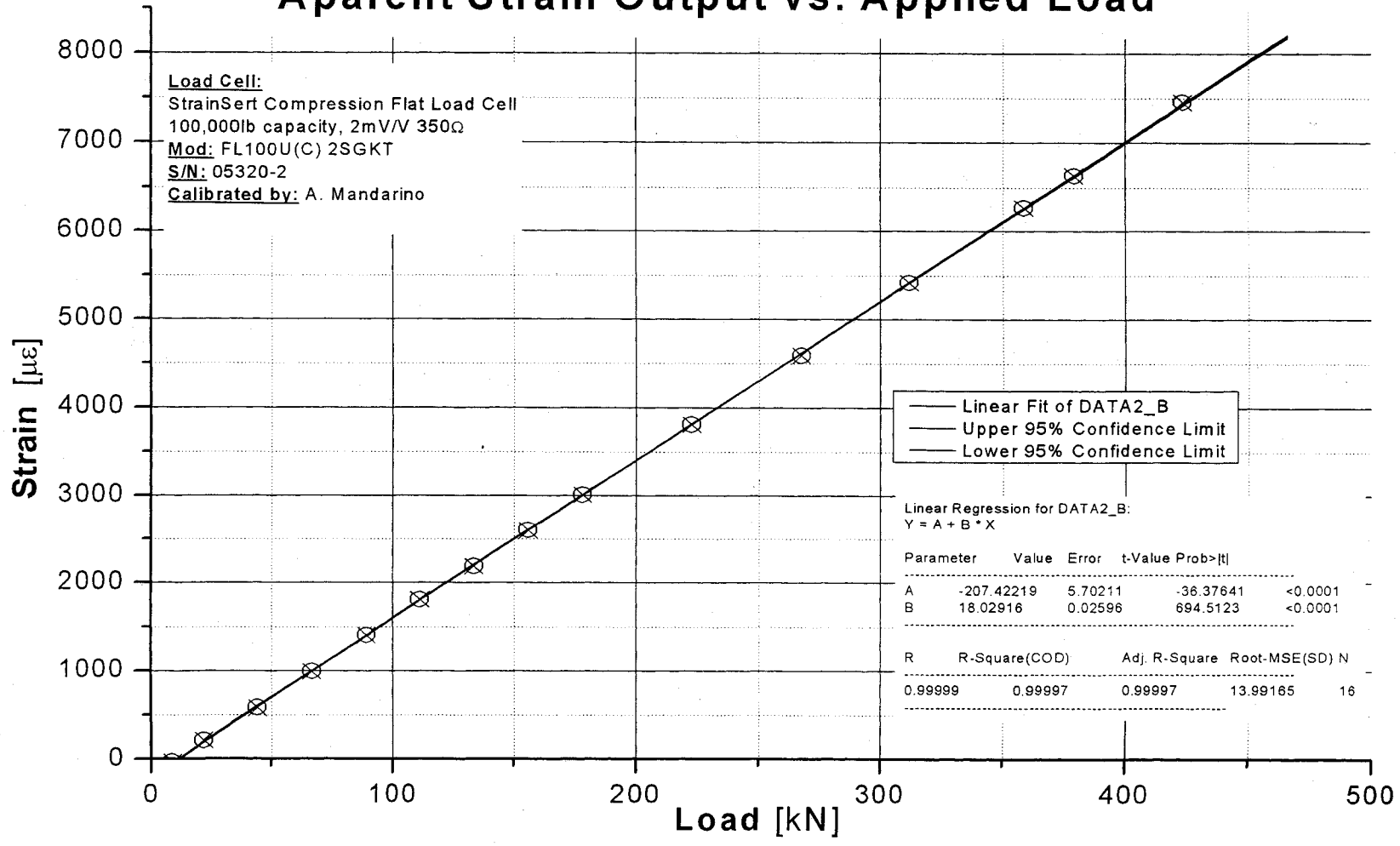
### Strain [ $\mu\epsilon$ ] Vs. Reaction Load [kN]



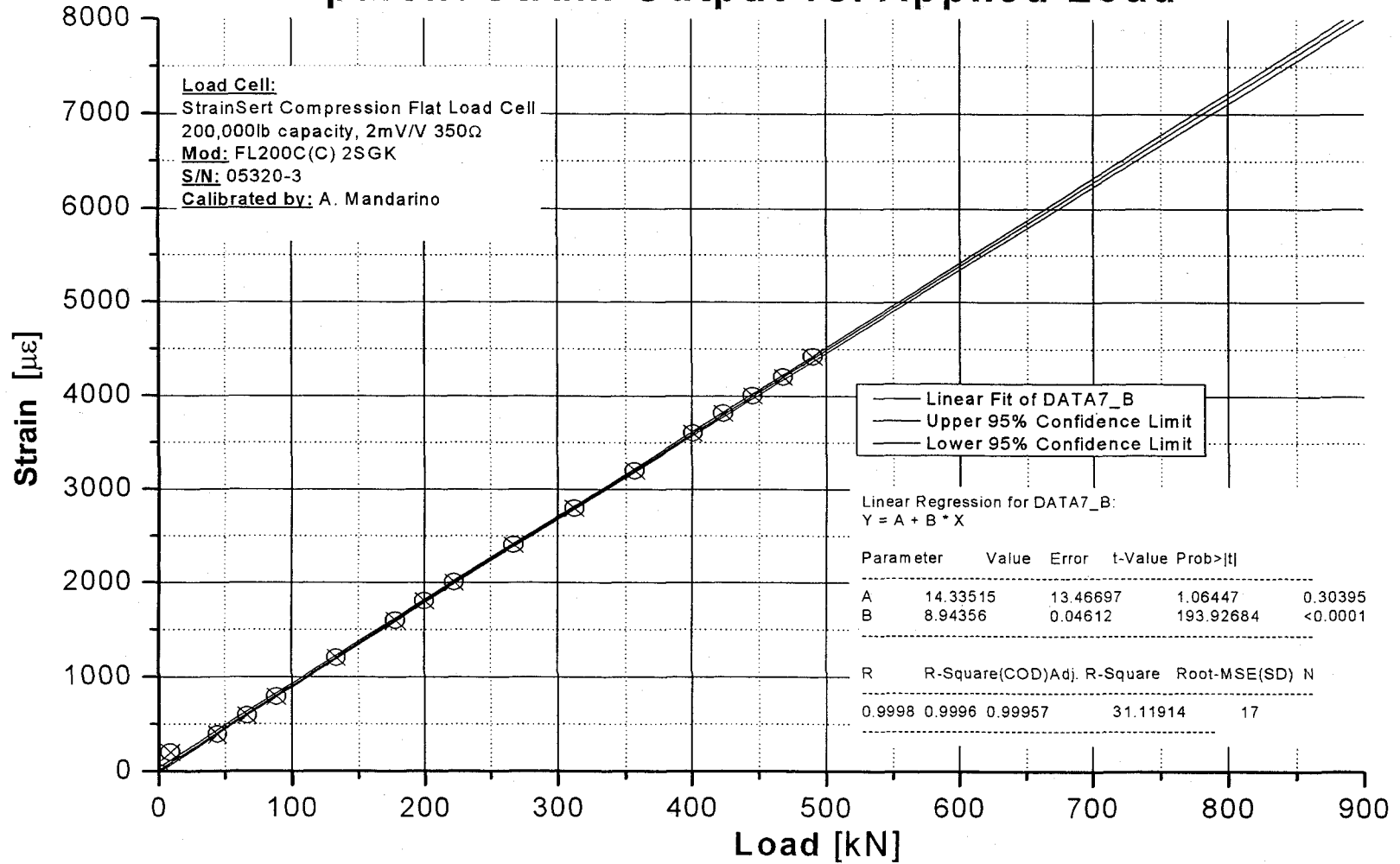




## Load Cell Calibration Curve: "100kip Cell" Aparent Strain Output vs. Applied Load



## Load Cell Calibration Curve: "200kip" Cell Aparent Strain Output vs. Applied Load





Structures Research Group

STAMP

Cazaly Hanger -Lab Scale Beam

University of Windsor

Cazaly Hanger Calculations by PCI/CPCI Methods

Date:

Date:

Anthony Mandarino EIT

Date:

The following calculations were performed by an EIT and DO NOT constitute an Engineered Design unless accompanied by the stamp of a Professional Engineer Registered in the Province of Ontario.

Basis:

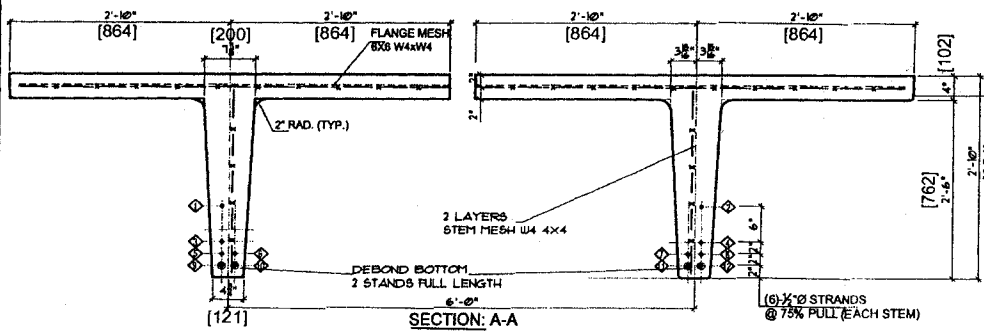
CAN/CSA A23.3-94 (for Concrete not discussed elsewhere) and CAN/CSA S16.1 (for Steel not discussed elsewhere)

Rem: Description

Basis

1.0 Geometric & Load Data

1.10



GENERAL NOTES

1. FINISH =
2. TOL =
3. TOL =
4. AIR ENTRAINMENT =
5. INITIAL CAMBER =
6. DEFLECTION CAMBER =
7. STRAND IN =
8. REINFORCING COVER =

BROOM FINISH  
3500 PSI @ RELEASE  
6000 PSI @ 28 DAYS

(From Fabrication Drawing with Metric Dimensions Added, See Figures)

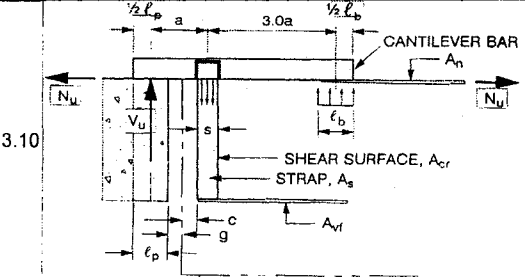
Basis

1.20	Length of Member [L]	4013 mm	13'-2" ft-in	Fabrication Drawing
1.30	Flange Width of Member [w]	1727 mm	5'-8" ft-in	Fabrication Drawing
1.40	Depth of Member [d]	864 mm	2'-10" ft-in	Fabrication Drawing
1.50	Web Thickness (bottom)	121 mm	4.75 in	Fabrication Drawing
1.60	Web Thickness (top)	200 mm	7.875 in	Fabrication Drawing
1.70	Dap Height (h)	500 mm		Design for 1/4 Scale
1.80	Cover	25.4 mm		Min Design Assumption
1.90	Load Application Point (distance from End)	50 mm		Design Assumption

2.0 Loading

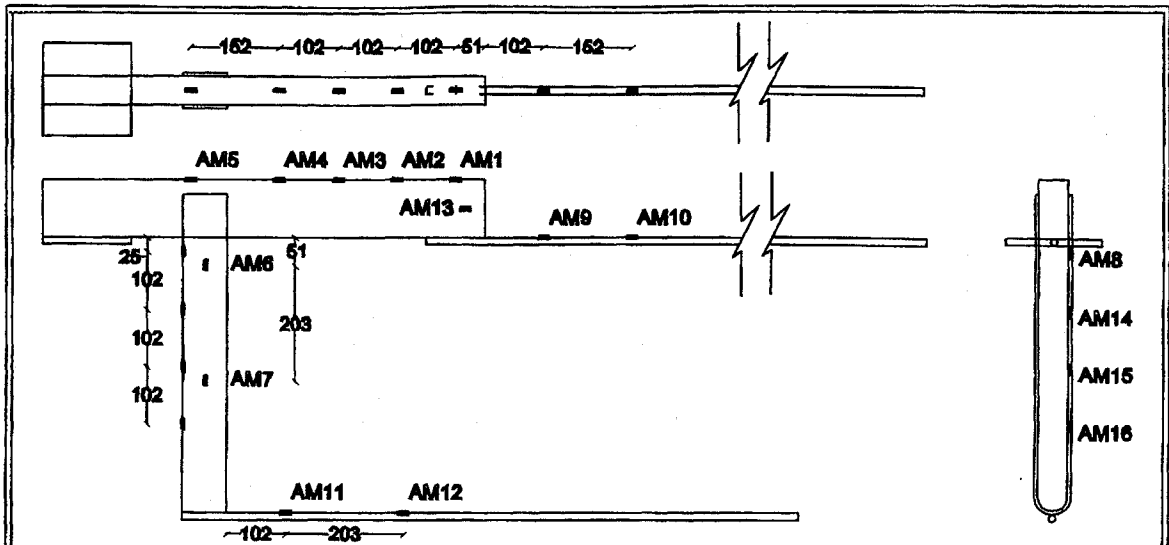
2.10	Vertical Design Reaction Per Stem [Vu]	122 kN	27 kip	Design for 1/4 Scale
2.20	Horizontal Design Reaction Per Stem [Nu]	24.3 kN	5.5 kip	CAN/CSA A23.3 Cl 11.5 ie. Min 0.20 * Rvf

3.0 Cazaly Hanger Design (PCI 5th Edition, 6-31)

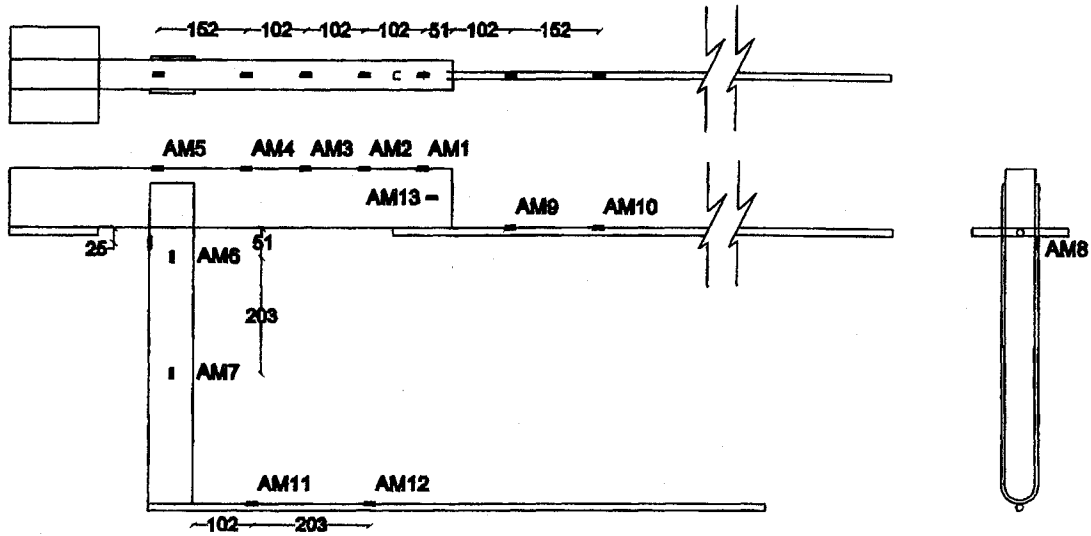


3.11	Fc'	41.5 Mpa	6000 psi	PSI Proprietary Mix Design
3.12	Fy(rft)	400 MPa	60 ksi	
3.13	Fy(steel)	245 MPa	36 ksi	
3.14	Steel Strength Reduction Factor, Φs	0.90	n/a	0.90 n/a
3.15	Bearing area 1 (assumed)	150 mm	6 in	
3.16	Bearing area 2 (assumed)	100 mm	4 in	
3.17	Cover, "c" (between strap and edge)	25.4 mm	1 in	
3.18	Gap spacing, "g" (between beam & ledge)	25.4 mm	1 in	
3.19	Plate Bearing Length, "lp" (worst case)	50 mm	6 in	
3.20	Size of Strap (s), from below	76.2 mm	3 in	
3.21	Strap to Force Application Distance, "a"	165 mm	6.5 in	

Strap Area						
4.01	Required Steel Area, $A_s$			1.12	in <sup>2</sup>	PCI Hbk 5th ed: 6.10.1 $A_s \geq 1.33V_u/(\phi_s F_y)$
4.02	Try 3/8" x 2" x 2 (2 sides)			1.50	in <sup>2</sup>	OK
4.03	Try 1/4" x 2.5" x 2 (2 sides)			1.25	in <sup>2</sup>	OK
4.04	Try 1/4" x 3.0" x 2 (2 sides)			1.50	in <sup>2</sup>	OK
Strap Weld Design						
5.01	Trial 1 Size of Weld	8.0	mm	0.313	in	Can use only if 3/8 bar used
5.02	Weld Resistance, $r_w$			10.0	kip/in	
5.03	Length of Weld Required			1.81	in	Can use less weld...
5.04	Trial 2 Size of Weld	5.0	mm	0.188	in	
5.05	Weld Resistance, $r_w$		kN/mm	4.18	kip/in	
5.06	Length of Weld Required		mm	4.34	in	
5.07	Design:	Use 1/4" bar, weld 2" on each side and 3" across top with 3/16" fillet weld using E70xx/E49xx electrodes.			To be welded in accordance with appropriate rebar welding standards, See Discussion on preheating of top bar	
5.08	Strap Design Thickness	6	mm	0.250	in	
5.09	Strap Design Width	76	mm	3.00	in	
5.10	Strap Weld Design Fillet	5	mm	0.188	in	
5.11	Strap Total Weld Length (Per Side)	178	mm	7.00	in	
Top Bar Design						
6.01	Moment to be resisted by bar			177	kip-in	PCI Hbk 5th ed: 6.10.2 $M_u = V_u \cdot a$
6.02	Assumed width of bar, $b$			2.0	in	
6.03	Required Section Modulus of Bar, $S_x$			5.47	in <sup>3</sup>	$S_x = M_u/\phi_s F_y$
6.04	Required Depth of Bar to meet $S_x$ , $d$			4.05	in	Since $S_x = bd^2/2$ , $d = \sqrt{S_x \cdot 6/2}$
6.05	Required Length of Embedded Bar (Recmnd)			19.5	in	Recommended Embedment Length = $3 \cdot a$
6.06	Total Length of bar			29.4	in	Total Length
6.07	Design:	Use a 2" (width) x 4" (height) bar. Total length of Bar to be 30in			To be welded in accordance with appropriate rebar welding standards, See Discussion on preheating of top bar	
Bearing Area Checks						
7.01	Concrete Ultimate Bearing Capacity Check			6.18	ksi	PCI Hbk 5th ed: 6.10.3 $f_{bu} = 0.85\phi f_c \sqrt{b_1/b}$
7.02	Bearing Area Length (lb)			0.73	in	



Gauging-Cazaly 1

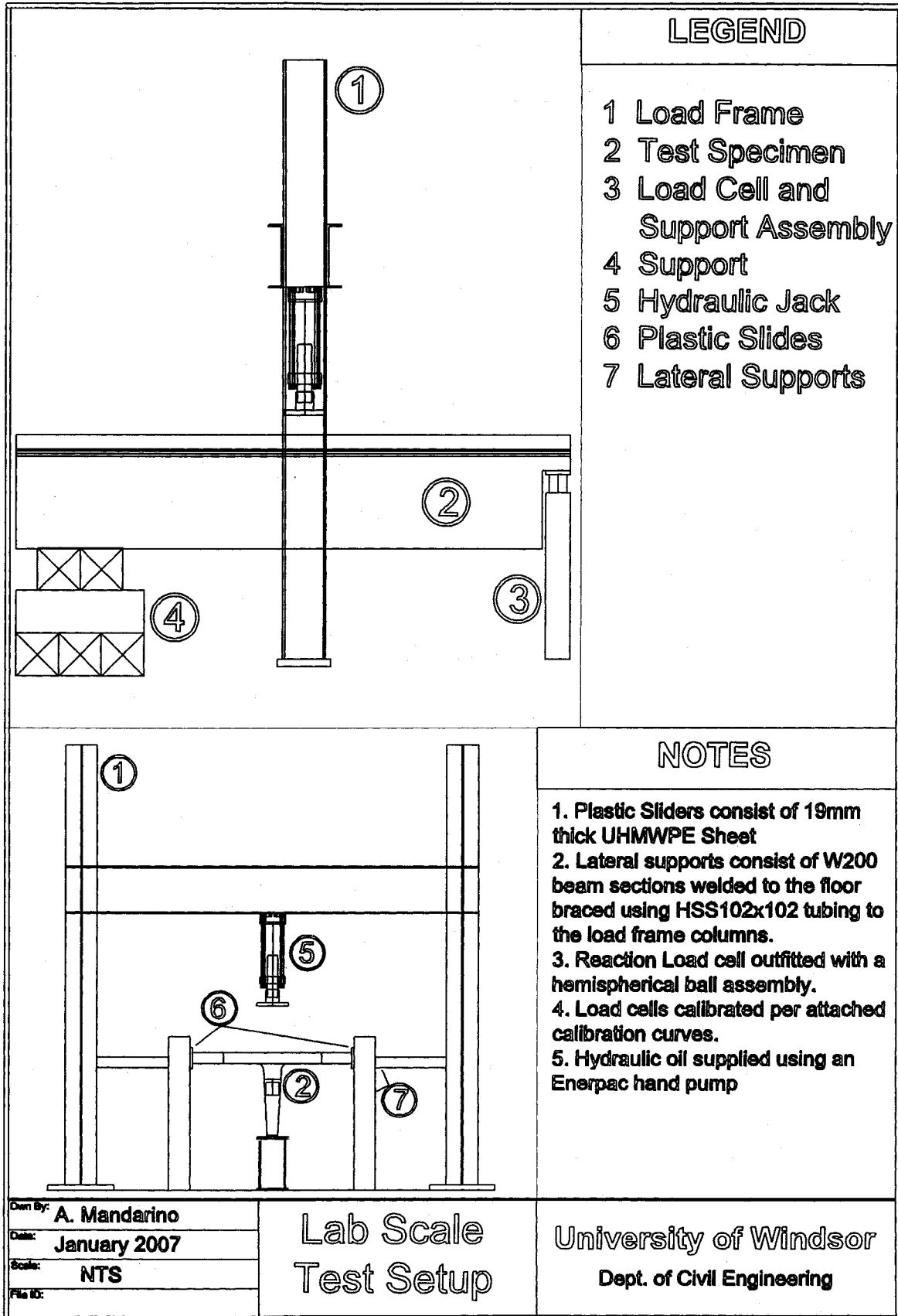


Gauging-Cazaly 2

Drawn By:	<b>A. Mandarino</b>
Date:	<b>January 2007</b>
Scale:	<b>NTS</b>
File ID:	

**Lab Scale Cazaly  
Hanger Gauges**

**University of Windsor  
Dept. of Civil Engineering**



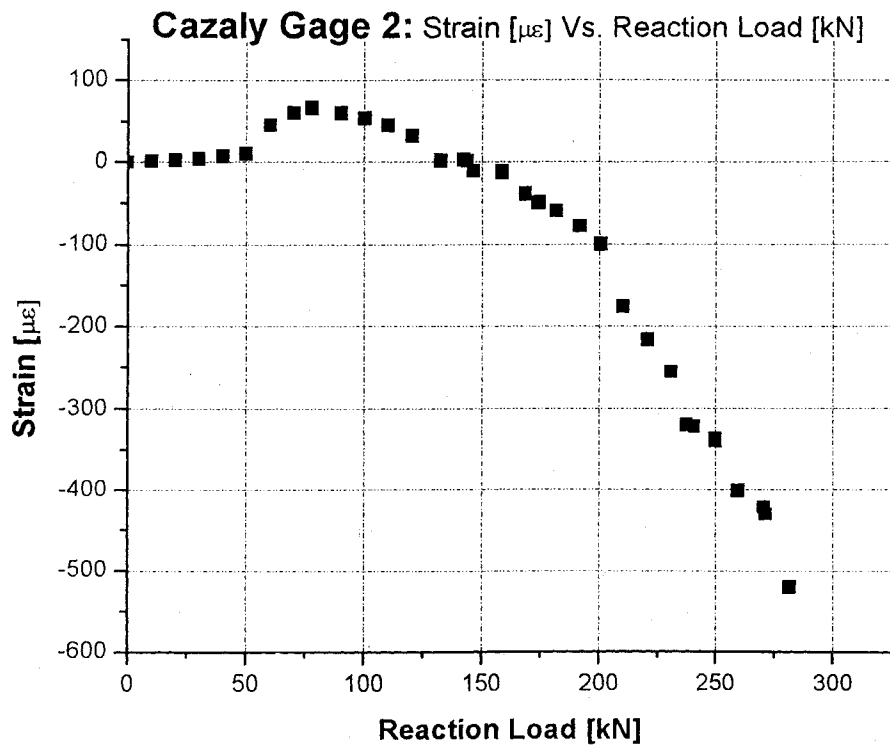
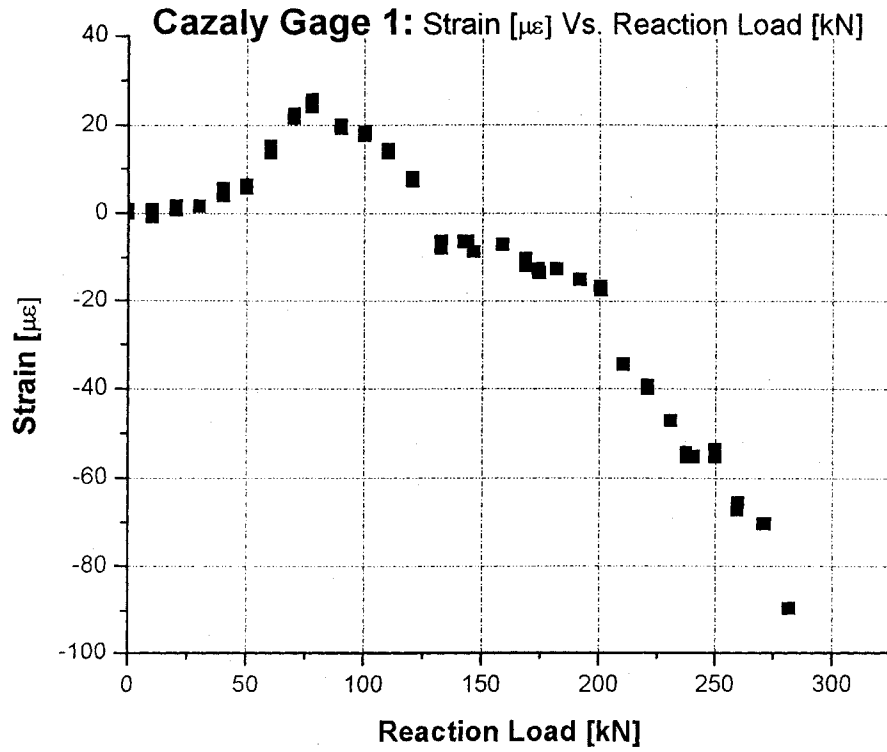
## Lab Scale Beam 1: Measurement Device Parameters

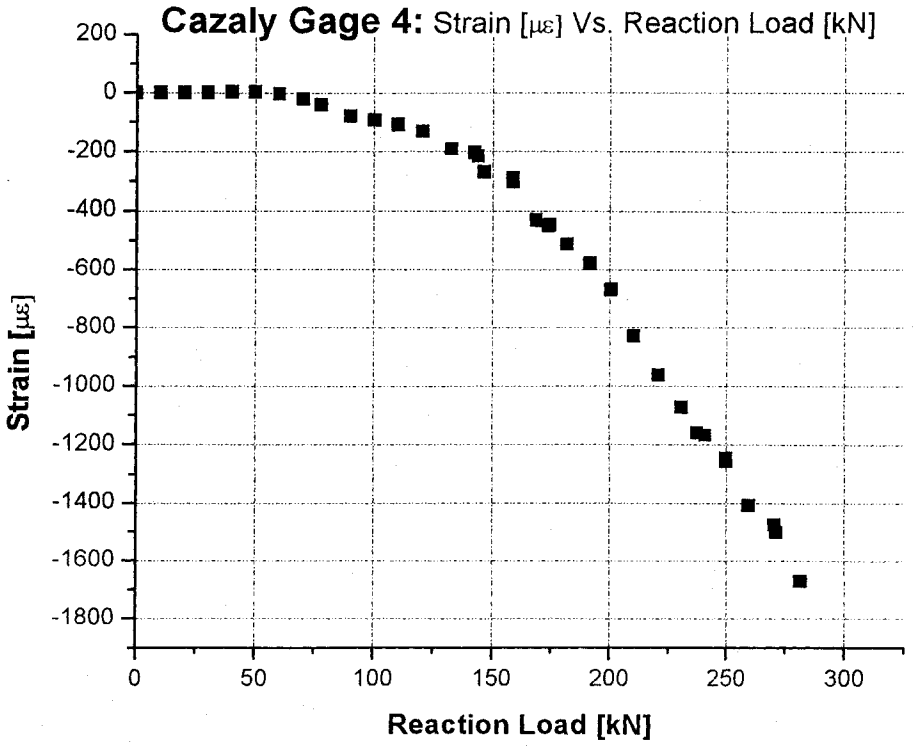
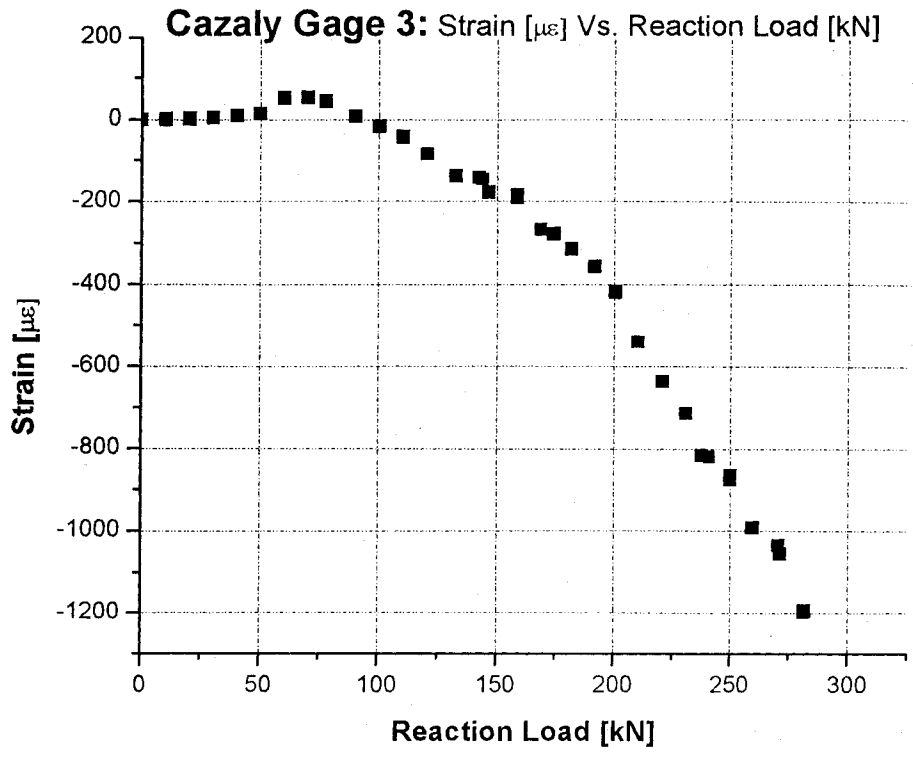
Parameter	Gauge Factor	Resistance	Temp Comp	Other Data
AM 1	2.11 +/- 1.0%	120Ω	11.7 ppm/°C	Kyowa 5mm KFG-05-120-C1-11
AM 2	2.11 +/- 1.0%	120Ω	11.7 ppm/°C	Kyowa 5mm KFG-05-120-C1-12
AM 3	2.11 +/- 1.0%	120Ω	11.7 ppm/°C	Kyowa 5mm KFG-05-120-C1-13
AM 4	2.11 +/- 1.0%	120Ω	11.7 ppm/°C	Kyowa 5mm KFG-05-120-C1-14
AM 5	2.11 +/- 1.0%	120Ω	11.7 ppm/°C	Kyowa 5mm KFG-05-120-C1-15
AM 6	2.11 +/- 1.0%	120Ω	11.7 ppm/°C	Kyowa 5mm KFG-05-120-C1-16
AM 7	2.11 +/- 1.0%	120Ω	11.7 ppm/°C	Kyowa 5mm KFG-05-120-C1-17
AM 8	2.11 +/- 1.0%	120Ω	11.7 ppm/°C	Kyowa 5mm KFG-05-120-C1-18
AM 9	2.11 +/- 1.0%	120Ω	11.7 ppm/°C	Kyowa 5mm KFG-05-120-C1-19
AM 10	2.11 +/- 1.0%	120Ω	11.7 ppm/°C	Kyowa 5mm KFG-05-120-C1-20
AM 11	2.11 +/- 1.0%	120Ω	11.7 ppm/°C	Kyowa 5mm KFG-05-120-C1-21
AM 12	2.11 +/- 1.0%	120Ω	11.7 ppm/°C	Kyowa 5mm KFG-05-120-C1-22
AM 13	2.11 +/- 1.0%	120Ω	11.7 ppm/°C	Kyowa 5mm KFG-05-120-C1-23
AM 14	2.11 +/- 1.0%	120Ω	11.7 ppm/°C	Kyowa 5mm KFG-05-120-C1-24
AM 15	2.11 +/- 1.0%	120Ω	11.7 ppm/°C	Kyowa 5mm KFG-05-120-C1-25
AM 16	2.11 +/- 1.0%	120Ω	11.7 ppm/°C	Kyowa 5mm KFG-05-120-C1-26
EG 1	2.05 +/- 1.0%	120Ω	11.7 ppm/°C	Vishay/MG Type 120 Embedment
EG 2	2.05 +/- 1.0%	120Ω	11.7 ppm/°C	Vishay/MG Type 120 Embedment
EG 3	2.05 +/- 1.0%	120Ω	11.7 ppm/°C	Vishay/MG Type 120 Embedment
CG 1	2.11 +/- 1.0%	120Ω	11.7 ppm/°C	Kyowa 30mm KFG-30-120-C1-11
CG 2	2.11 +/- 1.0%	120Ω	11.7 ppm/°C	Kyowa 30mm KFG-30-120-C1-11
CG 3	2.11 +/- 1.0%	120Ω	11.7 ppm/°C	Kyowa 30mm KFG-30-120-C1-11
CG 4	2.11 +/- 1.0%	120Ω	11.7 ppm/°C	Kyowa 30mm KFG-30-120-C1-11
CG 5	2.11 +/- 1.0%	120Ω	11.7 ppm/°C	Kyowa 30mm KFG-30-120-C1-11
CG 6	2.11 +/- 1.0%	120Ω	11.7 ppm/°C	Kyowa 30mm KFG-30-120-C1-11
CG 7	2.11 +/- 1.0%	120Ω	11.7 ppm/°C	Kyowa 30mm KFG-30-120-C1-11
CG 8	2.11 +/- 1.0%	120Ω	11.7 ppm/°C	Kyowa 30mm KFG-30-120-C1-11
LP 1	n/a	n/a	n/a	U Windsor Resistance Pot
LP 2	n/a	n/a	n/a	U Windsor Resistance Pot
LP 3	n/a	n/a	n/a	U Windsor Resistance Pot
LP 4	n/a	n/a	n/a	U Windsor Resistance Pot
Load Cell 1	See Cal'bn	n/a	n/a	See 100kip Cell Calibration Sheet
Load Cell 2	See Cal'bn	n/a	n/a	See 200kip Cell Calibration Sheet

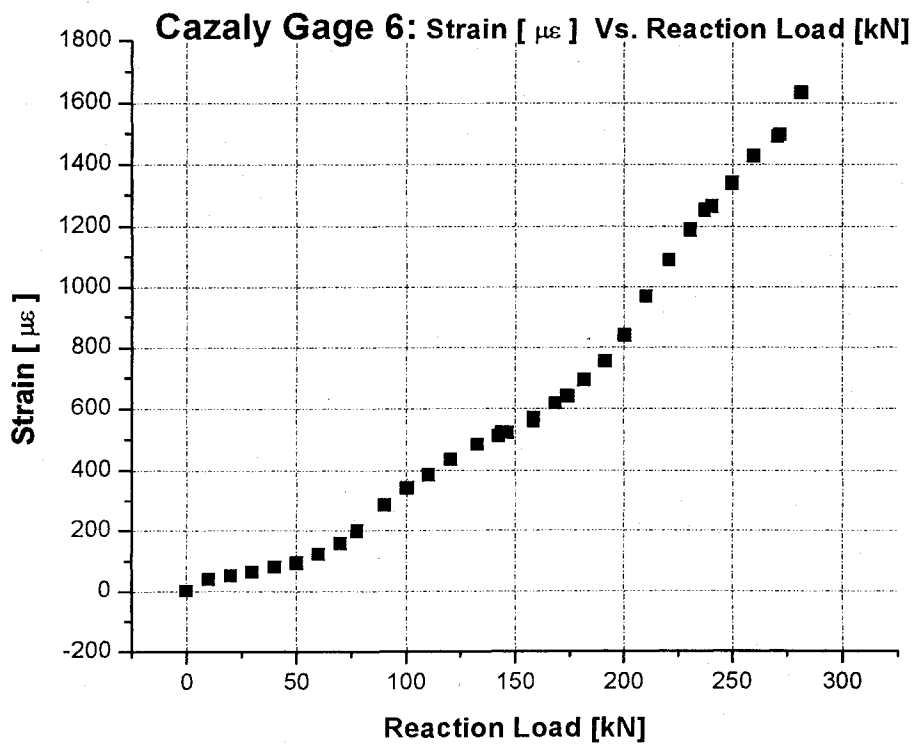
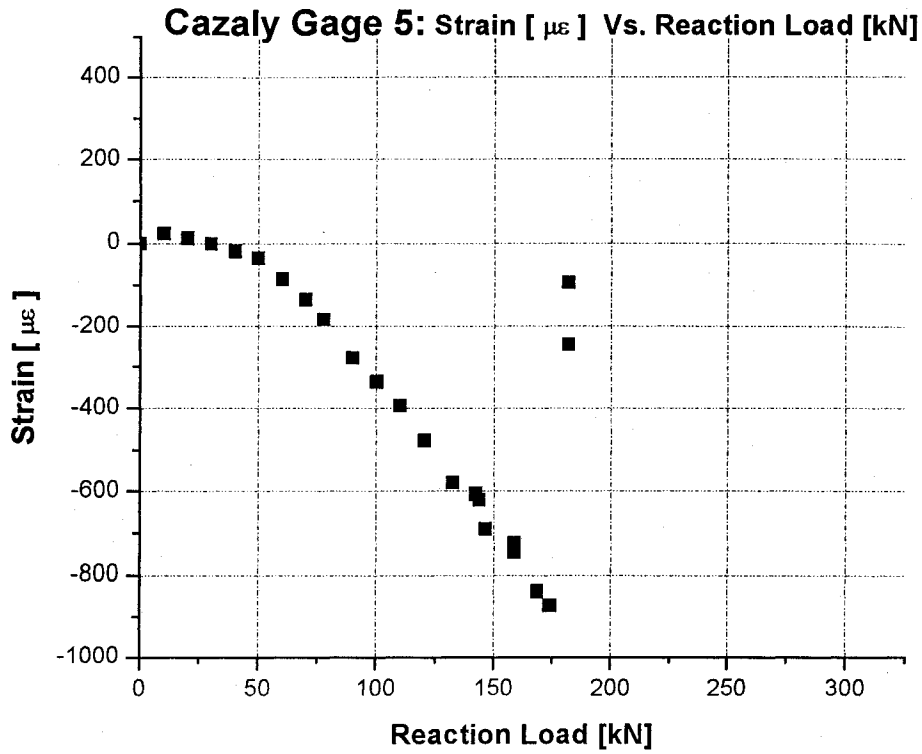
## Lab Scale Beam 2: Measurement Device Parameters

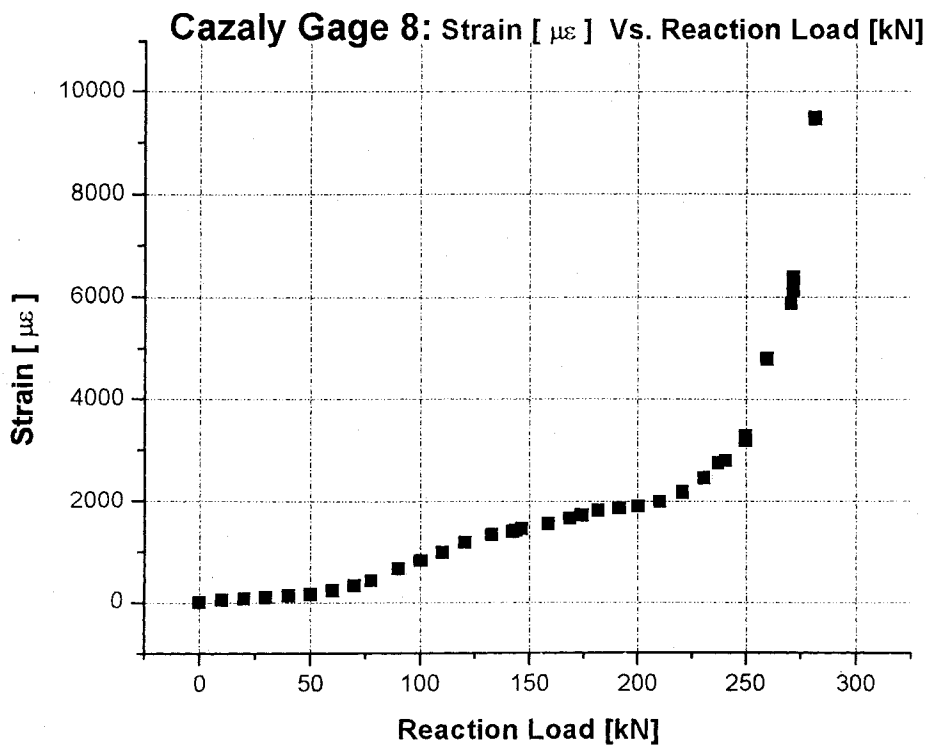
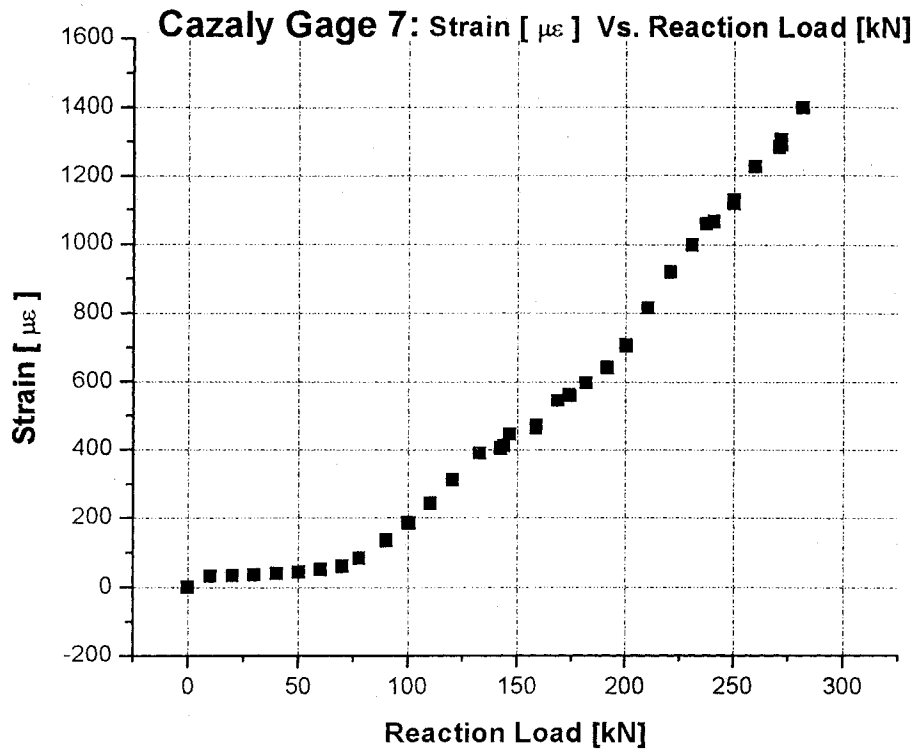
Parameter	Gauge Factor	Resistance	Temp Comp	Other Data
AM 1	2.11 +/- 1.0%	120Ω	11.7 ppm/°C	Kyowa 5mm KFG-05-120-C1-11
AM 2	2.11 +/- 1.0%	120Ω	11.7 ppm/°C	Kyowa 5mm KFG-05-120-C1-12
AM 3	2.11 +/- 1.0%	120Ω	11.7 ppm/°C	Kyowa 5mm KFG-05-120-C1-13
AM 4	2.11 +/- 1.0%	120Ω	11.7 ppm/°C	Kyowa 5mm KFG-05-120-C1-14
AM 5	2.11 +/- 1.0%	120Ω	11.7 ppm/°C	Kyowa 5mm KFG-05-120-C1-15
AM 6	2.11 +/- 1.0%	120Ω	11.7 ppm/°C	Kyowa 5mm KFG-05-120-C1-16
AM 7	2.11 +/- 1.0%	120Ω	11.7 ppm/°C	Kyowa 5mm KFG-05-120-C1-17
AM 8	2.11 +/- 1.0%	120Ω	11.7 ppm/°C	Kyowa 5mm KFG-05-120-C1-18
AM 9	2.11 +/- 1.0%	120Ω	11.7 ppm/°C	Kyowa 5mm KFG-05-120-C1-19
AM 10	2.11 +/- 1.0%	120Ω	11.7 ppm/°C	Kyowa 5mm KFG-05-120-C1-20
AM 11	2.11 +/- 1.0%	120Ω	11.7 ppm/°C	Kyowa 5mm KFG-05-120-C1-21
AM 12	2.11 +/- 1.0%	120Ω	11.7 ppm/°C	Kyowa 5mm KFG-05-120-C1-22
AM 13	2.11 +/- 1.0%	120Ω	11.7 ppm/°C	Kyowa 5mm KFG-05-120-C1-23
EG 1	2.05 +/- 1.0%	120Ω	11.7 ppm/°C	Vishay/MG Type 120 Embedment
EG 2	2.05 +/- 1.0%	120Ω	11.7 ppm/°C	Vishay/MG Type 120 Embedment
EG 3	2.05 +/- 1.0%	120Ω	11.7 ppm/°C	Vishay/MG Type 120 Embedment
CG 1	2.11 +/- 1.0%	120Ω	11.7 ppm/°C	Kyowa 30mm KFG-30-120-C1-11
CG 2	2.11 +/- 1.0%	120Ω	11.7 ppm/°C	Kyowa 30mm KFG-30-120-C1-11
CG 3	2.11 +/- 1.0%	120Ω	11.7 ppm/°C	Kyowa 30mm KFG-30-120-C1-11
CG 4	2.11 +/- 1.0%	120Ω	11.7 ppm/°C	Kyowa 30mm KFG-30-120-C1-11
CG 5	2.11 +/- 1.0%	120Ω	11.7 ppm/°C	Kyowa 30mm KFG-30-120-C1-11
CG 6	2.11 +/- 1.0%	120Ω	11.7 ppm/°C	Kyowa 30mm KFG-30-120-C1-11
CG 7	2.11 +/- 1.0%	120Ω	11.7 ppm/°C	Kyowa 30mm KFG-30-120-C1-11
CG 8	2.11 +/- 1.0%	120Ω	11.7 ppm/°C	Kyowa 30mm KFG-30-120-C1-11
CG 9	2.11 +/- 1.0%	120Ω	11.7 ppm/°C	Kyowa 30mm KFG-30-120-C1-11
CG 10	2.11 +/- 1.0%	120Ω	11.7 ppm/°C	Kyowa 30mm KFG-30-120-C1-11
CG 11	2.11 +/- 1.0%	120Ω	11.7 ppm/°C	Kyowa 30mm KFG-30-120-C1-11
CG 12	2.11 +/- 1.0%	120Ω	11.7 ppm/°C	Kyowa 30mm KFG-30-120-C1-11
CG 13	2.11 +/- 1.0%	120Ω	11.7 ppm/°C	Kyowa 30mm KFG-30-120-C1-11
LP 1	n/a	n/a	n/a	U Windsor Resistance Pot
LP 2	n/a	n/a	n/a	U Windsor Resistance Pot
LP 3	n/a	n/a	n/a	U Windsor Resistance Pot
LP 4	n/a	n/a	n/a	U Windsor Resistance Pot
Load Cell 1	See Cal'bn	n/a	n/a	See 100kip Cell Calibration Sheet
Load Cell 2	See Cal'bn	n/a	n/a	See 200kip Cell Calibration Sheet

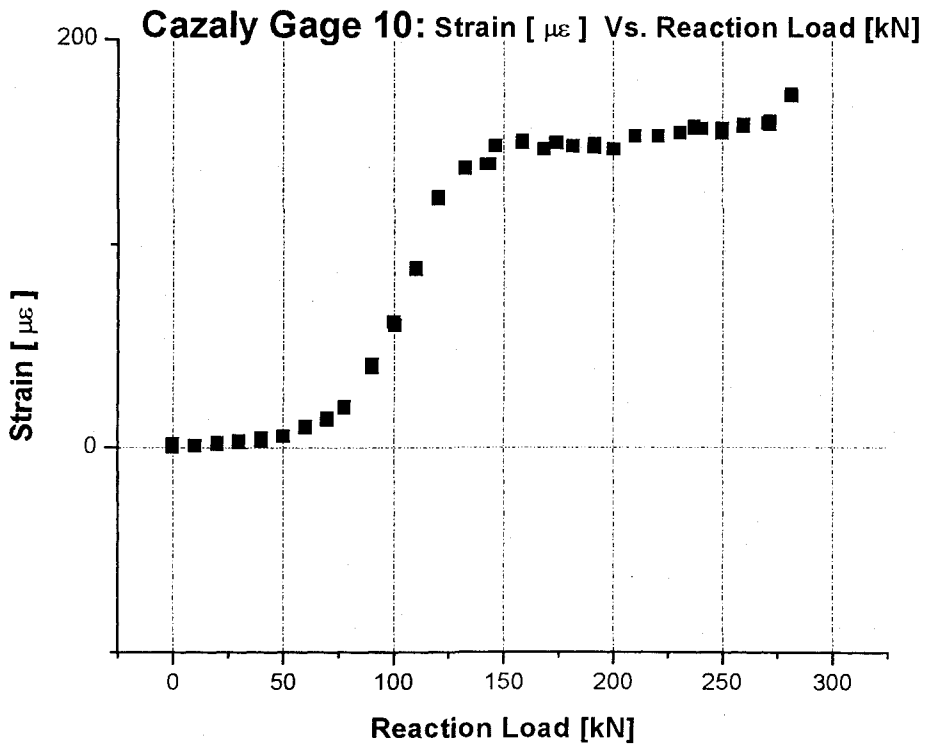
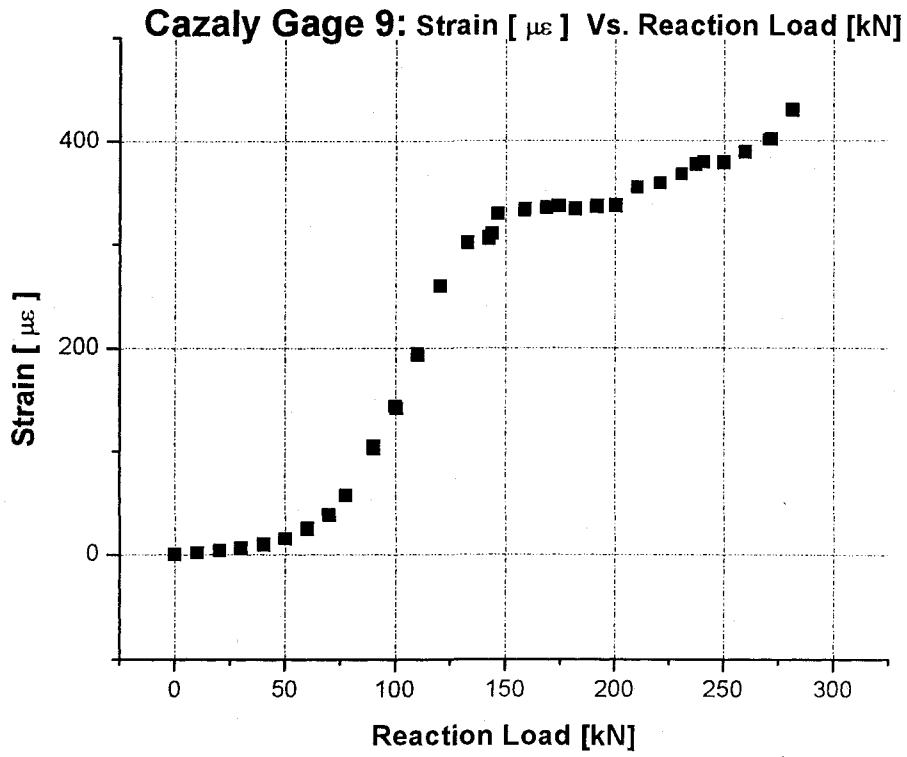


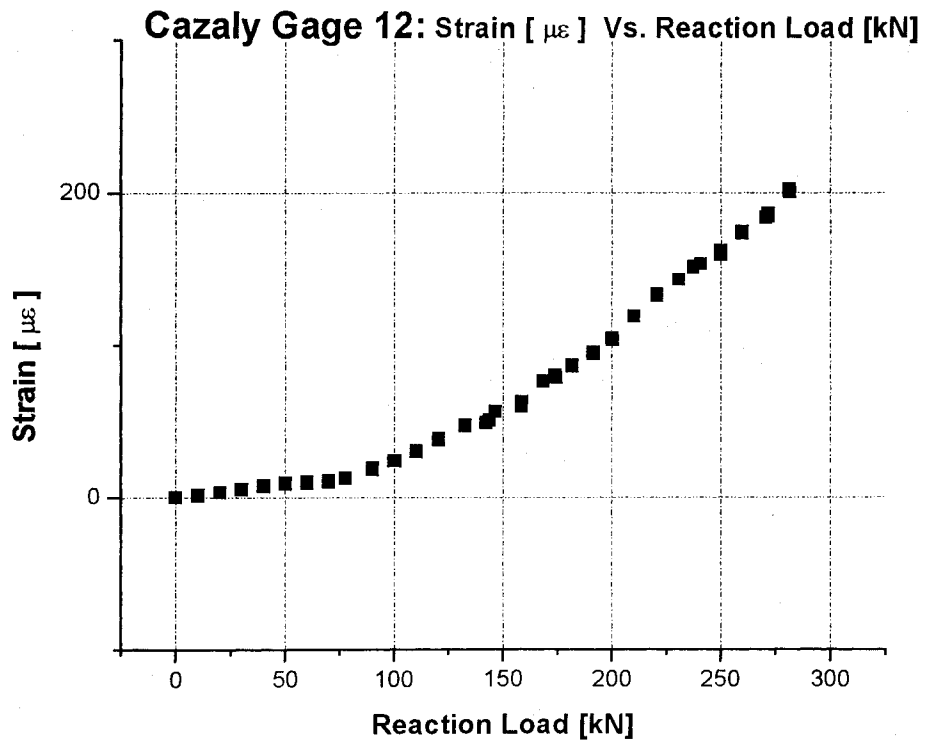
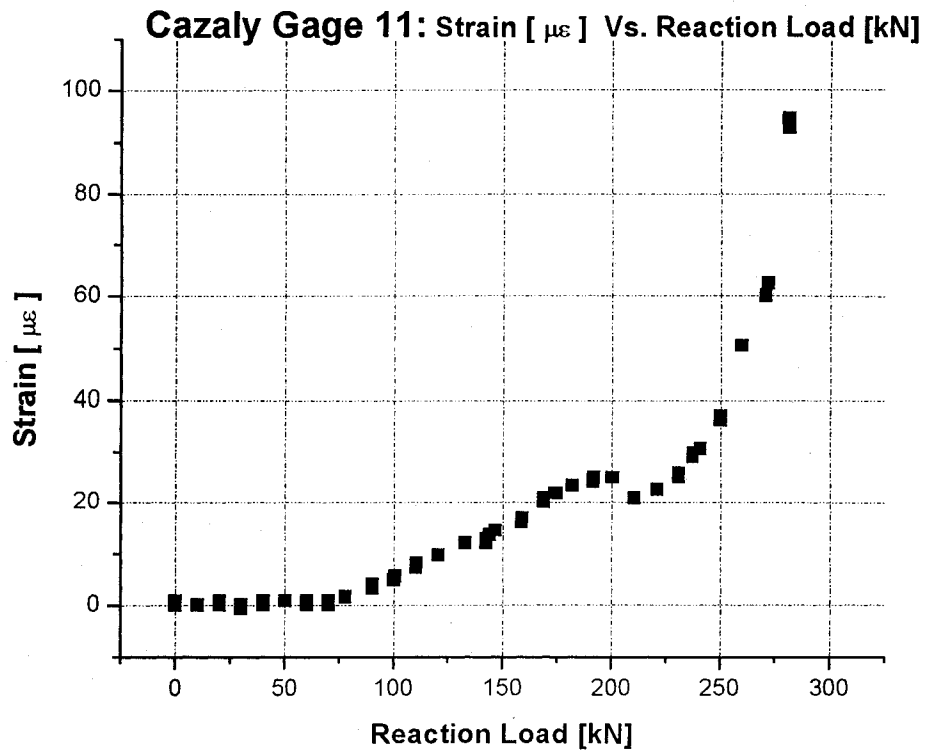


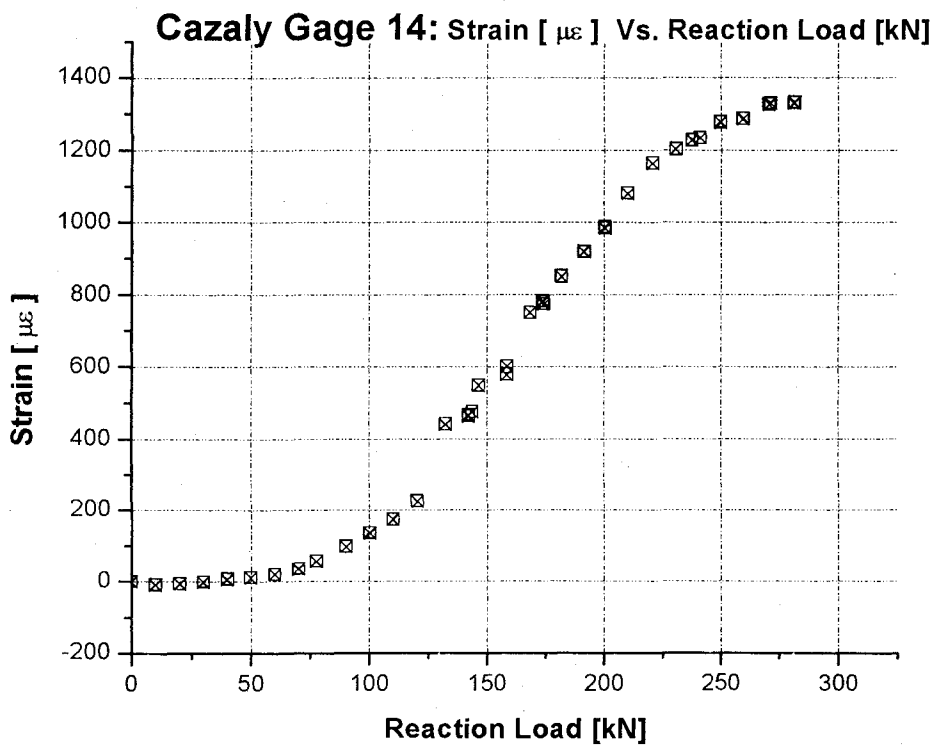
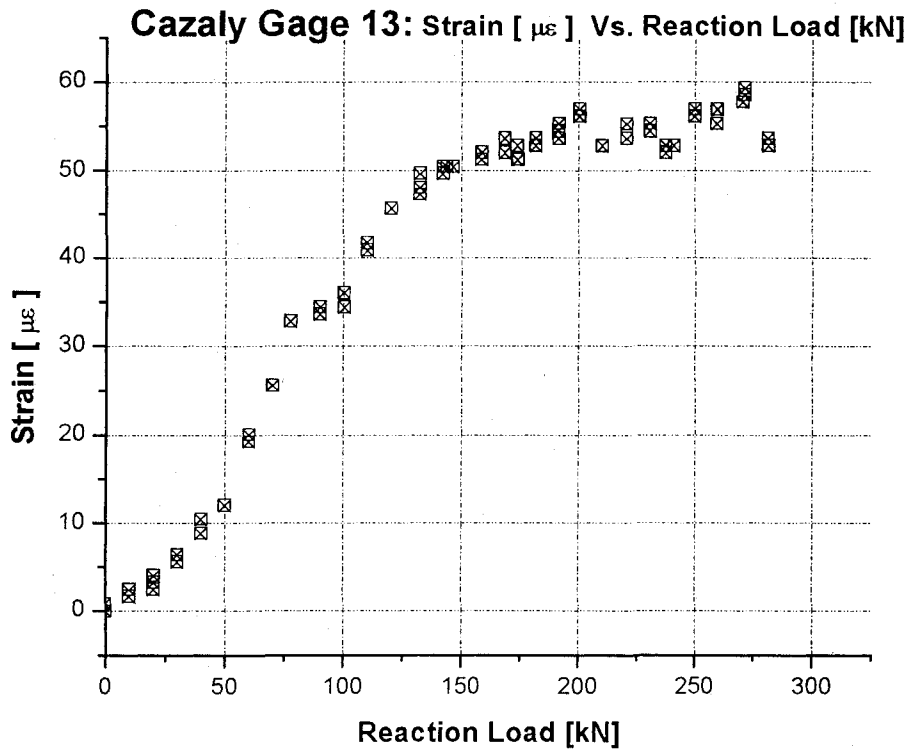


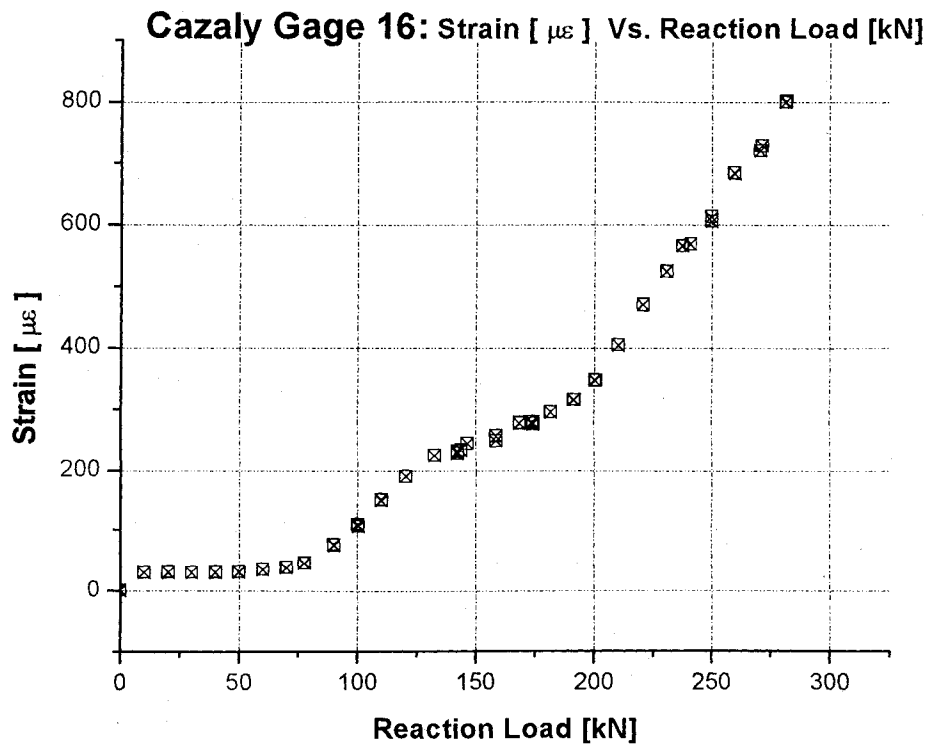
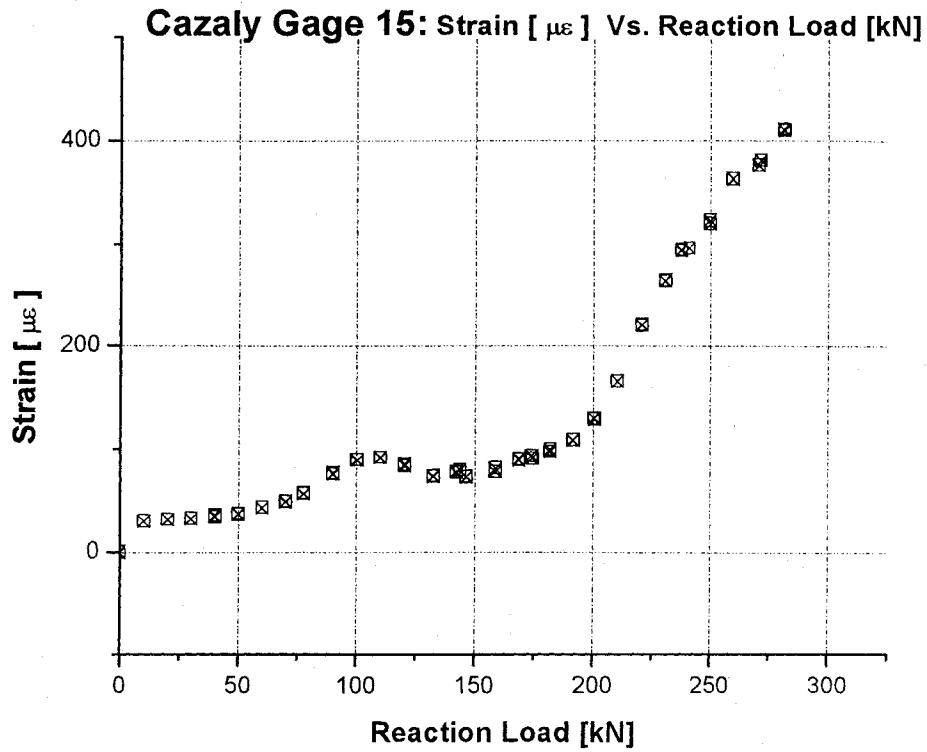




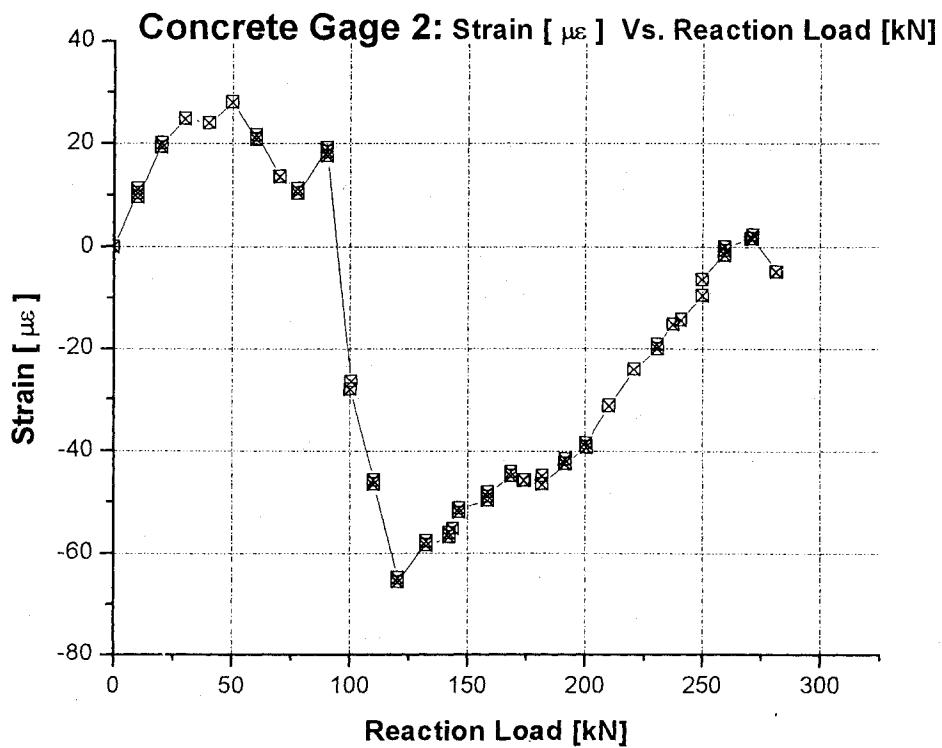
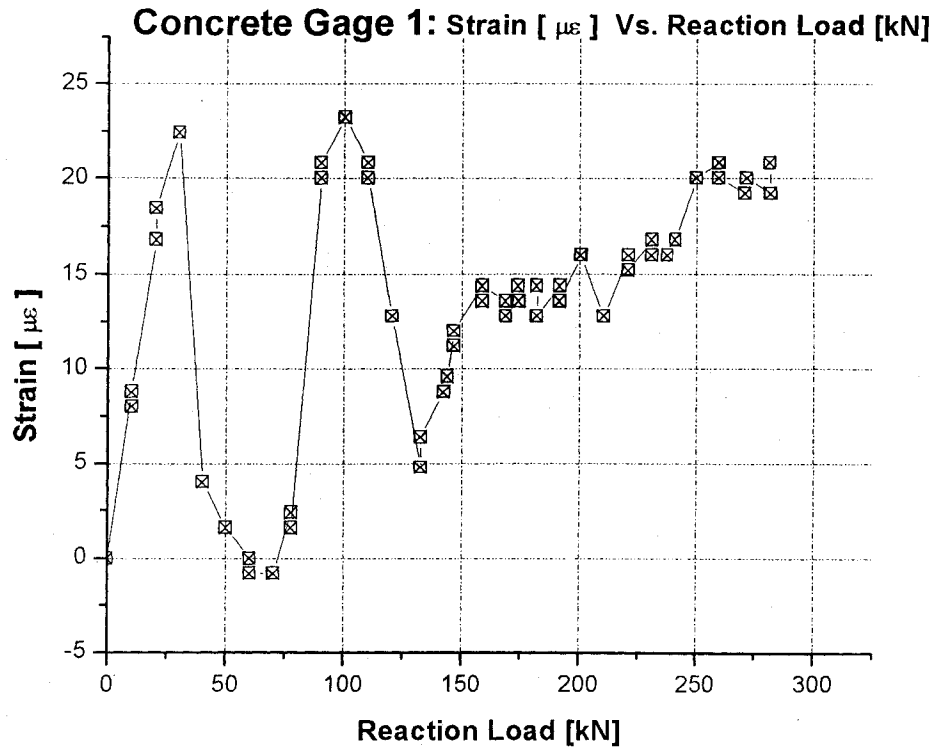


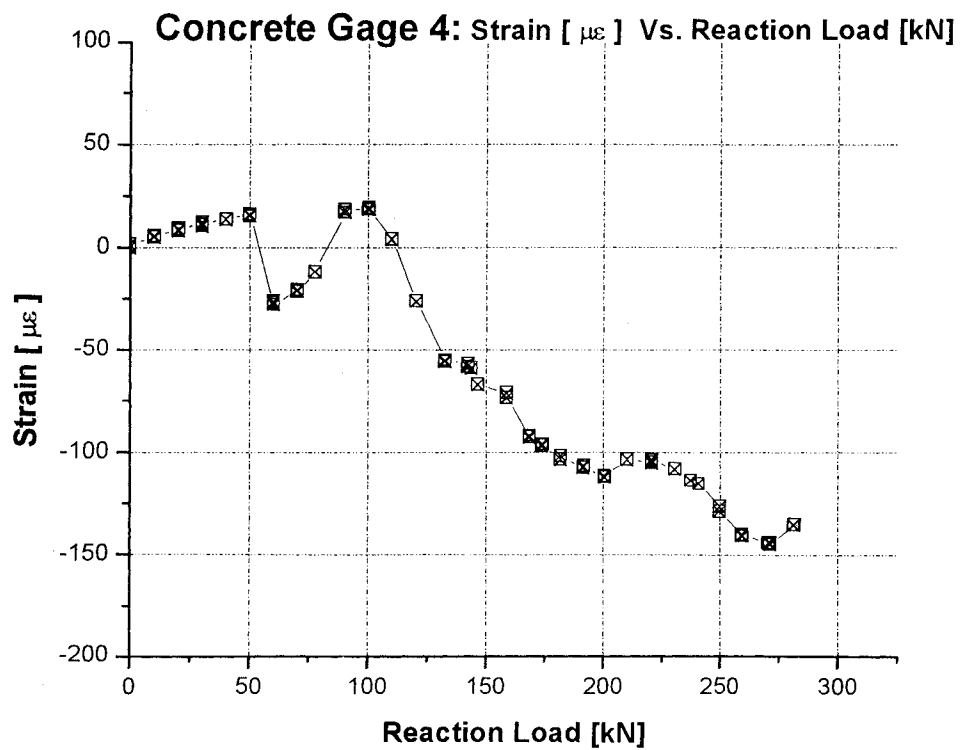
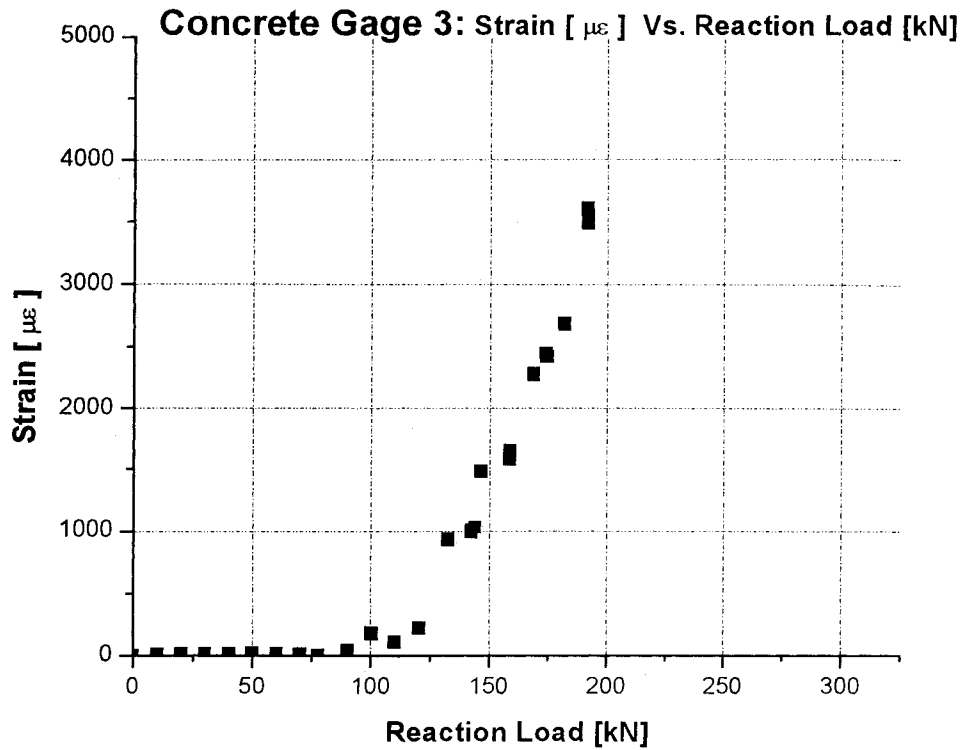


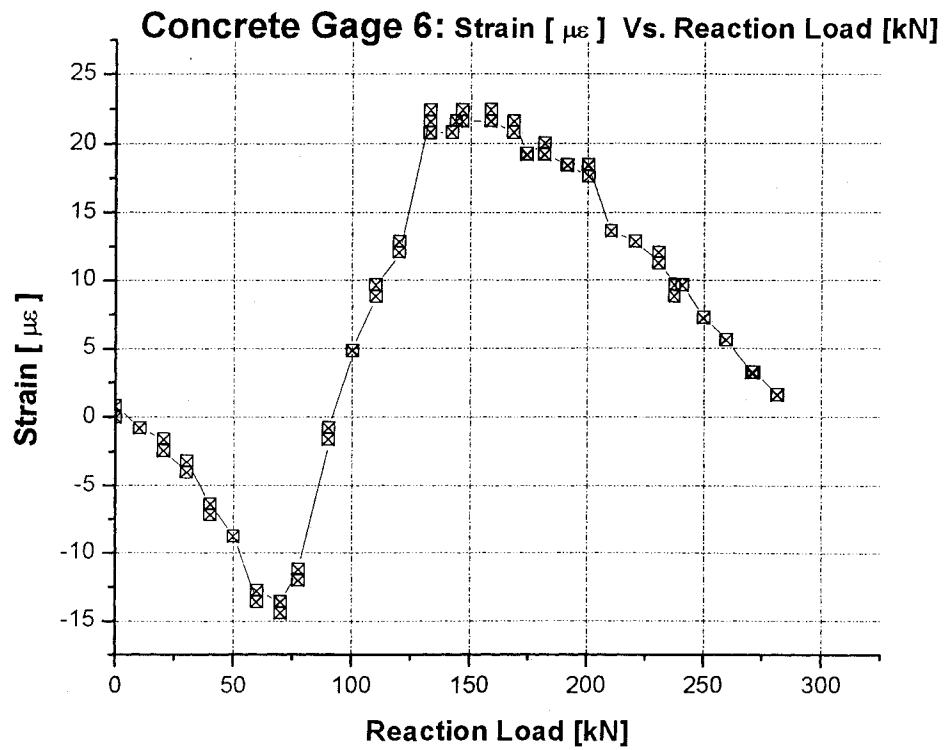
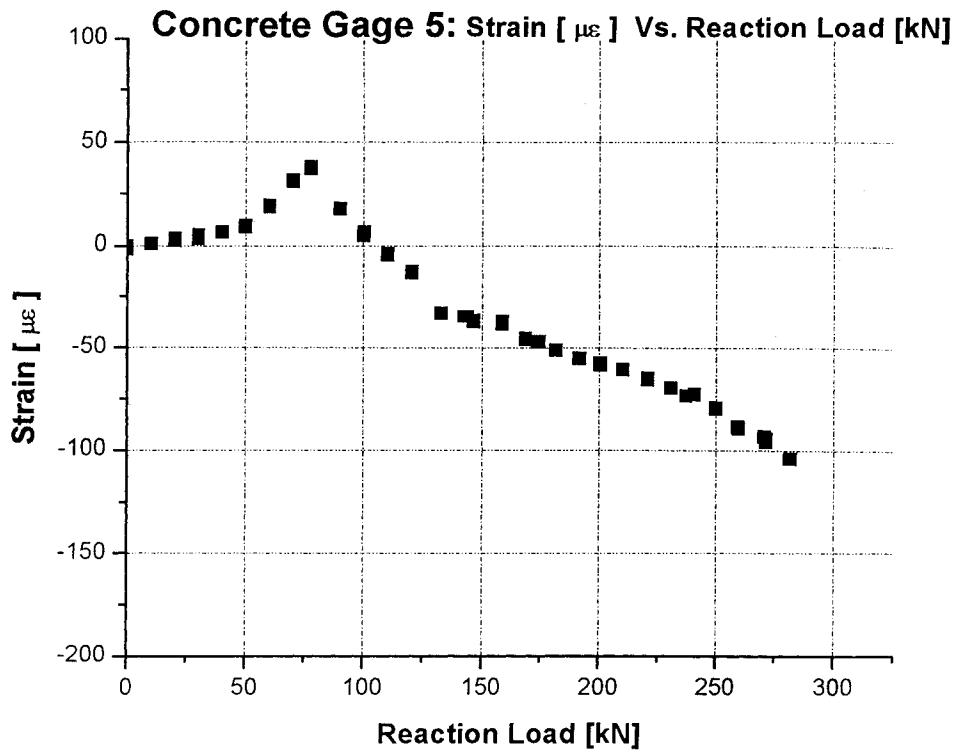


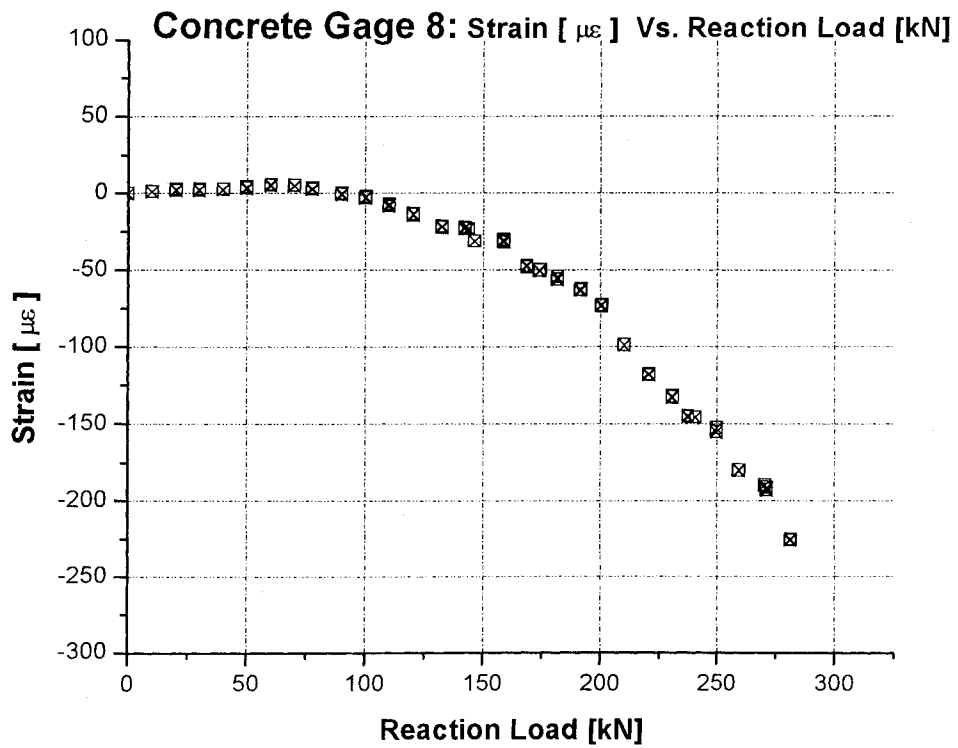
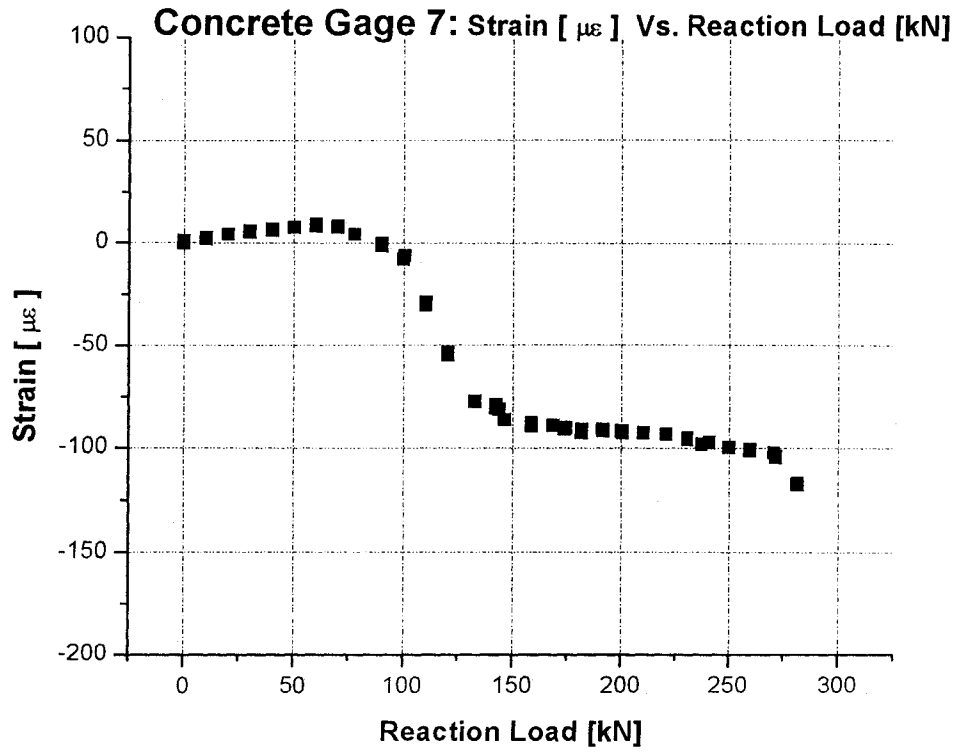


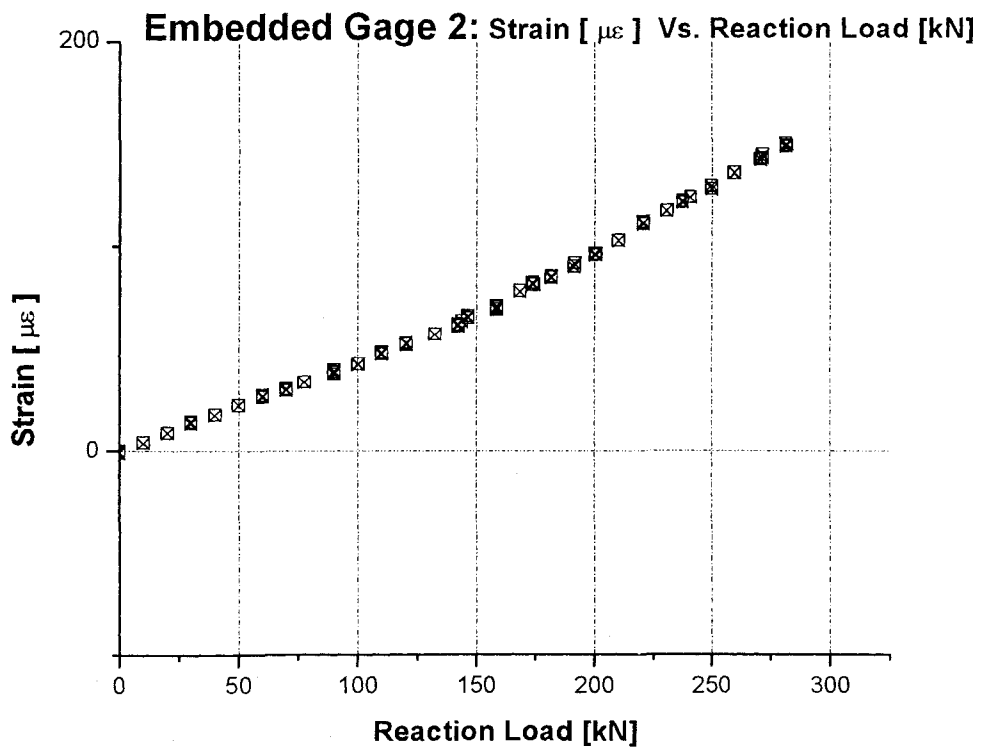
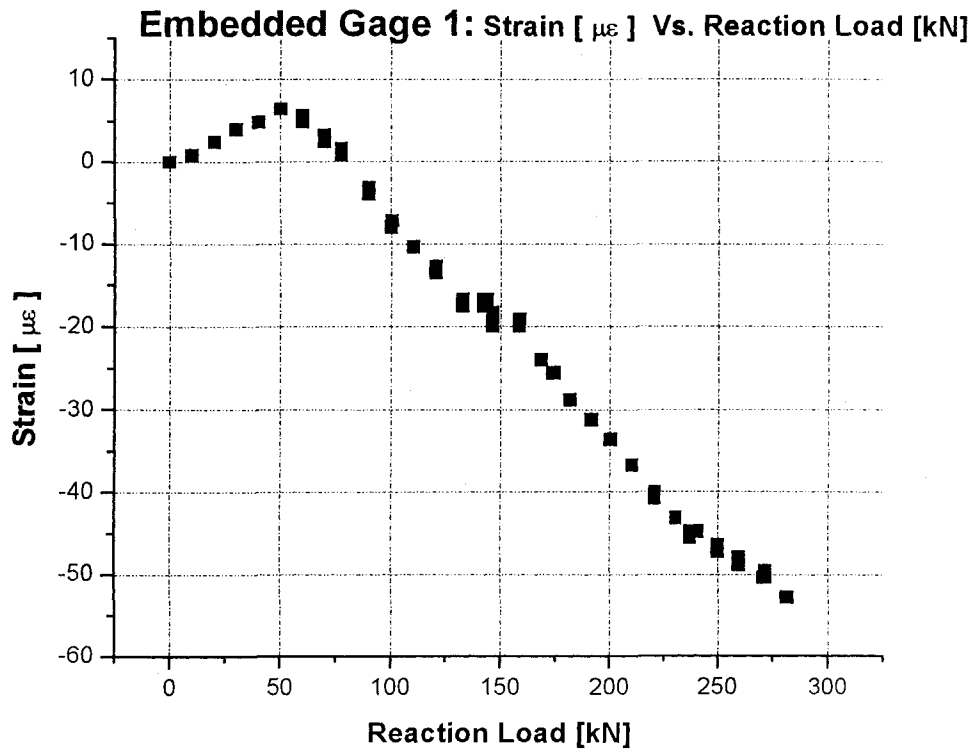


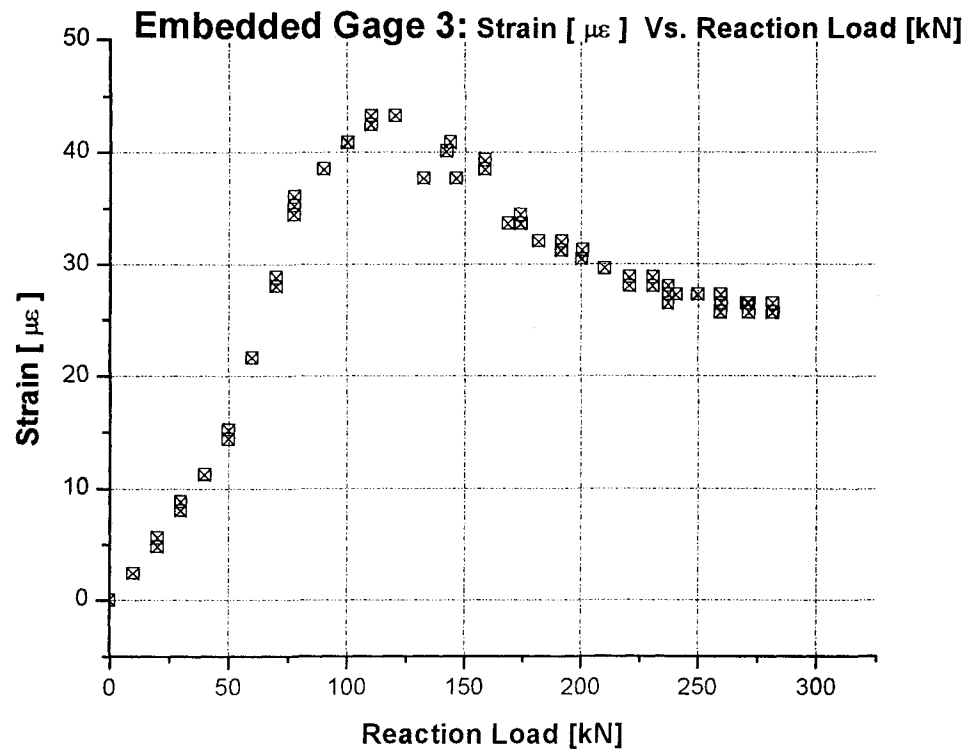


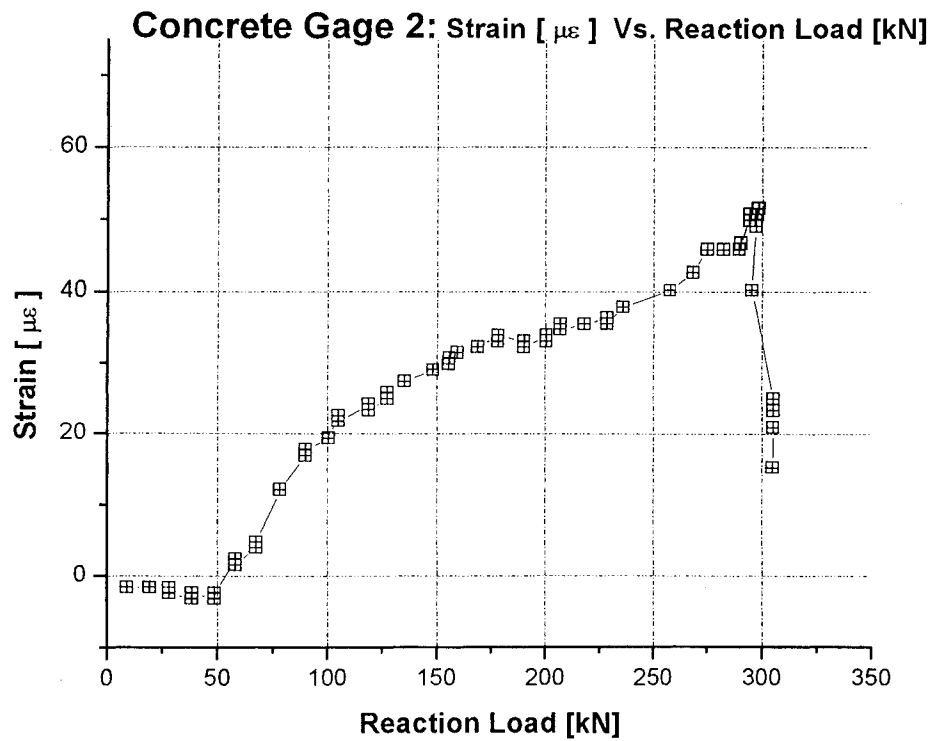
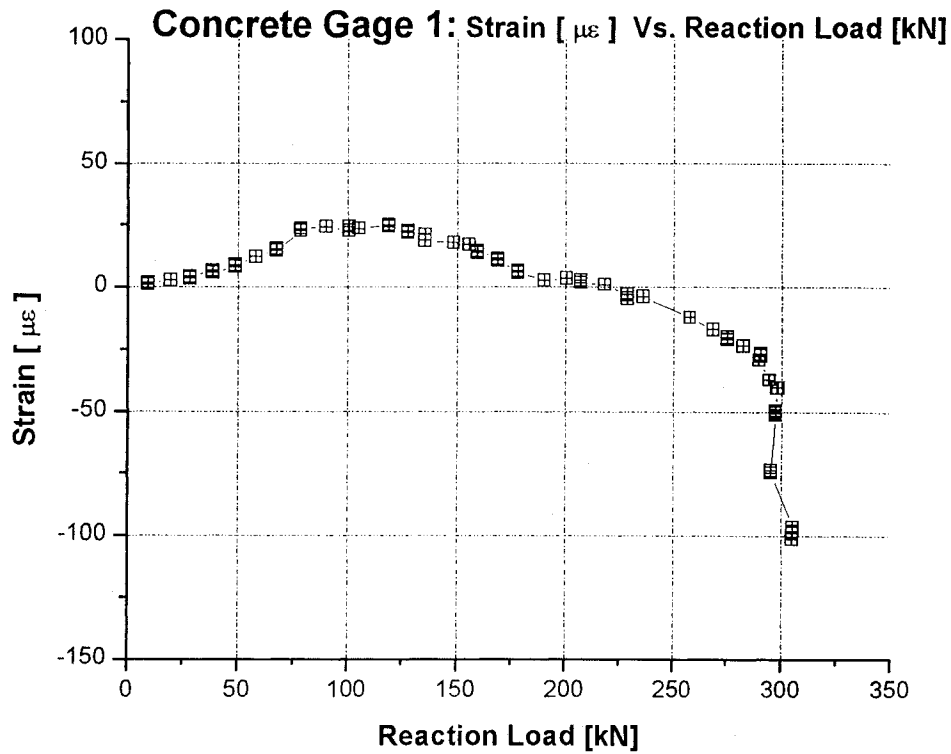


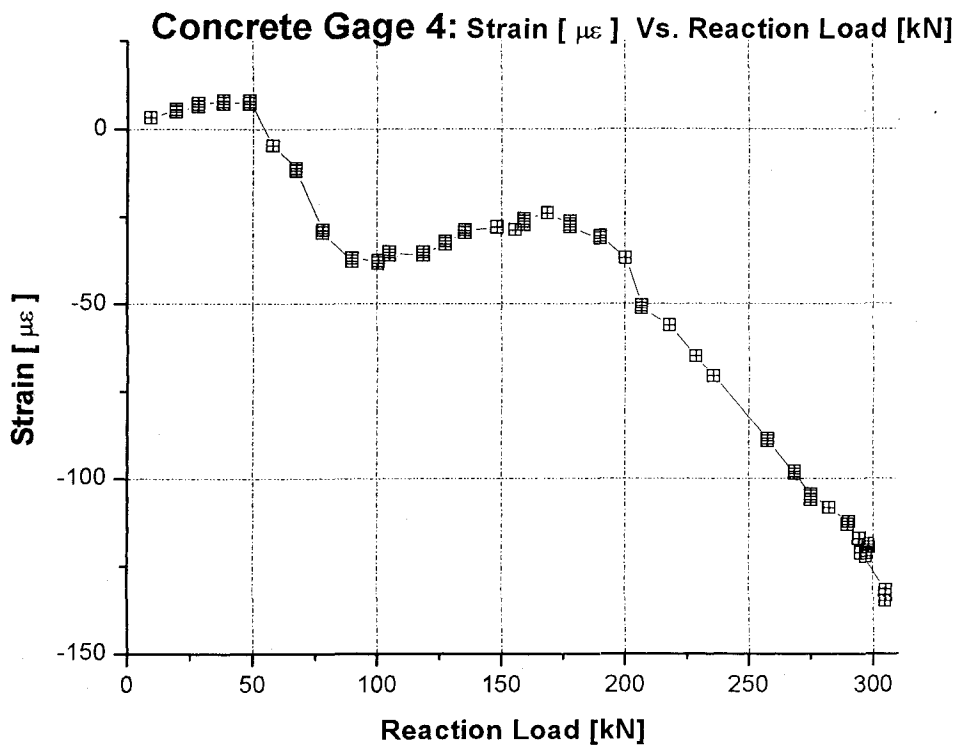
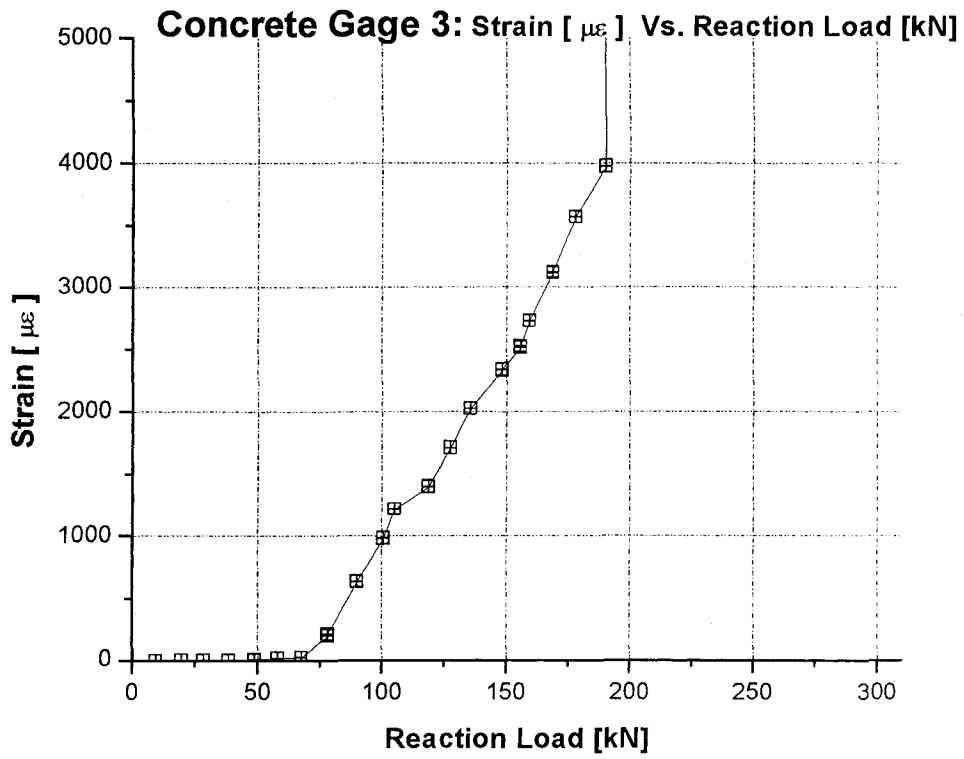




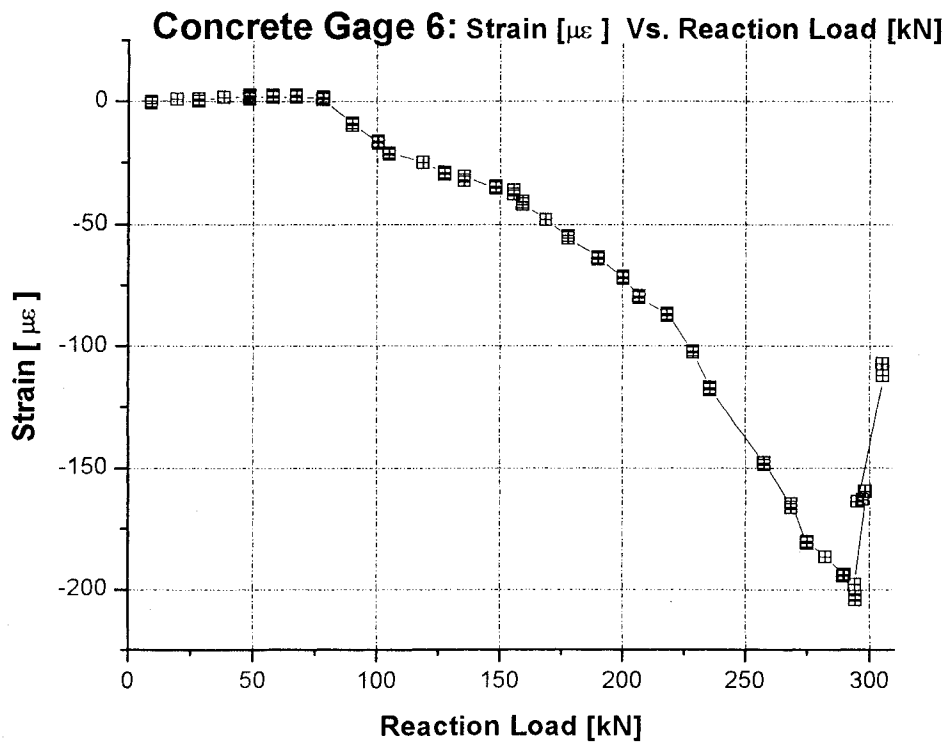
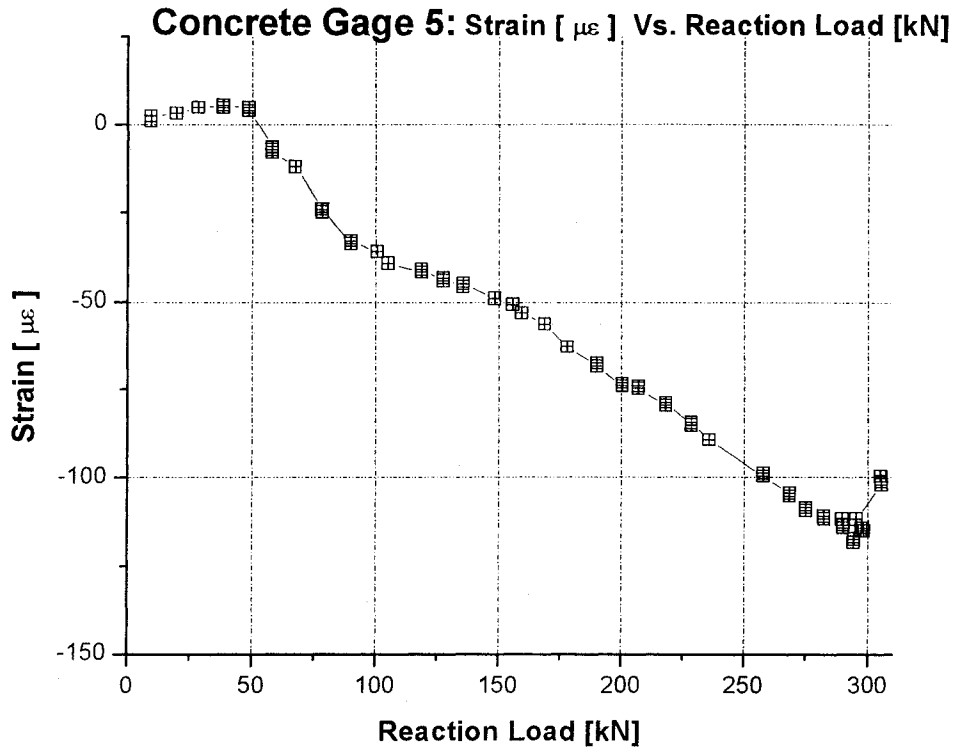


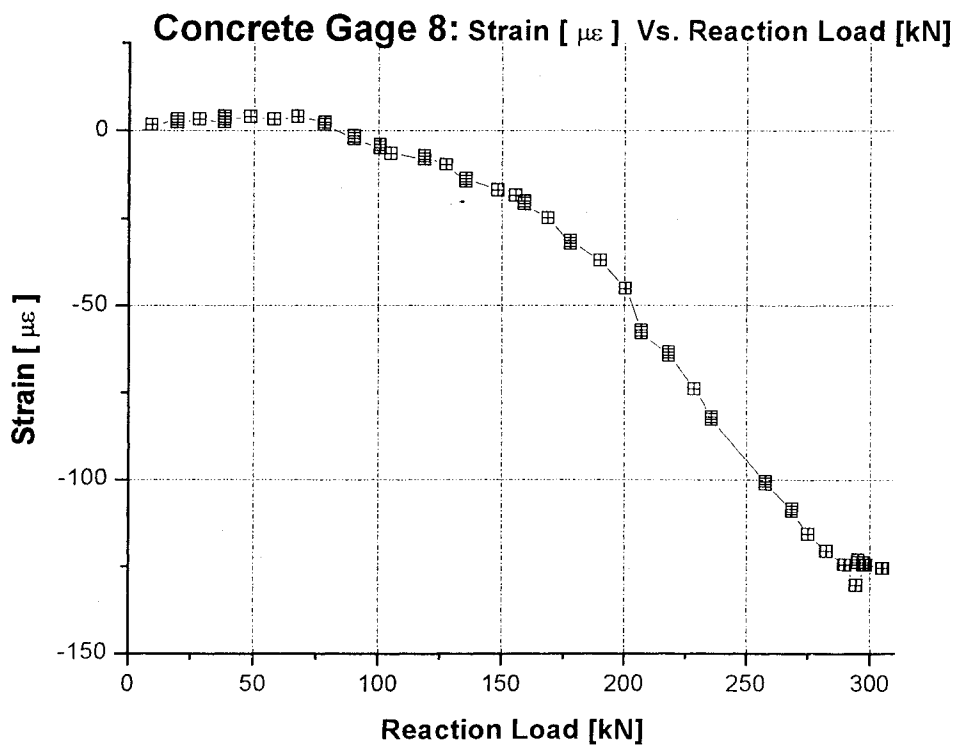
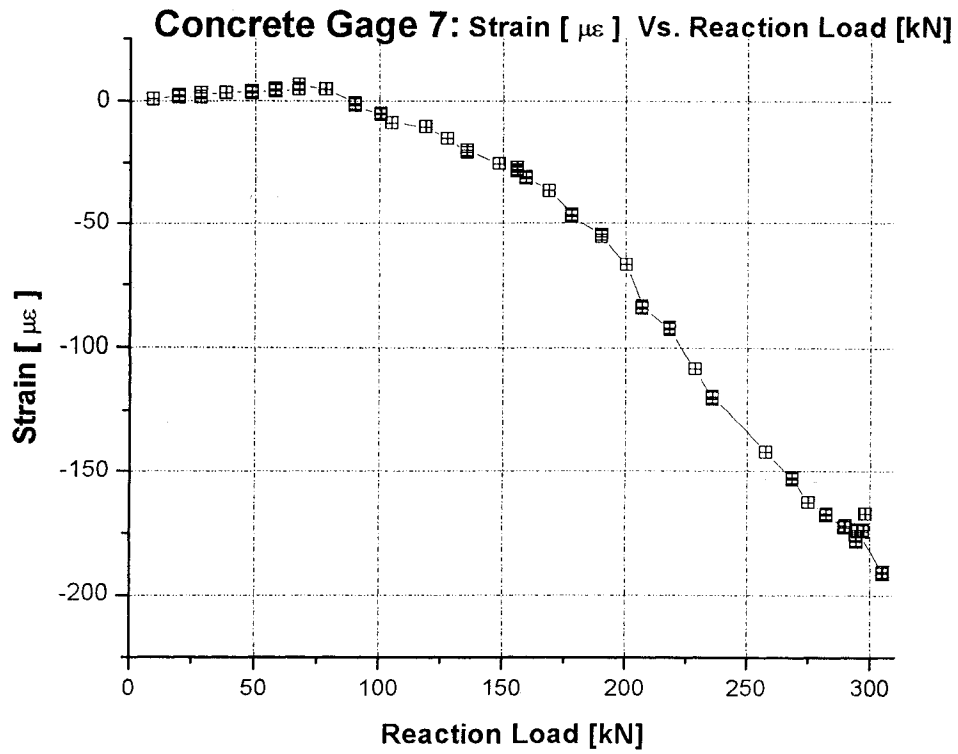


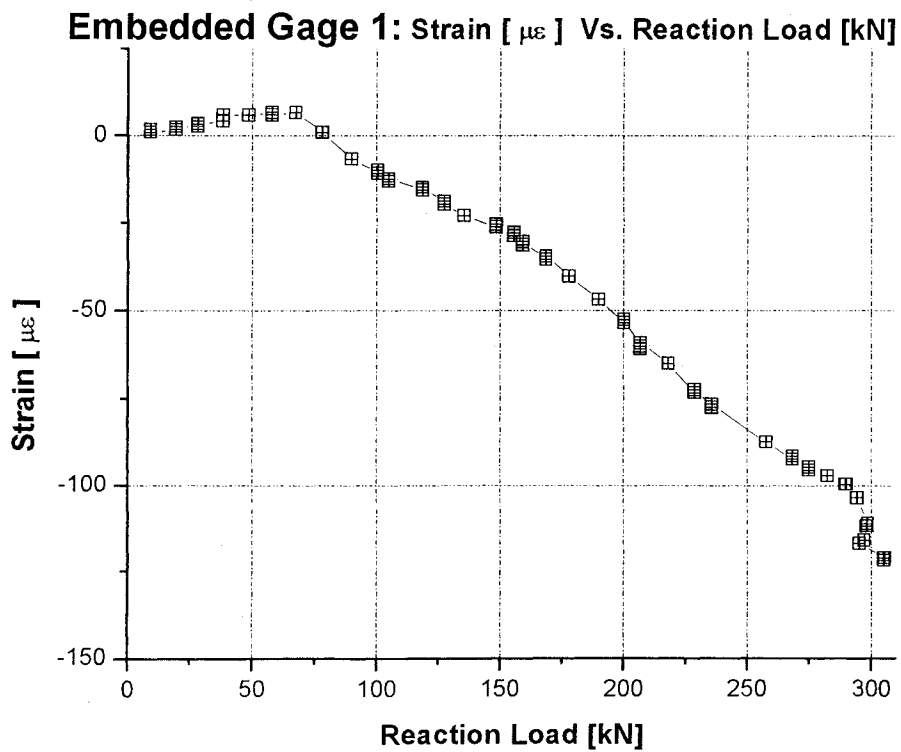
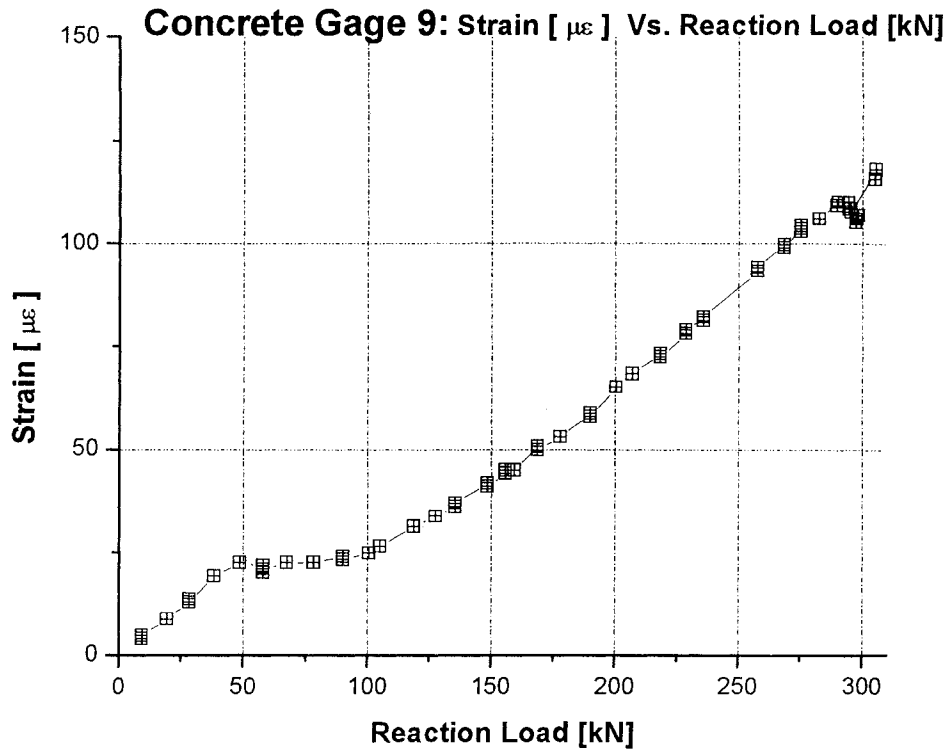




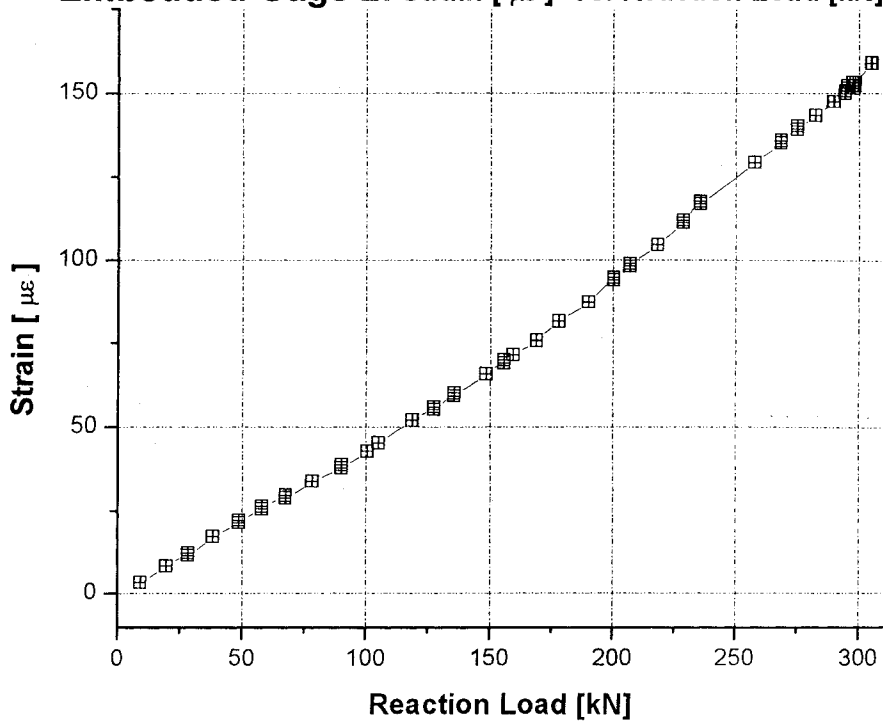




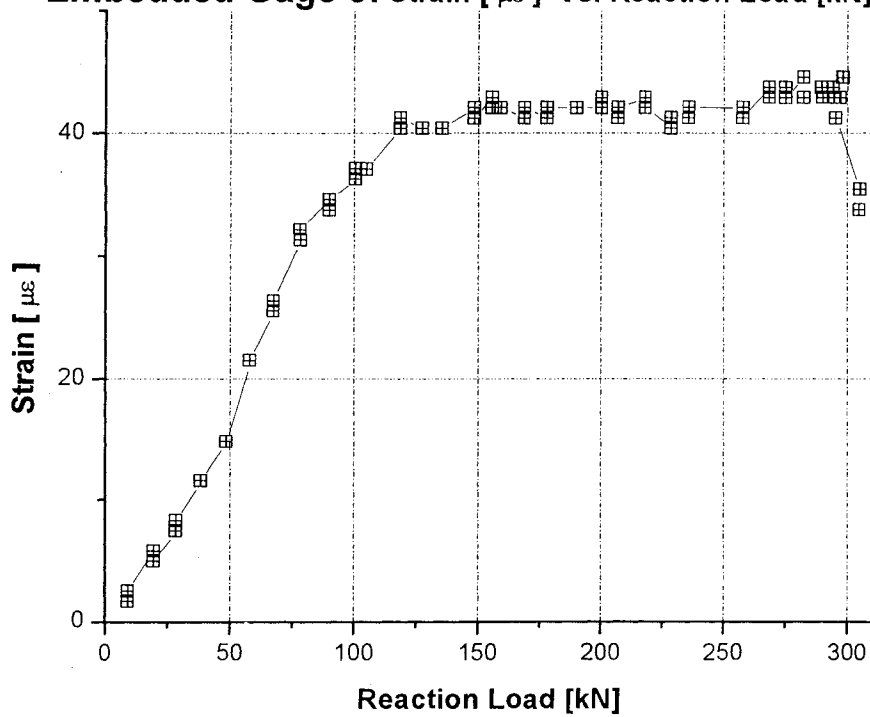




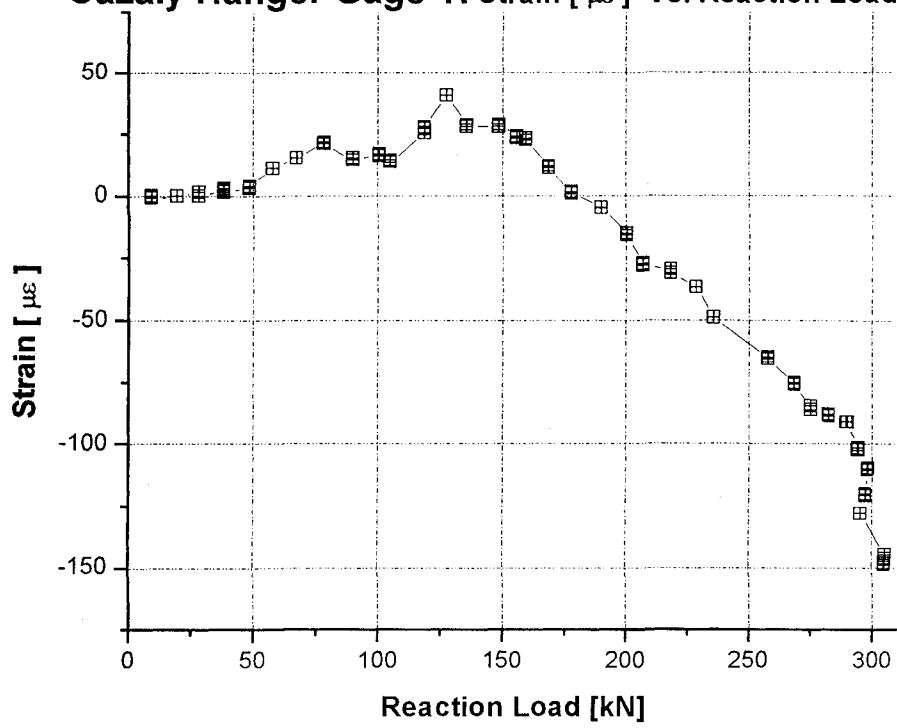
**Embedded Gage 2: Strain [ $\mu\epsilon$ ] Vs. Reaction Load [kN]**



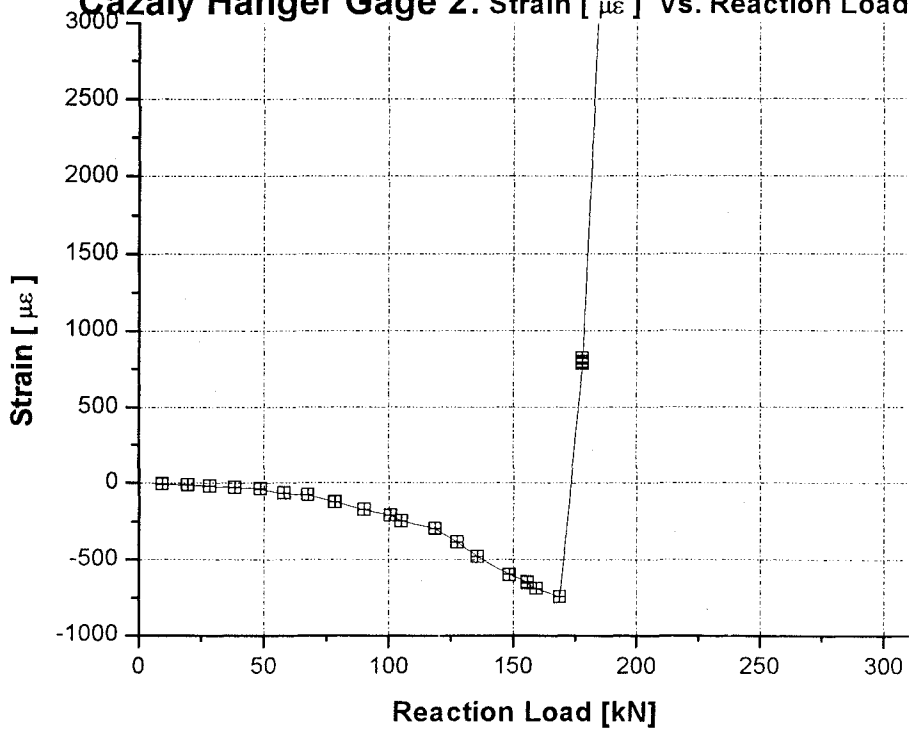
**Embedded Gage 3: Strain [ $\mu\epsilon$ ] Vs. Reaction Load [kN]**



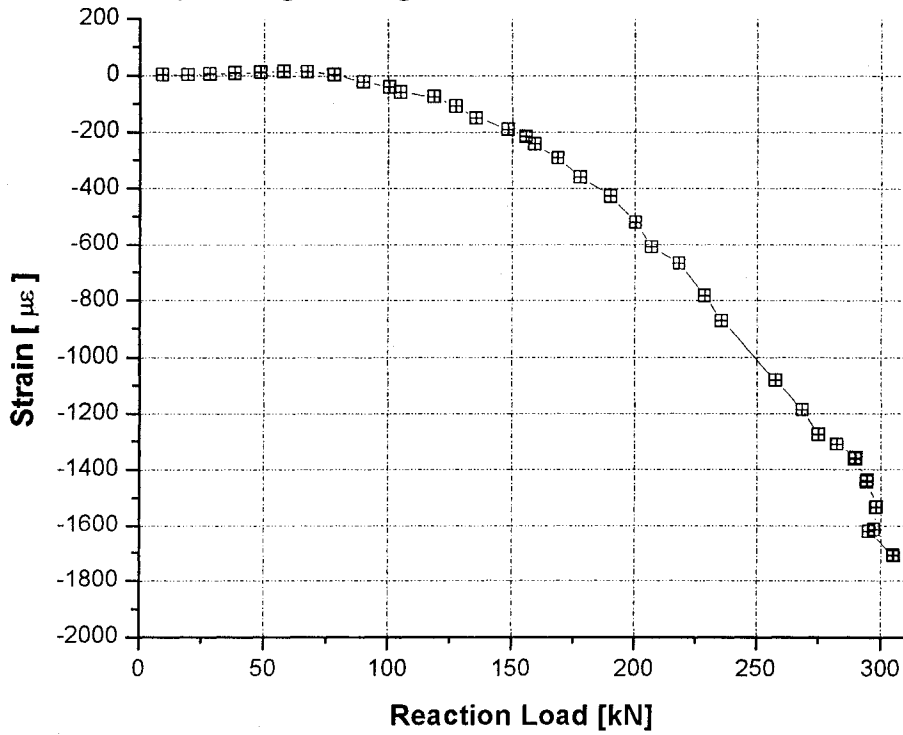
**Cazaly Hanger Gage 1: Strain [  $\mu\epsilon$  ] Vs. Reaction Load [kN]**



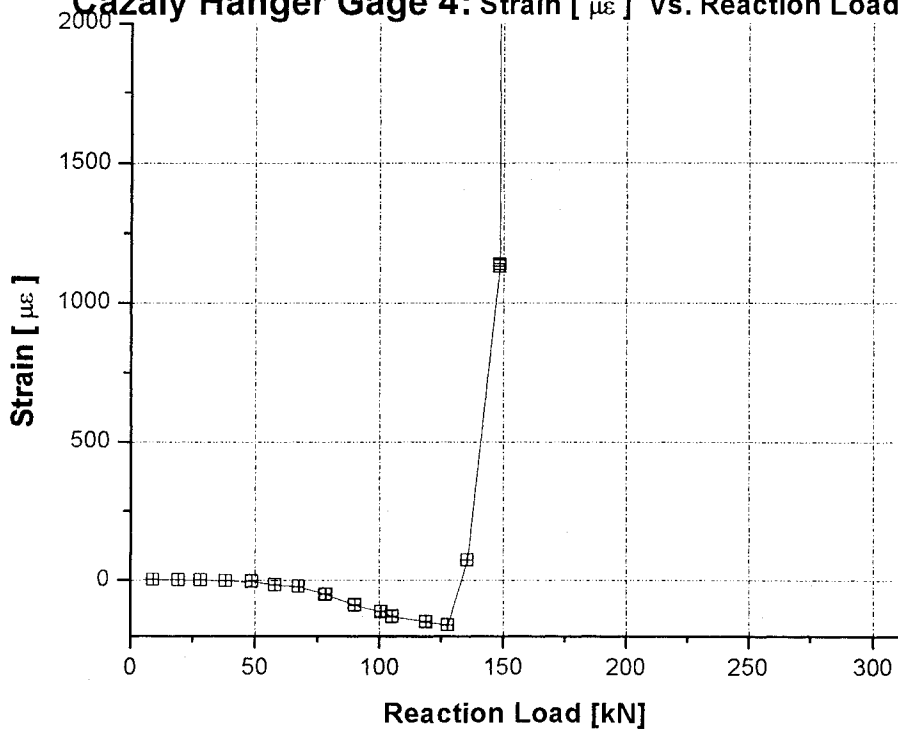
**Cazaly Hanger Gage 2: Strain [  $\mu\epsilon$  ] Vs. Reaction Load [kN]**



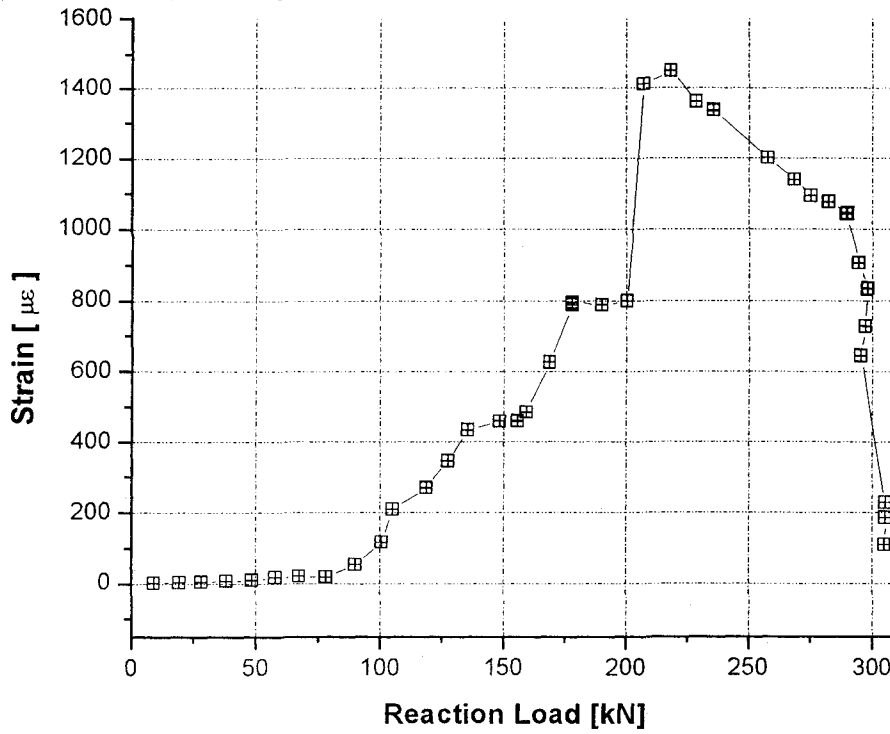
**Cazaly Hanger Gage 3: Strain [ $\mu\epsilon$ ] Vs. Reaction Load [kN]**



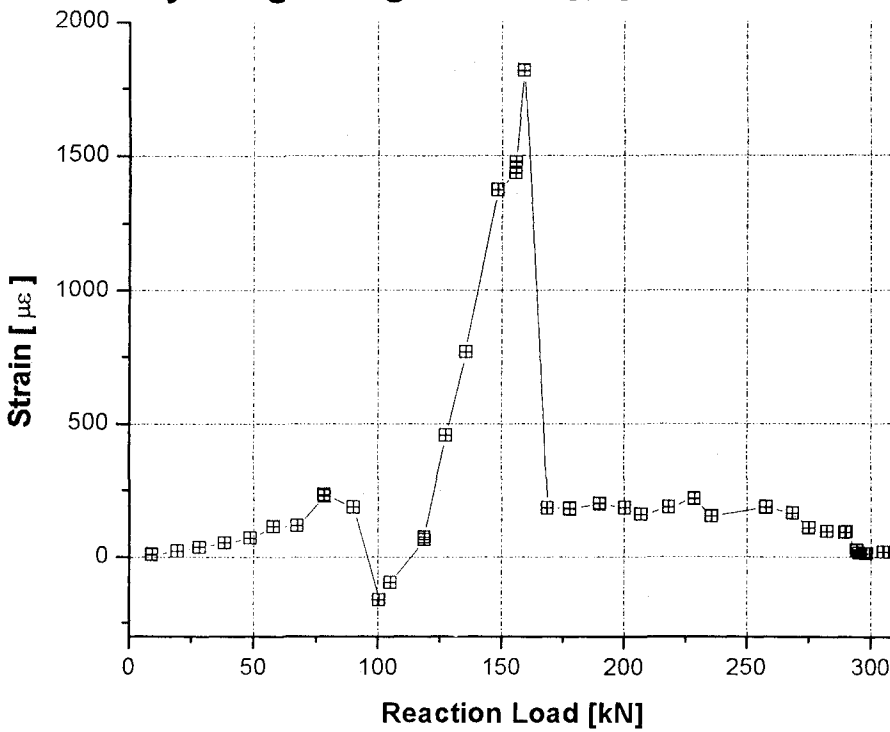
**Cazaly Hanger Gage 4: Strain [ $\mu\epsilon$ ] Vs. Reaction Load [kN]**

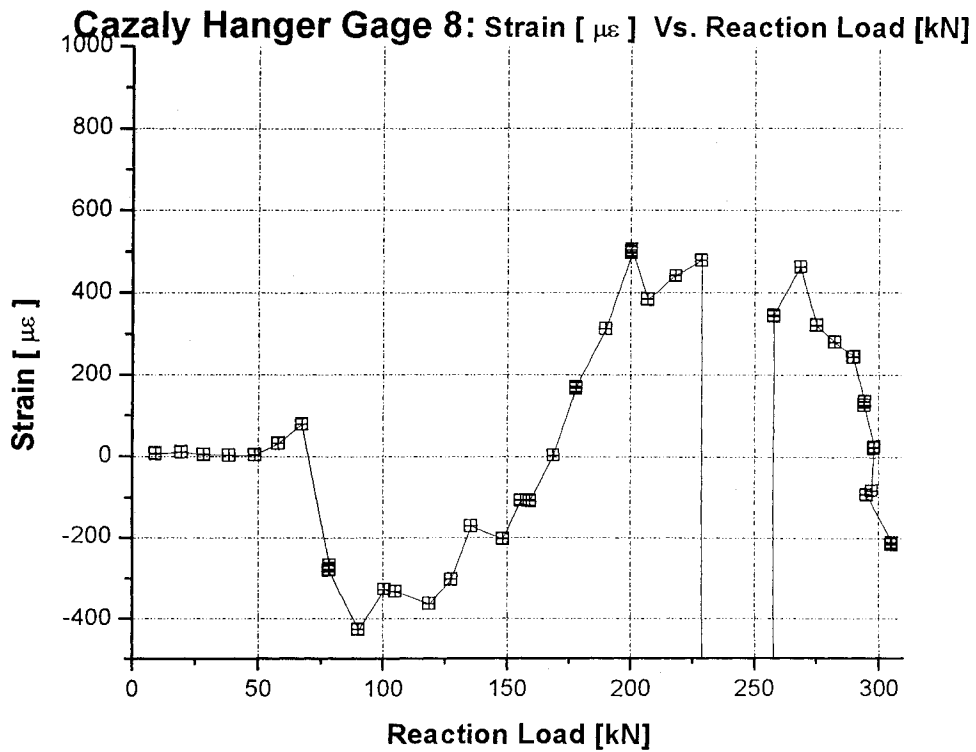
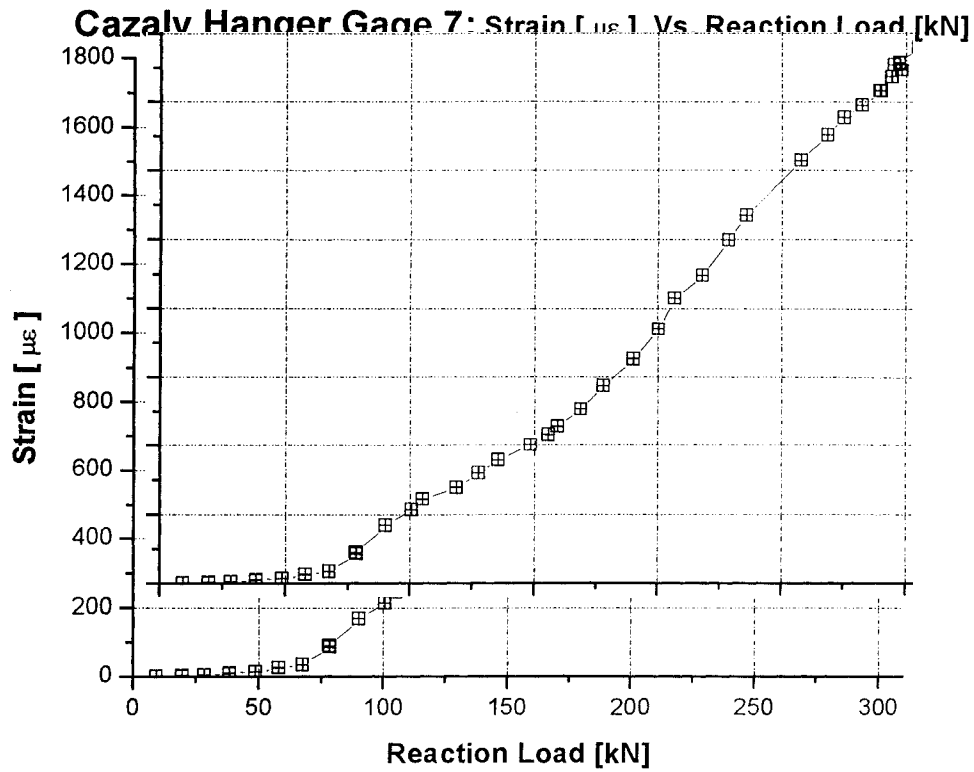


**Cazaly Hanger Gage 5: Strain [  $\mu\epsilon$  ] Vs. Reaction Load [kN]**

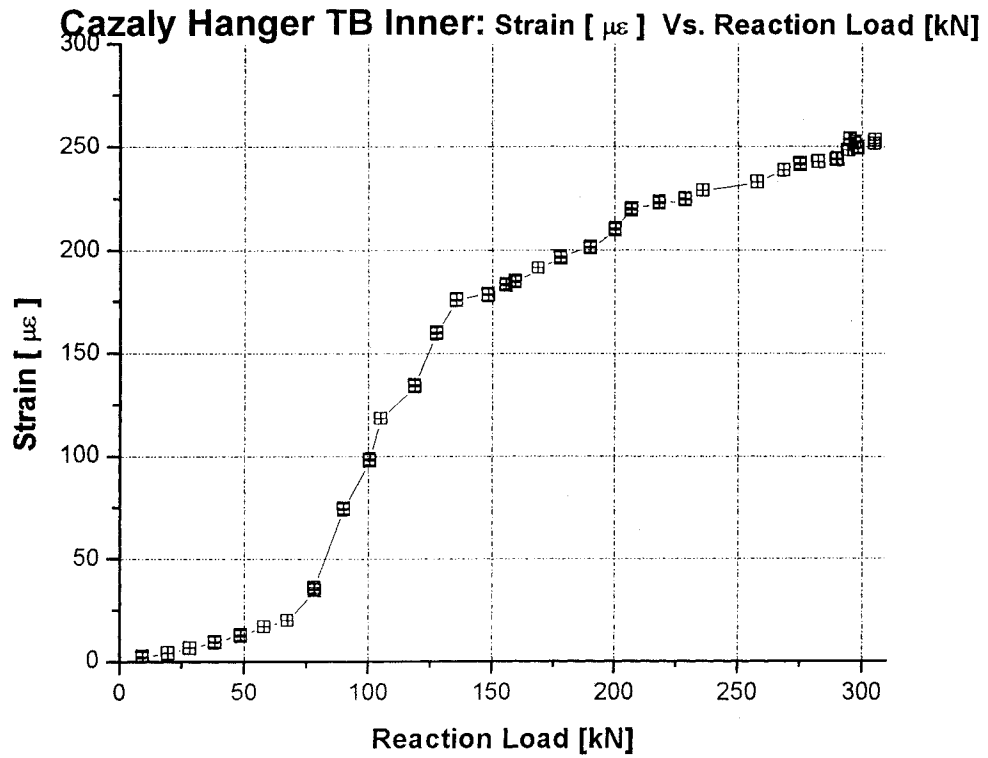


**Cazaly Hanger Gage 6: Strain [  $\mu\epsilon$  ] Vs. Reaction Load [kN]**









## VITA AUCTORIS

Anthony Mandarino

December 28, 1979

### **Education:**

Bachelor of Science (Chemistry)      University of Western Ontario      2002

Bachelor of Engineering Science      University of Western Ontario      2003  
(Structural Engineering)

Special Graduate Student      University of Western Ontario      2004  
Biomedical Engineering

**GENERAL NOTES**

- 1. FINISH = BROOM FINISH
- 2. TB = 350 PSI (@ RELEASE)
- 3. TP = 6000 PSI (@ 28 DAYS)
- 4. AIR ENTRAINMENT =
- 5. INITIAL CAMBER =
- 6. DEFLECTION CAMBER =
- 7. STRAND (IN) =
- 8. REINFORCING COVER =

**PRODUCTION NOTE:  
CAST-IN HARDWARE**

MARK #	QTY.	DESCRIPTION
4	STEM MESH W4xW4	
2	DECK MESH	
2	CASUALY HANGER PROVIDED	
4	SINGLE 2" LIFTING LOOPS	

**PRODUCTION - INFORMATION**

MARK #	QTY.	VOL. (m <sup>3</sup> )	AREA (ft <sup>2</sup> )	WGT. (lbs)
DT-UW	2	1.21		6,600

PROJECT: \_\_\_\_\_

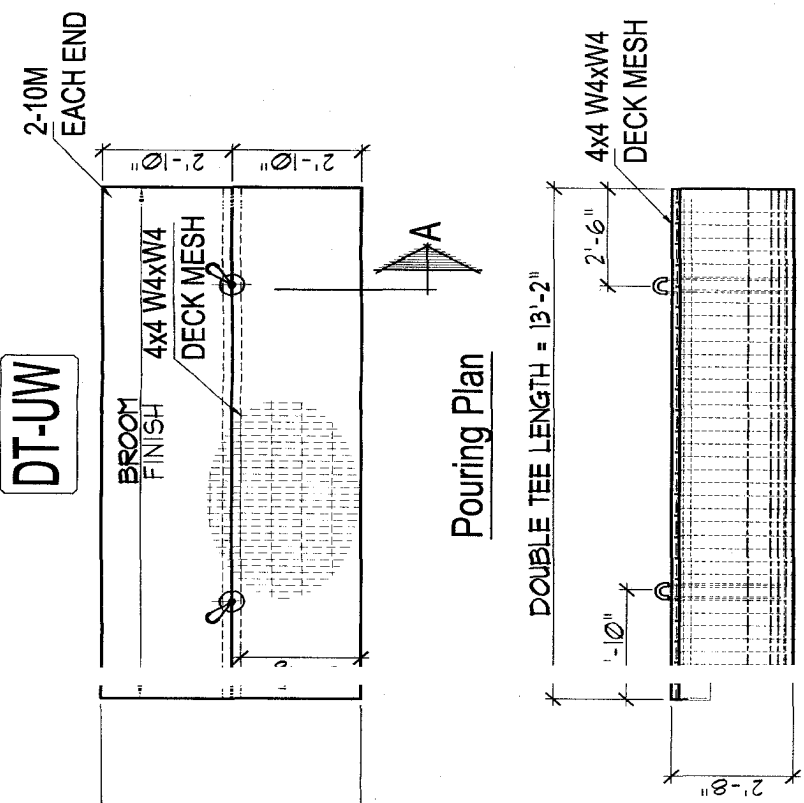
DRAWING TITLE: **Double-Tee**

P.M.: \_\_\_\_\_ SCALE: \_\_\_\_\_

CHECKED: \_\_\_\_\_

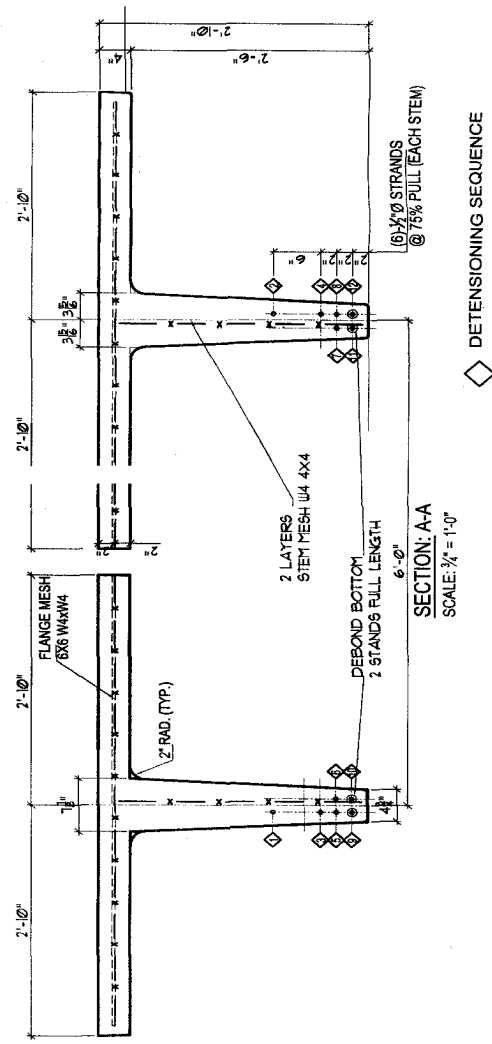
DRAWN: \_\_\_\_\_

PROJECT No.: \_\_\_\_\_ DRAWING No.: \_\_\_\_\_



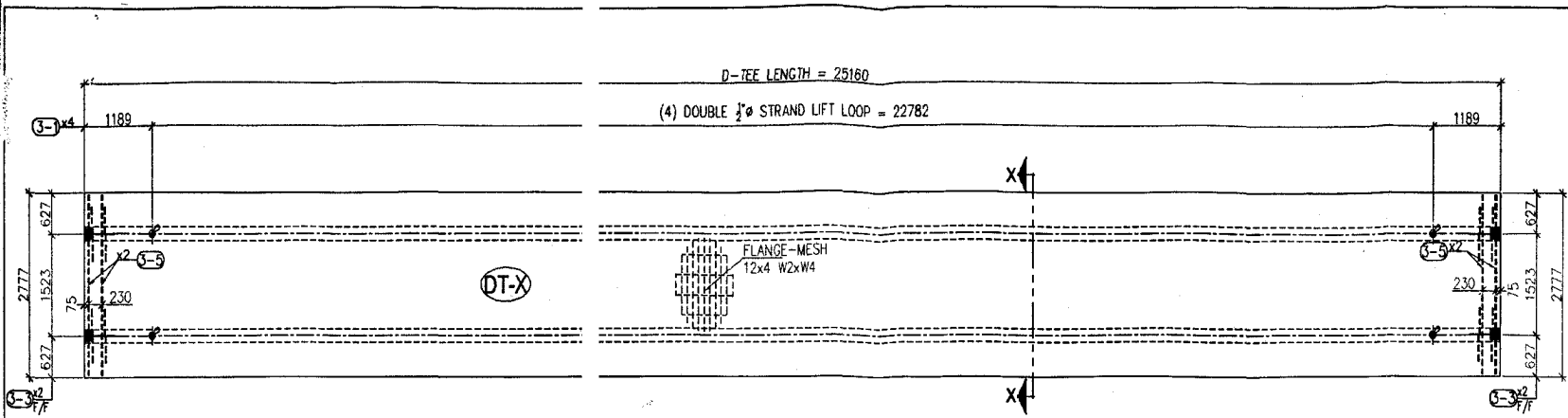
**Pouring Plan**

PRODUCTION NOTE:  
MARK THIS END WEST

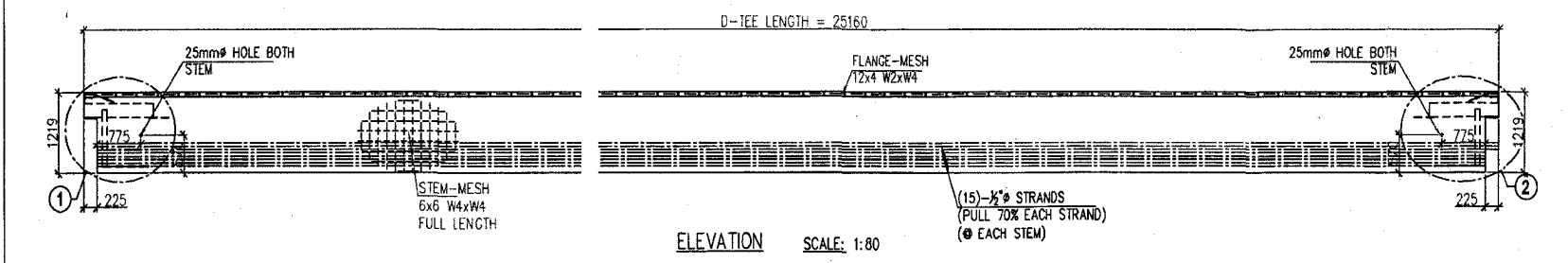


**SECTION: A-A**  
SCALE: 3/4" = 1'-0"

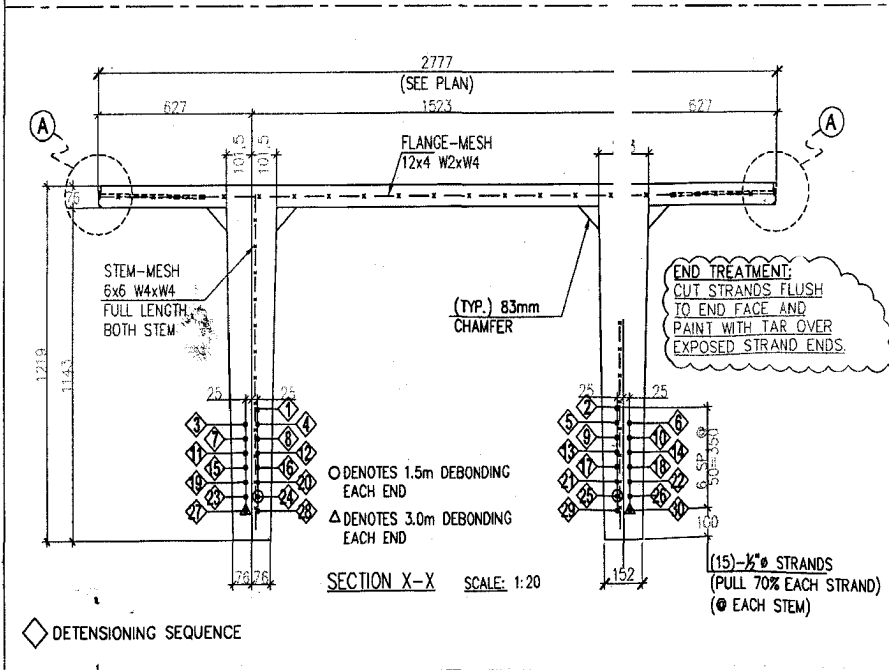
Reproduced with permission of the copyright owner. Further reproduction prohibited without permission.



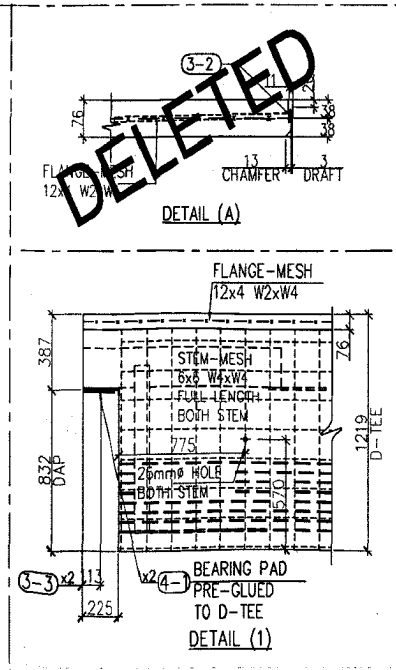
POURING PLAN SCALE: 1:80



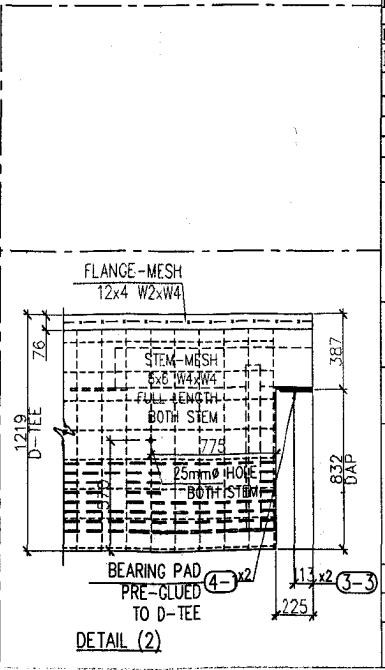
ELEVATION SCALE: 1:80



SECTION X-X SCALE: 1:20



DETAIL (A)



DETAIL (2)

**GENERAL NOTES**

- 1). FINISH = SEE SECTION
- 2).  $f_c$  = 48.3 MPa
- 3).  $f_{ci}$  = 28.0 MPa
- 4). AIR ENTRAINMENT = 5 ± 1%
- 5). COVER = 37 mm
- 6). INITIAL CAMBER = 30 mm
- 7). ERECTION CAMBER = 50 mm

**CAST-IN HARDWARE**

MK#	QTY.	DESCRIPTION
3-1	4	TRIPLE 1/2" STRAND LIFT LOOP (3" EMBED)
3-3	4	CAZALY HANGER (BEARING ASSEMBLY)
3-5	4	10M BARS ASSEMBLY FLANGE & STEM REINFORCING
4-1	4	13mm MASTICORD BRG. PAD

**REINFORCING SCHEDULE**

MK#	QTY.	LENGTH	DESCRIPTION

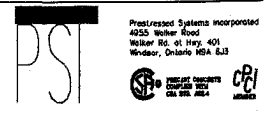
MARK TEST SPECIMEN

**PRODUCTION INFORMATION**

MK. #	QTY.	AREA (ft <sup>2</sup> )	VOL (m <sup>3</sup> )	WGT. (lbs)
DT-1	1	752	15.87	88882

**REVISIONS -- DRAWING ISS**

DATE	REVISION
Oct. 15/03	REVISED FOR PRODUCTION
June 27/05	ISSUED FOR PRODUCTION (TESTING)



PROJECT:

DRAWING TITLE:  
**DOUBLE TEE**

DRAWN:	SCALE: AS SHOWN
CHECKED:	FILE: P.C. D-1
PROJECT No.: 15588	DRAWING No.: DT-1